NTNU – Trondheim
Norwegian University of
Science and Technology

Effect of salinity shifts on microbial community composition in different nitrifying biofilms in continuous moving bed biofilm reactors.

Kjell Rune Jonassen

Chemical Engineering and Biotechnology
Submission date: June 2013
Supervisor: Kjetill Østgaard, IBT

Norwegian University of Science and Technology
Department of Biotechnology

Acknowledgements

This study was carried out at the Department of Biotechnology at the Norwegian University of Science and Technology (NTNU).

I would like to thank my supervisors Prof. Kjetill Østgaard, Prof. Olav Vadstein and PhD student Blanca Magdalena Gonzalez Silva for finding the time for weekly meetings and important feedback. Researcher Ingrid Bakke for guidance and help with DGGE. Fellow master students Are Johan Rønning and Ruben M. Sæther for all their shenanigans and engineer Randi Utgård for bringing (much needed!) coffee and chocolate during the 30 hour capacity and toxicity experiments.

A special thanks goes to all my loved ones and friends!

Abstract

Salinity is considered a common stress factor when nitrification is applied in waste water treatment. Observations often show a sub-optimal nitrification performance as a response to variations in in-fluent salinity. Recently, researchers have coupled microbial community dynamics and changes in the community structure to process stability, and there is a need for interdisciplinary research at the borderline between microbial ecology and process engineering to understand these links.

The aim of this study was to investigate and compare the community changes in two different nitrifying cultures adapted to different salinities as a response to a change in salinity.

Two continuous moving bed bio-film reactors were first operated at salinities corresponding to the community origin. These were a 0 ppt salinity adapted culture, originating from low salinity municipal waste water, and a 33 ppt salinity adapted culture originating from a recirculated aquaculture filter. After a period of continuous operation at those salinities the salinity were switched: operating the 0 ppt salinity adapted culture with a 33 ppt salinity based cultivation medium, and the 33 ppt adapted culture with a 0 ppt salinity based cultivation medium. Changes in community structure and community dynamics were monitored over time with denaturing gradient gel electrophoresis (DGGE). Average Bray-Curtis similarities within each community showed that a static nitrifying community was not essential for complete nitrification, but rather an advantageous community trait that gave a higher resilience towards fluctuations in environmental factors such as pH, temperature and nitrogen loading.

The results showed that the nitrifying culture adapted to 33 ppt salinity was more robust towards a change in salinity, and that the culture was halotolerant. Full nitrification was achieved from day 38 after the salinity change. The microbial adaptation strategy was not determined by either acclimation or by population shift, but rather a combination of the two determined by the community's inherent prerequisites. Further, it was demonstrated that during low salt adaptation a stable nitrification performance was not necessarily coupled to a stable community structure.

Population shift was probably the main adaptation strategy for the 0 ppt adapted culture when adapting to 33 ppt salinity. Observations during continuous operation at this salinity showed only partial nitrification from day 54 after the salinity change with low ammonium oxidation rates. Up towards this point in time, and towards the end of the experiment, the community structure was constantly changing.

Sammendrag

Salinitet er ansett som en vanlig stressfaktor når nitrifikasjon benyttes ved behandling av avløpsvann. Observasjoner viser ofte sub-optimale nitrifikasjonsrater som en reaksjon på variasjoner i influentens salinitet. Det har nylig blitt satt fokus på endringer og dynamikk i mikrobielle samfunn relatert til prosesstabilitet, og det er et er behov for ytterligere tverrfaglig forskning i grenseskillet mellom mikrobiell økologi og prosessteknikk for å forstå disse sammenhengene.

Målet med dette studiet var å undersøke og sammenligne mikrobielle samfunn i nitrifiserende biofilter adaptert til ulike saliniteter, og overvåke endringen i disse samfunnene som respons på en endring i salinitet.

To kontinuerlige reaktorsystem ble drevet, hvorav det ene med en kultur adaptert til 0 ppt salinitet, og det andre med en kultur adaptert til 33 ppt salinitet. Etter en periode med kontinuerlig drift ved disse salinitetene ble kultiveringsmediet byttet om og kulturen adaptert til 0 ppt salinitet ble forsynt med et medium med 33 ppt salinitet, og kulturen adaptert til 33 ppt salinitet ble forsynt med et kultiverings medium med 0 ppt salinitet. Endringer i samfunnets struktur og dynamikk ble overvåket over tid med denaturerende gradient gel-elektroforese (DGGE).

Gjennomsnittlig Bray-Curtis likheter innenfor hvert samfunn viste at et statisk mikrobielt samfunn ikke var avgjørende for fullstendig nitrifikasjon, men at et dynamisk samfunn var en fordel som ga en høyere elastisitet mot svingninger i miljøfaktorer som pH, temperatur og nitrogenbelastning.

Resultatene viste at kulturen adaptert til 33 ppt salinitet var mer robuste overfor en endring i salinitet, og at kulturen var halotolerant. Full nitrifikasjon ble oppnådd fra dag 38 etter endringen i kultiveringsmediets salinitet. Den mikrobielle tilpasningsstrategien ble ikke bestemt av akklimatisering eller ved samfunnsendringer, men snarere en kombinasjon av de to, bestemt av samfunnets naturlige iboende forutsetninger. Videre ble det vist at under adaptering til lav salinitet er stabile nitrifikasjonsrater ikke nødvendigvis koblet til en stabil samfunnsstruktur.

Samfunnsendring var mest sannsynlig den viktigste tilpasningsstrategien for kulturen adaptert til 0 ppt salinitet når denne ble forsynt med et 33 ppt salinitetsbasert kultiveringsmedium. Ved kontinuerlig drift ved denne saliniteten viste kulturen bare delvis nitrifikasjon fra dag 54 og utover etter salinitetsendringen. Ammoniumoksidasjonsratene var også lave i dette tidsrommet. Det mikrobielle samfunnet var i konstant endring under adapteringen.

Contents

1 Introduction **1**

1.1 Nitrification . . . 1
1.2 The microbiology of nitrification . . . 2
1.2.1 Ammonium oxidizing bacteria . . . 3
1.2.2 Nitrite oxidizing bacteria . . . 3
1.2.3 Nitrifying *Archaea* . . . 4
1.3 Salinity - effect and implications for nitrification and community structure 4
1.4 Characterization of microbial communities . . . 6
1.4.1 PCR-denaturing gradient gel electrophoresis (PCR-DGGE) . . . 6
1.4.2 Methodological biases . . . 7
1.5 Previous research at the Department of Biotechnology, NTNU, on nitrifying bio-films at different salinities . . . 8
1.6 Scope . . . 9

2 Materials and methods **11**

2.1 Experimental design . . . 11
2.2 Reactors, cultivation regimes and monitoring the nitrification rates . . . 13
2.2.1 Reactor set-up . . . 13
2.2.2 Cultivation media . . . 14
2.2.3 Sources of nitrifying bacteria and inoculation of the reactors . . . 16
2.2.4 Quantification of the nitrification activity . . . 17
2.3 Nitrification capacity and salinity toxicity tests . . . 18
2.4 Characterization of microbial community composition . . . 19
2.4.1 DNA sampling . . . 19
2.4.2 DNA extraction . . . 22
2.4.3 Polymerase Chain Reaction . . . 23
2.4.4 Denaturing gradient gel electrophoresis . . . 24
2.5 DGGE analysis and statistics . . . 26
2.5.1 DGGE anlysis . . . 26
2.5.2 Statistical analyses . . . 27

3 Results **28**
3.1 Operation of the nitrifying reactors 28
3.1.1 Operation of adapted and non-adapted cultures in previous experiments 28
3.1.2 The municipal waste water culture 29
3.1.3 The Trondheim Fjord culture 34
3.1.4 Data quality 37
3.2 Nitrification capacity and salinity toxicity tests 37
3.3 Bacterial community structure 39
3.3.1 Community dynamics at continuous operation at native salinities . 39
3.3.2 Microbial community composition in reactors before and after change in salinity 45

4 Discussion and conclusions **51**
4.1 Evaluation of molecular methods 51
4.2 Nitrification performance before and after the salinity change 52
4.3 Community structure and dynamics before the change in salinity 53
4.4 Community structure and dynamics after the change in salinity 55
4.5 Conclusions 58
4.6 Future perspectives 59

Appendices **67**

A Operation of the nitrifying reactor F, with biomass originating from low salinity municipal waste water **A1**

B Operation of the nitrifying reactor R2, with biomass originating from the Trondheim Fjord **B1**

C pH, temperature and dissolved oxygen measurements **C1**

D Capasity and toxicity tests **D1**

E DGGE protocol **E1**

List of Figures

1.1 Biological nitrogen sycle 2
1.2 Principle for separation of DNA fragments with DGGE. 7
1.3 Batch saline toxicity test. Jonassen (2012) 9

2.1 Flow scheme of the experimental design 12
2.2 Experimental setup for the nitrifying reactors 13
2.3 DNA sampling - reactor F 20
2.4 DNA sampling - reactor R2 21
2.5 DNA sampling - reactor R1 22
2.6 Sketch of DGGE gel with DNA samples from Jonassen (2012) project work 25
2.7 Sketch of DGGE gel with DNA samples from the municipal waste water culture and the Trondheim Fjord culture. 25

3.1 Concentrations of ammonium, nitrite and nitrite during continuous operation of Reactor F 29
3.2 Concentration measurements during continuous operation of Reactor F (zoomed in from day 75 of continuous operation) 31
3.3 Activity rates and volumetric nitrogen loading rate for Reactor F during continuous operation 32
3.4 Activity rates and volumetric nitrogen loading rate for Reactor F during continuous operation (zoomed in from day 40 of continuous operation) . . 33
3.5 Concentrations of ammonium, nitrite and nitrite during continuous operation of Reactor R2 34
3.6 Activity rates and volumetric nitrogen loading rate for Reactor R2 during continuous operation 36
3.7 Data quality. Nitrogen mass balances. 37
3.8 Batch capacity and saline toxicity experiments 38
3.9 DGGE gel, continuous operation at salinities corresponding to community origin 40
3.10 Average Bray-Curtis similarities within the communities in Reactor F, R1 and R2. 42
3.11 Average Bray-Curtis similarities within the communities in Reactor F, R1 and R2 plotted versus $\Delta salinity$. 42

3.12 NMMDS plot based on Bray-Curtis similarity measure of DGGE gel analysis results 43
3.13 DGGE gel from continuous operation before and after the change in salinity 45
3.14 NMMDS plot based on Bray-Curtis similarity measure of DGGE gel analysis results. 46
3.15 Average Bray-Curtis similarities within the four groups F_{start}, F_{end}, $R2_{start}$ and $R2_{end}$ 47
3.16 Comparison of the average Bray-Curtis values for F_{start} with the time series towards F_{end} 48
3.17 Comparison of the average Bray-Curtis values for $R2_{start}$ with the time series towards $R2_{end}$ 49

4.1 Comparison of Bray-Curtis similarities between samples 54
4.2 Comparison of Bray-Curtis similarities between samples after salinity switch 57

List of Tables

2.1 Composition of tap water media (0 ppt salinity). 15
2.2 Composition of sea water based based media (33 ppt salinity). 15
2.3 Composition of metal stock solution. 15
2.4 PCR reagents 23
2.5 PCR temperature regime. 24

3.1 Band richness(k), Shannon (H') and Evenness diversity indices for reactor F, R1 and R2. 41
3.2 One-way ANOSIM test for significant differences between the nitrifying cultures adapted to different salinities. (P-values: Bon-Ferroni sequential.) 44
3.3 Similarity percentage - Showing the ten most influential bands contributing to the total difference between the groups in Figure 3.9. 44
3.4 Diversity between Reactor F and R2. 46
3.5 Diversity between the groups F_{start}, F_{end}, $R2_{start}$ and $R2_{end}$. 47
3.6 One-way ANOSIM bonferroni seq. F_{start}, F_{end}, $R2_{start}$ and $R2_{end}$. 49
3.7 Similarity percentage - Showing the ten most influential bands contributing to the total difference between the groups in Figure 3.13 50

Chapter 1

Introduction

1.1 Nitrification

Nitrogen occurs in a wide range of oxidation states, from +5 (nitrate) to -3 (ammonium), thus functioning as an important electron donor and acceptor in a variety of chemical and biological reactions and transformations. In environments rich in oxygen, such as rivers and many lakes, nitrate is the most abundant form of fixated nitrogen. In oxygen depleted environments, such as swamps, sediments and waste water, ammonium dominates. These two pools of dissolved inorganic nitrogen are connected through the process of microbial nitrification, which is a process that links the mediated transformation of nitrogen in its most reduced state (ammonium) to its most oxidised state (nitrate). Nitrification is a two step process where ammonia is first converted to nitrite by the action of ammonia oxidizing bacteria (AOB). The nitrite is then further converted to nitrate by the nitrite oxidising bacteria (NOB) (Ward et al., 2011). Both these groups of bacteria are autotrophic *i.e.* they fixate CO_2. The chemical reactions in Equations 1.1 and 1.2 are performed by the ammonia oxidising bacteria in two sequential steps by two different enzymes. Equation 1.1, where ammonia is converted to hydroxylamine, is catalysed by the enzyme ammonia monooxygenase. The hydroxylamine is further oxidised to nitrous acid as shown in Equation 1.2. This reaction is catalysed by the enzyme hydroxylamine oxireductase (Madigan et al. (2009) and Ward et al. (2011)).

$$NH_3 + O_2 + 2H^+ + 2e^- \rightarrow NH_2OH + H_2O \tag{1.1}$$

$$NH_2OH + \frac{1}{2}O_2 \rightarrow HNO_2 + 2H^+ + 2e^- \tag{1.2}$$

The over all energy yield from from the aerobic oxidation of NH_3 to NO_2^- is $\Delta G_0^{'} = -137$ $kJ \cdot mol^{-1}$. This energy is used both for production af ATP and reducing power for reduction of CO_2.

The nitrite oxidising bacteria consume nitrite and convert it to nitrate through the

reaction shown in Equation 1.3. The reaction is catalysed by the enzyme nitrite oxioreductase (Madigan et al. (2009) and Ward et al. (2011)).

$$NO_2^- + \frac{1}{2}O_2 \rightarrow NO_3^- \tag{1.3}$$

Figure 1.1 shows the biological nitrogen cycle. The process of nitrification and its position in the cycle is shown. Ammonia is released through break-down of organic matter mediated through the process of ammonification and excretion by animals.

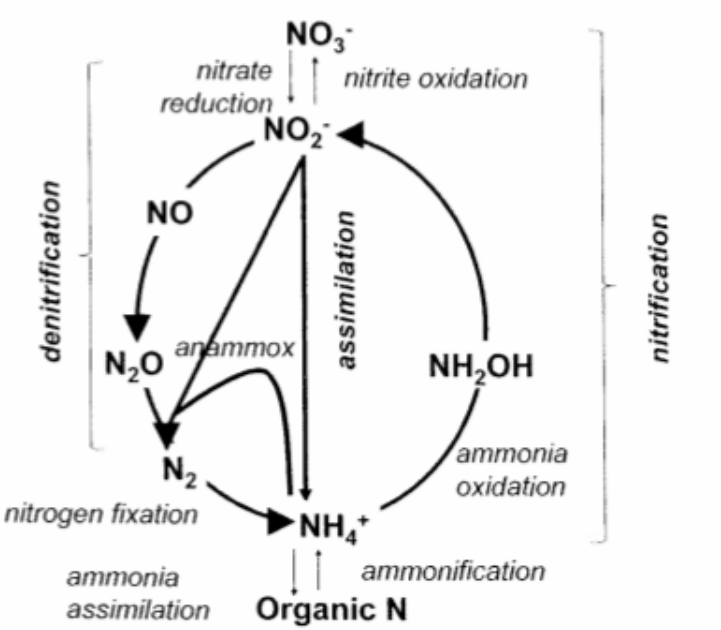

Figure 1.1: Biological nitrogen cycle. Figure adapted from Ward et al. (2011).

.

1.2 The microbiology of nitrification

As shown in Equation 1.1 - 1.3, the nitrifying bacteria are aerobic, but the energy yield of nitrification is poor. As a consequence, the nitrifying bacteria are slow growers with maximum specific growth rates (μ_{max}) in the region of 0.34 to 2.2 day^{-1} (Henze et al. (1987), Sedlak (1991) and Jimenez et al. (2011)). The nitrifyers are chemolithoautotrophs and thus utilize CO_2 as a source of carbon. This means that they do not compete with fast growing organo-heterotrophs for carbon sources under aerobic conditions.

Nitrifying bacterial communities are sensitive to environmental factors such as temperature, pH, dissolved oxygen concentration (Hellinga et al., 1998), the availability of substrate and inhibitory compounds (Moussa et al., 2006). In utilization of nitrifyers

for industrial purposes it is therefore a necessity to monitor the environmental factors closely. This is due to the fragile mutalism between the ammonium oxidizing bacteria and the nitrite oxidisers (Graham et al., 2007) that often causes a sub-optimal nitrification performance in real applications.

pH regulation is of particular importance as pH influences the concentration of free ammonia and nitrous acid which can inhibit the AOB and NOB. Equation 1.4 shows the relationship between pH, temperature and ammonium concentration and the concentration of ammonia. Ammonia levels between 10 and 150 mg-N/L, and between 0.1 and 10 mg-N/L have been reported to inhibit the AOB and NOB (Anthonisen et al., 1976).

$$C_{NH_3} = \frac{17}{14} \frac{\sum(NH_4^+ - N \cdot 10^{pH})}{exp(\frac{6344}{273+T}) + 10^{pH}} \tag{1.4}$$

Equation 1.5 shows the relationship between pH, temperature and nitrite concentration and the concentration of nitrous acid. Nitrous acid levels above 0.2 mg-N/L have been reported to inhibit both AOB and NOB (Anthonisen et al., 1976).

$$C_{HNO_2} = \frac{17}{14} \frac{\sum NO_2^- - N}{exp(\frac{-2300}{273+T}) \cdot 10^{pH}} \tag{1.5}$$

1.2.1 Ammonium oxidizing bacteria

The ammonia oxidizing bacteria (AOB) are obligate chemolithotrophs that support growth and metabolism solely from the oxidation of ammonium. The AOBs belong to two different classes of bacteria; the γ-proteobacteria and the β-proteobacteria. Within the the β-proteobacteria the genera *Nitrosomonas*, *Nitrosovibrio* and *Nitrosospira* cover most of the ammonium oxidizing species. Ammonia oxidizing species organized in the genus *Nitrosococcus* belong to the γ-proteobacteria group.

AOBs are distributed in a wide array of environments, with reported findings of γ- and β-proteobacteria in marine-, estuarine- and freshwater systems (including waste water and other engineered treatment systems), and also in terrestrial systems such as soil (Ward et al., 2011).

1.2.2 Nitrite oxidizing bacteria

Nitrite oxidizing bacteria (NOB) belong to five genera from two different phyla of the bacterial domain. The genera *Nitrospina*, *Nitrotoga* and *Nitrococcus* belongs to the δ-, α- and γ-genera of the proteobacteria phylum, respectively. The *Nitrobacter* and *Nitrospira* belongs to the α-proteobacteria and to the second phylum, Nitrospirae. (Ward et al., 2011). Nitrite is usually scarce in natural environments, so the presence of NOBs are tightly linked to the ammonium oxidisers and are found in all environments that harbour AOBs (Section 1.2.1).

1.2.3 Nitrifying *Archaea*

It has recently been shown that *Archaea* probably plays a key role in the nitrification process in marine environments. Genes similar to the ammonia monooxygenase genes of AOBs were in 2005 identified in a group of *Archaea* abundant in fresh water and marine environments (Treusch et al., 2005). Konneke et al. (2005) discovered ammonia oxidizing metabolism in *Archaeal* isolates. It was later reported that *Archaea* have an important role in the global biological nitrogen cycle, Figure 1.1 (Francis et al., 2007). Ammonia oxidizing archaea have later been found present in a variety of environments including waste water sludge and marine sediments (Bernhard et al., 2010). Bernhard et al. (2010) showed that the abundance of ammonia oxidizing *Archaea* was greater than that of ammonia oxidizing bacteria along an estuarine salinity gradient, but the abundance did not correlate with nitrification activities.

The presence of *Archaeal* nitrifyers will not be examined in this study.

1.3 Salinity - effect and implications for nitrification and community structure

Saline effluent streams have been in researchers attention for quite some time, and according to Gutierrez-Wing and Malone (2005) factors such as water quality, water quantity, environmental impacts, cost of land and diseases are driving aquaculture and other industries to adopt more environmental friendly technologies. These industries include aquaculture, cheese manufacturing, seafood processing, the production of chemicals and oil and gas recovery among others. Furter, more countries are examining the possibility of using saline water for flushing due to scarcity of freshwater. This will eventually lead to an increase in the waste water salinity that reaches municipal waste water treatment plants (Moussa et al., 2006).

In Norway, fish farming is one of the most important export industries with a revenue of 53 BNOK in 2011 (Regjeringen.no, 2012). Fish farming has mainly been run with open pen nets in open seas, and is reported to be the largest contributor of inorganic nutrient emissions in Norway (Norwegian Climate and Pollution agency, Selvik J. (2007)). Conversion to land based aquaculture farms could limit these emissions substantially, as a land based farm will allow more control of the emissions. Land based aquaculture farms pose other problems such as accumulation of salts potentially toxic to the farmed fish, with ammonia being one of the key players (Wright and Wood, 2012). It is therefore a need for efficient methods of removing this fish toxin from the recirculated stream. A biological nitrification filter could be a good and environmental friendly method of converting ammonia to a more oxidised and less lethal form - nitrate.

Studies on the effect of salt on nitrification are difficult to compare and often show somewhat contradictory results. Catalan-Sakairi et al. (1997) and Sudarno et al. (2010) reported that nitrite accumulation occurred at high salinities with adapted cultures, both with the use of marine genera adapted to high salinities. On the contrary Hunik et al. (1992) used batch assays to examine the effects of different salts on a nitrifying

culture, and reported that ammonia oxidation was more sensitive to the inhibitory effect of high salt concentrations. Moussa et al. (2006) hypothesised that the reasons for the contradictions in the literature could be system configuration and instability in the experimental conditions with respect to temperature, pH, presence of inhibitory compounds/factors. The way salt is introduced to the system (pulse or gradual increase), the species involved (use of pure or mixed cultures) or the use of adapted or non-adapted communities.

Most of the studies regarding salt adaptation do not report on the role of community dynamics during the adaptation. According to Moussa et al. (2006) there is a need for interdisciplinary research in the fields of microbial ecology and process engineering to understand how the microbial diversity is linked to process stability and efficiency. Miura et al. (2007a) compared community structures in membrane bio reactors treating low salinity municipal waste water and linked community stability with reactor performance. It was found that stable communities were not required for consistent reactor performance, but rather that small perpetual fluctuations in community structure seemed to be of importance for stable operation, indicating a flexibility to adapt to minor changes in the environment. This was also shown by Wittebolle et al. (2008) who quantified community dynamics of nitrifyers in functionally stable sequential batch- and membrane bio reactors. Non of the reactors showed a static microbial community and it was concluded that the stability of the microbial communities were not essential for maintaining the functional stability of the nitrification process. Pareto-Lorentz evenness curves based on AOB denaturing gradient gel electrophoresis (DGGE) profiles showed that only a small group of different AOBs played a numerically dominant role in the reactors, which led to speculations that the less dominant species constituted some sort of reserve being able to proliferate and dominate if conditions were changed.

The effects of variations in pH, dissolved oxygen concentration and ammonium on community structures of waste water nitrifying bacteria were studied by Princic et al. (1998). ARDRA similarity indexes were calculated and compared before and after changes, and when the cultures were restored to the original conditions. They showed that high ammonium levels in the in-fluent resulted in a reversible community change. Running reactors at pH extremities of 5.8 and 8.5 also resulted in community changes, but these were irreversible and the communities did not regain their initial composition when returning the communities to the normal pH range of 7.0 - 8.0. Changes in the dissolved oxygen concentrations did only result in community changes at low concentrations (1%), but then the nitrification rates were also reduced. Princic et al. (1998) looked at the effect of in-fluent concentrations of ammonium and nitrite on communities of AOBs in activated sludge continuous reactors. Differences in the composition of dominant AOBs were discovered at low/high ammonium loading rates. Addition of nitrite showed that some AOB were more significantly inhibited than others.

As mentioned above, most studies regarding salt adaptation do not include the changes in the microbial community during adaptation and how this influences the functional performance. Still, there has been some reports on salt adaptation and its effect on the microbial diversity related to nitrification activity. Bassin et al. (2012) studied

the effect of different salt adaptation strategies related to microbial diversity and activity in sequencing batch reactors. Two different salt adaptation strategies were applied; salt was first increased in an incremental manner - 5, 10, 15 and 20 g/L of NaCl, and in a more shock-wise manner - 10 and 20 g/l NaCl. They concluded that different salt adaptation strategies both resulted in good nitrification performance, but caused different shifts in the microbial community. Ammonia oxidation activity was more affected with a shock load adaptation strategy, than the nitrite oxidisers.

1.4 Characterization of microbial communities

1.4.1 PCR-denaturing gradient gel electrophoresis (PCR-DGGE)

PCR-DGGE, first introduced by Muyzer et al. (1993), is a common genetic fingerprint technique to study and assess the community structure and to describe the community dynamics in response to environmental variations in environmental samples. Commonly, this identification is based on differences in the nucleic acids corresponding to genes encoding the bacterial ribosomal 16S rDNA (Bakke et al. (2011)), and is used as a marker for bacterial diversity. The literature describing its application is wide, and PCR-DGGE have been applied in studying microbial communities in a wide array of habitats; waste water treatment plants (Boon et al., 2002), soil (Shimano et al., 2012), food (Bibiloni et al., 2005), micro biota of animals (Bibiloni et al., 2005) and fish (Brunvold et al., 2007) among others.

Traditional methods regarding investigating microbial communities often involves microscopic identification of morphological characteristics and investigation of different traits; as the ability to grow in different cultivation media. A common problem with these techniques is that many bacteria have similar morphologies, but are in fact different species. Furthermore, with cultivation based techniques only a small proportion of the microbial communities are detectable due to lacking knowledge regarding the real conditions in which bacteria is growing in their natural habitats - commonly referred to as *The great plate count anomaly* (Staley and Konopka, 1985). Opposed to culture dependent methods PCR-DGGE and other PCR based fingerprinting methods are culture-independent, and overcomes many of the problems associated to culture dependent techniques.

The technique is based on separation of equal length PCR amplicons with different melting behaviours due to differences in base composition of these amplicons. The PCR amplified DNA from an environmental sample is run through an acrylamide gel with a denaturing gradient (Figure 1.2). Double stranded DNA will migrate through the gel when subjected to an electric field. While the double-stranded amplicons initially migrate freely through the gel matrix, they eventually encounter a concentration of denaturant where the sequence of interest dissociates, resulting in a "mobility arrest." The melting properties of DNA is dependent on the DNAs guanine (G) and cytocine (C) content, which means that variations in the DNA sequences constituting an environmental sample will result in different melting characteristics. Elaborated, a high content of G

and C will make a need for harsher denaturing conditions in order to melt the DNA fragment and *vice verca* for fragments with a low GC content. The resulting gel will contain bands of DNA at different positions (ideally one band per species) and functions as an estimate of the microbial diversity in the sample. The different bands can be cut out of the gel for accurate species determination with the use of DNA sequencing techniques.

DNA needs to be extracted and amplified before the DGGE analysis. General primers targeting all bacteria, genus specific primers, or primers targeting genes of enzymes unique for a particular function can be used. General primers often target regions of the 16S rRNA gene. The primers are often modified with a GC clamp ($\approx$ 40 bp GC rich sequence) (Figure 1.2). The GC-clamp prevents complete strand separation and ensures that the DNA samples will not migrate through the gel. As shown by Myers et al. (1985) attatching a GC-clamp allows the separation of almost similar DNA sequences, often differing in only one base substitution. They further showed that substitutions do not lead to a distinct separations in the DGGE gels when the fragments were not modified with the GC-clamp. In the same study theoretical calculations and analysis of a large number of different mutations showed that approximately 95% of all possible single base substitutions should be separable when attached to a GC-clamp.

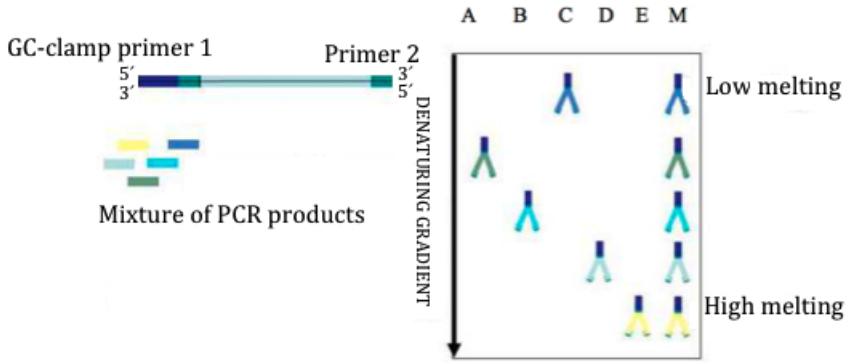

Figure 1.2: Principle for separation of DNA fragments with DGGE. Figure adapted from Plant Research International (2013).

.

The final result is a community fingerprint which is unique for the the environmental sample being studied. The bands represented on the gel are relative to the microbial species present in the sample. Further computational and statistical methods can be applied in order to compare different samples.

1.4.2 Methodological biases

PCR-DGGE is an effective way of studying microbial communities since many samples can be analysed simultaneously. There are still some limitations to the technique, lim-

itations that can lead to wrong conclusions regarding identification of species and also wrongly estimating the community richness or diversity. In extraction of nucleic acids from an environmental sample different extraction protocols often suffer from inadequacies which include incomplete cell lysis, DNA binding to surfaces, co-extraction of humic acids that inhibit the DNA–DNA hybridization and enzymatic reactions influencing the extraction efficiency, according to Mumy and Findlay (2004). The PCR reaction also generates several possible biases due to various PCR generated artefacts. Kusar and Avgustin (2012) describe several biases that arise from the amplification of a complex mixture of DNA targets and includes sequence mismatches, heteroduplexes, chimeric molecules, and single-stranded DNA (ssDNA). But as PCR related biases will influence all the samples equally it is possible to compare the relative amounts of different taxa/bands between different samples. DGGE is also known to be prone to possible co-migration of DNA fragments from different taxa to the same positions within the DGGE gel, resulting in different species constituting one band in the gel (Gafan and Spratt, 2005).

Even if DGGE gives information regarding presence of DNA present in an environmental sample, the possible errors introduced from the methodological biases makes it hard to conclude if the bands on the gel correspond to key-players in the habitat sampled. Poor resolution makes the number of separable bands limited. The limited resolution of the gels also makes it hard to detect the presence of minor populations within the community *e.g.* on the 16S rDNA level, as weak bands may not be visible on the DGGE gel (Miura et al., 2007a).

1.5 Previous research at the Department of Biotechnology, NTNU, on nitrifying bio-films at different salinities

Kristoffersen (2004) performed an experiment on the acute toxic effects of different salinities on two different nitrifying cultures adapted to different salinities (0- and 22 ppt). This experimental study found the nitrifying activity in the 0 ppt salinity adapted culture to decrease as response to elevation in salt concentrations. This was also observed in the 22 ppt. salinity adapted culture, but here the effect was not as substantial as observed in the 0 ppt salinity adapted culture.

Hjort (2010) continued operating the same bacterial cultures as Kristoffersen (2004). She showed that denaturing gradient gel electrophoresis (DGGE) was a useful method for investigating the microbial communities and that the 22 ppt. adapted culture had a lower microbial diversity compared the non-adapted culture. Different species also seemed to dominate when comparing the two bio-films. DGGE analysis revealed that the 0 ppt salinity adapted culture revealed higher microbial diversity compared to the 22 ppt. salinity adapted culture.

In Jonassen (2012) project work three enriched nitrifying cultures were continuously operated in moving bed bio-film reactors at different salinities. Two of these were the same cultures utilized in the experiments of Hjort (2010) and Kristoffersen (2004). The third culture was a 33 ppt. salinity adapted culture. A batch salinity toxicity experiment

(Figure 1.3) showed that the two bacterial cultures adapted to high salinities seemed to tolerate high salinities better than the culture adapted to 0 ppt salinity. The 22 and 33 ppt salinity adapted cultures also demonstrated high nitrification rates in a tap water based cultivation medium, which indicated that the microbial communities adapted to these salinities were halotolerant, and thus had a competitive advantage towards variations in salinity. (Figure 1.3).

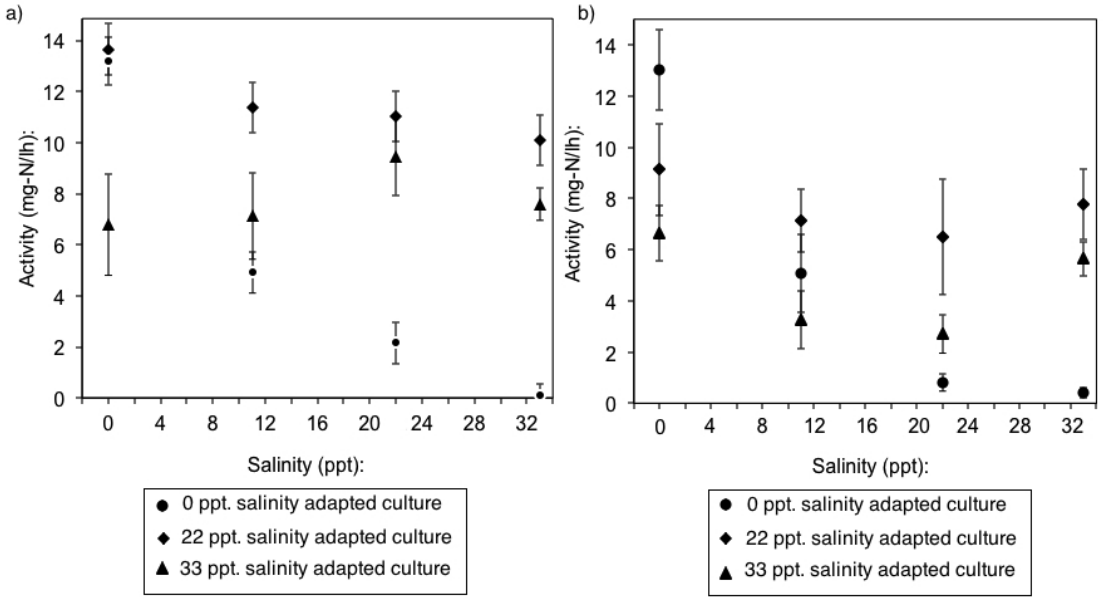

Figure 1.3: Nitrification calculations for batch saline toxicity test at different salinities (Jonassen, 2012). The 0, 22 and 33 ppt adapted cultures were subjected to different salinities and the concentration of ammonium, nitrite and nitrite were monitored over time. Linear regression gave the nitrification activities which were plotted versus salinity for the three cultures. **a)** Ammonium removal rates ($mg{-}N/l{\cdot}h$) for the 0, 22 and 33 ppt salinity adapted cultures at different salinities. **b)** Nitrate forming rates ($mg - N/l \cdot h$) for the 0, 22 and 33 ppt salinity adapted cultures at different salinities.

Each culture was sampled for a preliminary DGGE analysis at various times during continuous operation of the nitrifying reactors at culture adapted salinities. Comparison of different bio-film samples showed that there was clear differences in the composition of the microbial communities between the reactors.

1.6 Scope

Salinity is considered a common stress factor in biological nitrogen removal in waste water treatments plants. The treatment of saline waste waters often shows sub-optimal nitrification. It is therefore a need for interdisciplinary research at the border line between process engineering and microbial ecology in order to understand the links between

microbial diversity, community dynamics and process stability.

The aim of this thesis was to study the long term effect on the community structure and community dynamics as a response to a major change in salinity with two nitrifying cultures; adapted to 0 ppt and 33 ppt salinity. The work included operation of two continuous moving bed bio-film nitrifying reactors at culture adapted salinities, which was followed by a change in salinity where the 0 ppt adapted culture was subjected to a salinity of 33 ppt, and the 33 ppt adapted culture was subjected to 0 ppt salinity. The experiment also included a nitrification capacity test and a saline toxicity test, which was performed before the switch in salinity. Nitrification rates were monitored, and the change in the microbial communities were characterized by analysing gradient gel electrophoresis (DGGE) community fingerprints.

The nitrifying cultures, and the DNA samples from the experiments of Jonassen (2012) were available for further studies regarding microbial community structure and dynamics in this project.

Chapter 2

Materials and methods

2.1 Experimental design

To study the community dynamics as a response to an abrupt change in salinity in different enrichments of nitrifying bacteria adapted to different salinities, a two stage experiment was designed. In the first stage three bench scale moving bed bio-film reactors were first operated at native saline conditions in order to determine community structure and stability under constant salinity. The cultures originated from environments with a salinity corresponding to tap water (salinity of 0 ppt.), brackish water (salinity of 21 ppt) and sea water (salinity of 32 ppt). The culture adapted to tap water salinity originated from municipal waste water and the culture operated at a salinity of 22 ppt originated from an aerated lagoon near Statoil Mongstad Oil Refinery. The third culture, adapted to sea water salinity, originated from the Trondheim Fjord. DNA were sampled at various points during continuous operation. These three cultures were operated by Jonassen (2012) as a part of a project work during the fall of 2012.

The second stage was performed in the present study. It involved two of the cultures previously operated by Jonassen (2012). These were the municipal waste water culture, adapted to tap water salinity (0 ppt), and the Trondheim Fjord culture, adapted to sea water salinity (33 ppt). The cultures were first operated at native salinities until they were operating consistently. Then the growth medium was interchanged: supplying the municipal waste water culture with a sea water based medium (33 ppt), and the sea water culture with a tap water based medium (0 ppt). Before the medium switch a batch capacity test and a saline toxicity test was conducted on both cultures.

During operation DNA samples were sampled at regular time intervals before and after the change in salinity. A part of the variable 3 region of the bacterial 16S rRNA gene was amplified with the use of PCR, and the PCR products were separated based on melting behaviour with denaturing gradient gel electrophoresis (DGGE). The band pattern of the DGGE gel was used in further computational and statistical analysis with the software Gel2k (Norland, 2004) and PAST (Hammer et al., 2001) to determine the community dynamics before and after the change in salinity.

Details regarding reactor set-up, bio-film origin and history, composition of culti-

vation media and the inoculation of the reactors are explained in chapters 2.2.1 and 2.2.3. Chapter 2.2.4 describes the methodology of sampling in order to monitor the nitrification activity in each reactor. The capacity- and salinity toxic response test are described in chapter 2.3, followed by a description of assays regarding molecular biology techniques; DNA extraction, PCR and DGGE, in chapter 2.4. The basis behind the computational analysis of the DGGE gels and statistical analysis is explained in chapter 2.5. Figure 2.1 shows a schematic scheme of the experimental design used in this experiment.

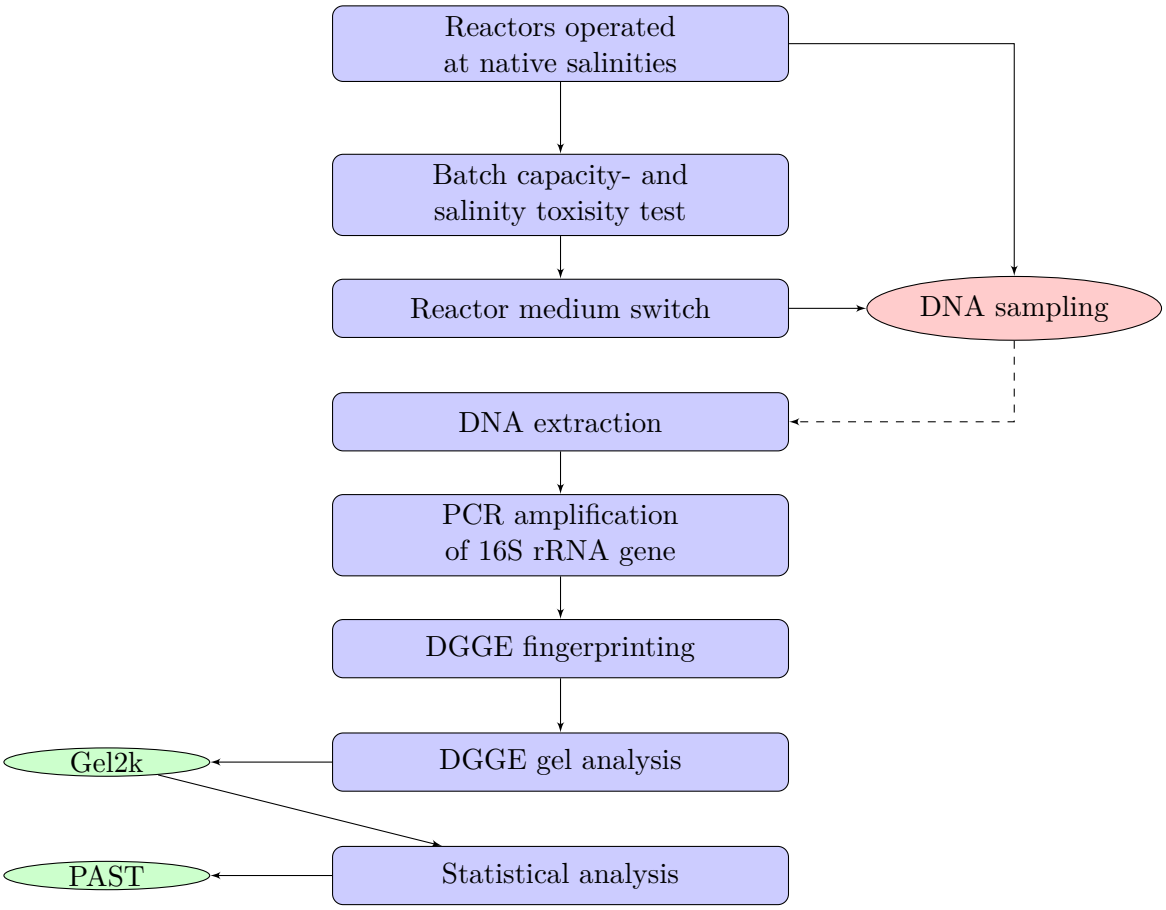

Figure 2.1: Flow scheme of the experimental design. Blue nodes shows the main steps in the experiment. Red nodes shows at which points DNA were sampled, and green nodes shows the steps in which computational and statistical methods were applied.

2.2 Reactors, cultivation regimes and monitoring the nitrification rates

Small bench scale moving bed bio-film reactors were set up in continuous flow in order to cultivate nitrifying bacteria originating from sources of different salinities. The reactors were fed with media containing 0 ppt. (only tap water) and 100% sea water. The sea water had a salinity content of 33 ppt.. The bio-film carriers used was the AnoxKaldnes^{TM}K1 bio-film carriers. These carriers had an already established bio-film originating from different environments with different salinities.

2.2.1 Reactor set-up

The reactors consisted of a glass housing with a glass heating jacket (Figure 2.2). A silicone lid with drilled holes allowed for easy placement of a pH electrode, inlet tubing for the cultivation media, tubing for acid and base related to pH regulation and inlet tubing for aeration. A magnetic stirrer was applied to mix the bio-film carriers evenly throughout the reactor, as well as to evenly mix the cultivation media and to disperse the air bubbles evenly in the reactor volume. During operation each reactor was covered with black plastic or fabric in order to prevent most of the light from penetrating into the reactors. This was done in order to minimize the possibility of phototrophic growth inside the reactors. A settler was mounted on the outlet of the reactor. This allowed for sedimentation of biomass carried out in the effluent stream.

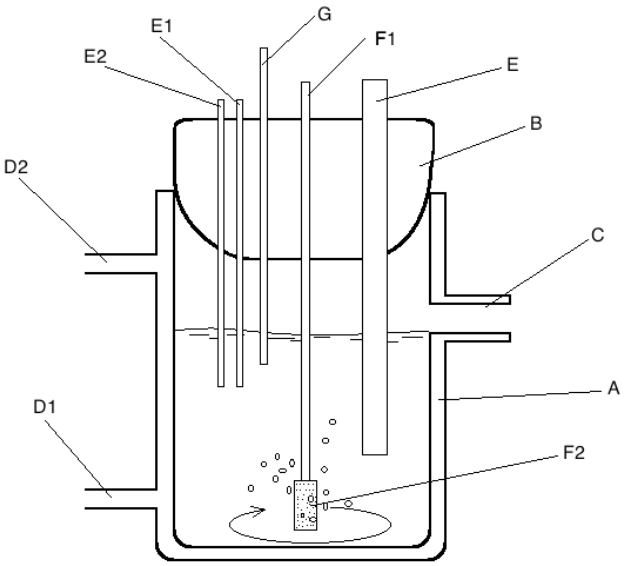

Figure 2.2: Experimental setup for the nitrifying reactors. A: Reactor. B: Silicone lid. C: Outlet. D1/2: Inlet/outlet for heating jacket. E/1/2: pH electrode and acid and base inlets. F1/2: Inlet for air and aquarium air stone. G: Inlet for cultivation medium.

All the tubing through the various pumps and connectors were of two different types of Masterflex^{TM}tubing (model no.: 6404-14 and 6404-16). Only clean "out of the box" tubing was used. Tubing and connectors were flushed in distilled water before use. Influent flow of cultivation media into the reactors was controlled with adjustable $Ismatec^{®}$ MCP pumps (model no.: ISM404B) with ISM734B pump heads.

Air was supplied to the reactors through a Rexroth R412004415 regulator, which allowed for regulation of air flow into the reactors. The regulator had an integrated filter to remove any possible compressor fluids prior of entering the reactor. In order to maximize the mass transfer of oxygen the air was passed through an aquarium air stone to ensure small air bubble size in the reactors. Nitrifying bacteria are sensitive to low oxygen concentrations, and inhibition have been reported at dissolved oxygen concentrations below 2 $mg\ O_2/L$ (Ward et al. (2011). The concentration of dissolved oxygen ($mg\ O_2/L$) was measured by a Oxi 3315 hand held digital meter connected to a $FDO^{®}$ 925 oxygen electrode (WTW), and aeration was regulated if necessary.

The temperature of the reactors was kept at 25 °C by a circulating water bath (Cole Parmer $Polystat^{®}$) which pumped heated water in and out of the heating jacket of the reactors.

pH was regulated by a Consort R301 automatic pH controller with pH set points between 7.2 and 7.8 . The controller received a signal from a Mettler HA405-DDA-SC-S8/225 combination pH electrode placed inside the reactors. The controller signalled Easyload^{TM}Masterflex pumps (model no.; 7518-00) to add 0.5 M NaOH or 0.5 M HCl when necessary.

The nitrifying reaction is consuming alkalinity (Equation 1.1, 1.2 and 1.3), but as the system was bicarbonate buffered (Chapter 2.2.2) the pH was mainly regulated by the effect of aeration on the gas/liquid equilibrium of CO_2 (Equation 2.1):

$$H_2O + CO_2 \rightleftarrows H_2CO_3 \rightleftarrows H^+ + HCO_3^- \tag{2.1}$$

Stripping of CO_2 will generate alkaline conditions in the initial phases of reactor start up, and addition of hydrochloric acid is expected. As a result of increasing nitrification rates (Chapter 2.2.4) the production of protons from the nitrification process outweighs the effects of CO_2 stripping, making addition of sodium hydroxide necessary.

2.2.2 Cultivation media

The media composition (2.1 and 2.2) is derived from Ostgaard et al. (1994). The sole energy source was ammonium sulphate ($(NH_4)_2SO_4$). Sodium hydrogen carbonate ($NaHCO_3$) added to the media acted as a carbon source and as a buffer. The source of phosphorous in the tap-water based medium was di-potassium hydrogen phosphate (K_2HPO_4). In the sea water based medium the source of phosphorous was sodium di-hydrogen phosphate ($NaH_2PO_4 \cdot H_2O$). The trace metal solution was prepared according to Table 2.3 and was stored at 4 °C in darkness.

The sea water used in the experiments was collected from approximately 70 meters depth in the Trondheim Fjord. It was stored at room temperature in a 1 m^3 plastic container covered in plastic. Prior to use the sea water was filtered through a type 692 $1\mu m$ glass fibre filter (VWR) with the use of a VacSafe 15 vacuum pump (ScanVac).

The cultivation media was placed at room temperature when connected to the reactors. Prior to reactor hookup the pH in the medium was adjusted to pH 7.5 with the use of 6 M HCl or 6 M NaOH. The containers were covered in black plastic in order to minimize the growth of phototrophs when connected to the reactors.

Table 2.1: Composition of tap water media (0 ppt salinity).

Compound	Amount added to 1 L media
$(NH_4)_2SO_4$	Varying
$NaHCO_3$	1 g
K_2HPO_4	0.4 g
Metal stock solution	10 mL
Tap water	990 mL

Table 2.2: Composition of sea water based based media (33 ppt salinity).

Compound	Amount added to 1 L media
$(NH_4)_2SO_4$	Varying
$NaHCO_3$	1 g
$NaH_2PO_4 \cdot H_2O$	0.005 g
Metal stock solution	10 mL
Sea water	990 mL

Table 2.3: Composition of metal stock solution.

Compound	Amount added per 1 L
$MgSO_4 \cdot 7H_2O$	2.5 g
$MnCl_2 \cdot 4H_2O$	0.55 g
$CaCl_2 \cdot 2H_2O$	0.05 g
$ZnCl_2$	0.068 g
$CoCl_2 \cdot 6H_2O$	0.12 g
$NiCl_2 \cdot 6H_2O$	0.12 g
$FeCl_2$	0.4 g

2.2.3 Sources of nitrifying bacteria and inoculation of the reactors

The bio-film carriers used were the AnoxKaldnes^{TM}K1 bio-film carriers. These carriers had an established bio-film originating from different environments. The bio-film history is described below.

The inoculation was done by thawing frozen carriers directly in the reactors while these were operated at continuous flow.

Tap water adapted nitrifying culture - Reactor F

The bio-film carriers originated from an inoculation with municipal waste-water from the city of Trondheim, Norway, established during a student course in Environmental Biotechnology (TBT4130) at NTNU in the spring of 2012. After this course, the carriers were stored at -20 °C for approximately 6 months prior to use in Jonassen (2012) project work during the fall of 2012. The carriers were operated with a tap-water based cultivation medium in a continuous moving bed bio-film reactor for 63 days. In the work of Jonassen (2012) about half of the carriers were subjected to a salinity toxic response test. This experiment lasted for twelve hours and the carriers were subjected to several incremental increases in salinity during that time. Following the experiment the carriers were flushed in tap water before they were pooled and stored with the rest at -20 °C. After approximately one month of storage the carriers was re-inoculated in the present experiment. The carriers thus had an established bio-film with nitrifyers originating from low salinity conditions.

A total of 200 mL of carriers were used, which gave a hydraulic filling degree of approximately 29 %.

Sea water adapted nitrifying culture - Reactor R2

The carriers used were donated by the SINTEF Sea lab in Trondheim. They originated from a recirculating aqua culture system for marine fish larvae, and had been continuously inoculated with sea water (salinity of 33 ppt) from 60 meters depth from the Trondheim Fjord. They had been operated on and off for about 1.5 years until the fall of 2012. They were then used in Jonassen (2012) experiment and were operated in a moving bed bio-film reactor with a sea water based cultivation medium for 56 days.

In Jonassen (2012) work about half of the carriers were subjected to a salinity toxic response test, and was subjected to different medium changes with a incremental reduction in salinity ranging from 33 to 0 ppm salinity (tap water). Following this experiment the bio-film carriers were flushed in sea water before they were pooled and stored with the remaining carriers at -20 °C. After approximately one month of storage the carriers were re-inoculated in the present experiment. The carriers thus had an established bio-film with nitrifyers originating from high salinity conditions.

A total of 200 mL of carriers were used, which gave a hydraulic filling degree of approximately 29 %.

Brackish water adapted culture - Reactor R1

The bio-film carriers originated from carriers previously enriched by Hjort (2010) and Kristoffersen (2004), with biomass originating from an aerated brackish lagoon (salinity of approximately 22 ppm) in Mongstad, Norway. The lagoon is used to treat waste water from the nearby Statiol oil refinery. Some raw sludge collected by Norevik (2004), also originating from Mongstad, was added to further enrich the bio-film. Both the carriers (stored since 2010) and the sludge (stored since 2004) was stored at -20 °C prior to the new inoculation in the experiment of Jonassen (2012).

2.2.4 Quantification of the nitrification activity

The nitrification activity ($mg - N/L \cdot h$) was monitored by measuring the concentration of ammonia ($N - NH_4^+$), nitrite ($N - NO_2^-$) and nitrate ($N - NO_3^-$), and the hydraulic retention time (HRT). Samples from the reactors were taken at various time intervals during the experiment: every day at the start of the experiment, and from once to twice a week towards the end. The sample volume was in the range of 3 - 5 mL. Every sample was filtered trough a Sarstedt 0.45 μm sterile syringe filter. When the cultures were operated at sea water salinity the samples were filtrated through a Dr. Lange chloride elimination syringe (LCW 925). The ammonium, nitrite and nitrate concentrations were measured with the use of Dr. Lange cuvette tests LCK 303, LCK 341 and LCK 339 respectively. The measurements were done photometrically with a Dr. Lange Lasa100 spectrophotometer.

Whenever new cultivation medium was prepared a sample was taken and the concentration of ammonium, nitrite and nitrate were measured according to the description above. The concentration measurements were only performed once, as the cultivation medium was replaced with fresh medium approximately every week. It is possible that some oxidation of the ammonium sulphate may have occurred in the period between each medium remake due to bacterial growth or oxidation. As bacterial growth was not observed in the medium containers, and these were covered in black plastic, the concentration of ammonium, nitrite and nitrate were assumed to be constant.

The hydraulic retention time (HRT) is given in Equation 2.2 and is calculated by dividing the volume of the reactor (mL) with the feed flow, Q (mL/h), of cultivation medium (The volume of the bio-film carriers were not included calculating the HRT).

$$HRT = \frac{V_{reactor}}{Q} \tag{2.2}$$

Equation 2.3 shows how the ammonium consumption rate was calculated. The measured inlet concentration of ammonia ($C_{N-NH_4^+,in}$) was subtracted from the concentration of ammonia in the effluent ($C_{N-NH_4^+,out}$) and divided by the hydraulic retention time (h).

$$Activity = \frac{C_{N-NH_4,in} - C_{NH_4,out}}{HRT} \tag{2.3}$$

Equation 2.4 shows how the rate of nitrate production rate was calculated. The concentration of nitrate in the outlet ($C_{N-NO_3,out}$) was subtracted with the concentration of nitrate in the in-fluent ($C_{N-NO_3,in}$)and divided by the hydraulic retention time (HRT).

$$Activity = \frac{C_{N-NO_3,out} - C_{N-NO_3,in}}{HRT} \tag{2.4}$$

Equation 2.5 shows the volumetric nitrogen load rate (VNLR), providing a correlation between flow, volume and the total mass of nitrogen fed to the reactor per time unit.

$$VNLR = \frac{C_{N_{tot,in}}}{HRT} \tag{2.5}$$

2.3 Nitrification capacity and salinity toxicity tests

To determine the maximum nitrification activity for each reactor before the planned change in salinity both reactors were subjected to a capacity test in order to monitor the batch nitrification kinetics. The capacity test was immediately followed by a salinity toxic response test in order to compare the nitrification rates before and after the change in salinity, and to give information on how the microbial community adapted/responded to an abrupt increase/decrease in salinity.

In these tests the reactors were run in batch mode with aeration and the pH control units attached. The amount of cultivation media used corresponded to the volume of each reactor: 700 mL for the municipal waste water culture, and 690 mL for the Trondheim Fjord culture. The cultivation media was otherwise prepared in the same manner as described in Chapter 2.2.2.

Nitrification activities were calculated by linear regression. The regressions were done with the StatPlus software (AnalystSoft, 2012). Probabilities for correlation coefficients, which is the extent to which N points, $(x_1, y_1)...(x_N, y_N)$, fit a straight line were calculated (Taylor, 1997).

The linear correlation coefficient, given in Equation 2.6, always lies in the interval $-1 \leqslant r \leqslant 1$. Values close to ± 1 indicates a good linear correlation.

$$r = \frac{\sum(x_i - \overline{x})(y_i - \overline{y})}{\sqrt{\sum(x_i - \overline{x})^2 \sum(y_i - \overline{y})^2}} \tag{2.6}$$

The probability that the variables are not linearly correlated is given in Equation 2.7, which gives a more quantitative measure of the fit. For any given value of r_o, $Prob_N(|r| \geqslant |r_o|$ is the probability that N measurements of two uncorrelated variables would give a coefficient r as large as r_o. In other words, if a correlation coefficient, r_o, is obtained for which $Prob_N(|r| \geqslant |r_o|$ is small, it is correspondingly less likely that the variables are uncorrelated. If $Prob_N(|r| \geqslant |r_o|) \leqslant 0.05$ the correlation is significant.

$$Prob_N(|r| \geq |r_o| = \frac{2\Gamma[(N-1)/2]}{\sqrt{\pi}\Gamma[(N-2)/2]} \int_{|r_o|}^{1} (1-r^2)^{(N-4)/2} dr \tag{2.7}$$

For the capacity test the content of each reactor was emptied and the bio-film carriers were flushed with fresh native medium before the experiment started. The concentration of ammonium, nitrite and nitrate were monitored at regular time intervals over a period of four hours. The concentration of ammonium, nitrite and nitrate was analysed in the same way as described in Chapter 2.2.4. The concentrations of ammonium, nitrite and nitrate were plotted versus time, and the nitrification rates were calculated by regression analysis.

For the salinity toxicity test the content of each reactor was emptied and the bio-film carriers were flushed with fresh medium before the experiment started. The 0 ppt salinity adapted culture was flushed with the sea water based medium (33 ppt salinity), and the 33 ppt salinity adapted culture was flushed with the tap water based medium (0 ppt salinity). The nitrification activities were monitored at regular time intervals over a period of 24 hours for the culture originating from municipal waste water, and over a period of 13 hours for the culture originating from the Trondheim Fjord. Concentrations of ammonium, nitrite and nitrate was analysed in the same way as described in Chapter 2.2.4. The concentrations of ammonium, nitrite and nitrate were plotted versus time, and the nitrification rates were calculated by regression analysis.

2.4 Characterization of microbial community composition

In order to characterize and describe the changes within and between the two microbial communities different molecular and computational techniques were applied. These were DNA extraction from the different cultures, polymerase chain reaction (PCR) for amplification of parts of the 16S rRNA gene of the extracted DNA, denaturing gradient gel electrophoresis (DGGE) for separation of the PCR products and to produce community fingerprints, and computational and statistical analysis to calculate similarities between groups and individual samples. Only bacterial primers were used. Assay for sampling, DNA extraction, PCR and DGGE is described in Chapters 2.4.1 throughout 2.4.4. Computational analysis of the DGGE gels and statistical interpretation of the data is covered in Section 2.5

2.4.1 DNA sampling

DNA were sampled at regular time intervals during operation of the nitrifying reactors. Samples from both reactors were taken at three regular occasions before the change in salinity, and at nine regular occasions after the change in salinity. Bio-film coated carriers were collected with a sterile pair of tweezers and flushed in milliQ water before they were cut into two pieces and rapidly cooled down in liquid nitrogen. The samples

were then stored at −80 °C until DNA extraction (Chapter 2.4.2). The DNA samples of Jonassen (2012) experimental work was available for use in this experiment and had been stored at −20 °C for approximately three months prior to DNA extraction.

Details regarding sampling days is depicted in the time-lines in Figure 2.3, 2.4 and 2.5. which graphically summarizes the points of sampling during continuous operation.

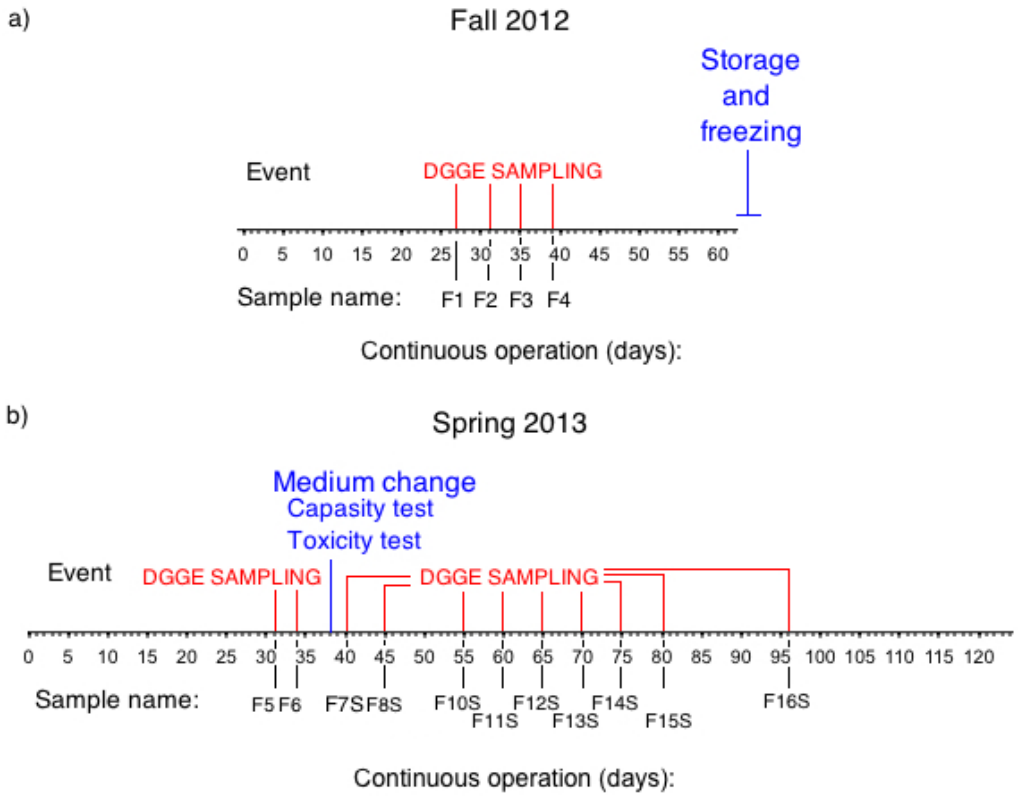

Figure 2.3: Time-lines showing days of continuous operation of reactor F. **a)** DNA sampling days after initiation of continuous operation of Reactor F with biomass adapted to 0 ppm. salinity during the experiment of Jonassen (2012). The reactor was operated with a tap water based culture medium. DNA samples were taken at four day intervals on day 27, 31, 35 and 39 of continuous operation and were available for use in the present experiment. **b)** Two DNA samples were taken at three day intervals at day 31 and 34 before the batch capacity- and saline toxicity tests performed at day 37/38. The tests were followed by a change in cultivation medium on day 38: from a tap water based cultivation medium to a 33 ppt saline sea water based culture medium. During continuous operation DNA were sampled every fifth day from day 45 and until day 80, with a gap at day 50. Due to changes in nitrification activity (Section 3.1) additional DNA were sampled at day 96.

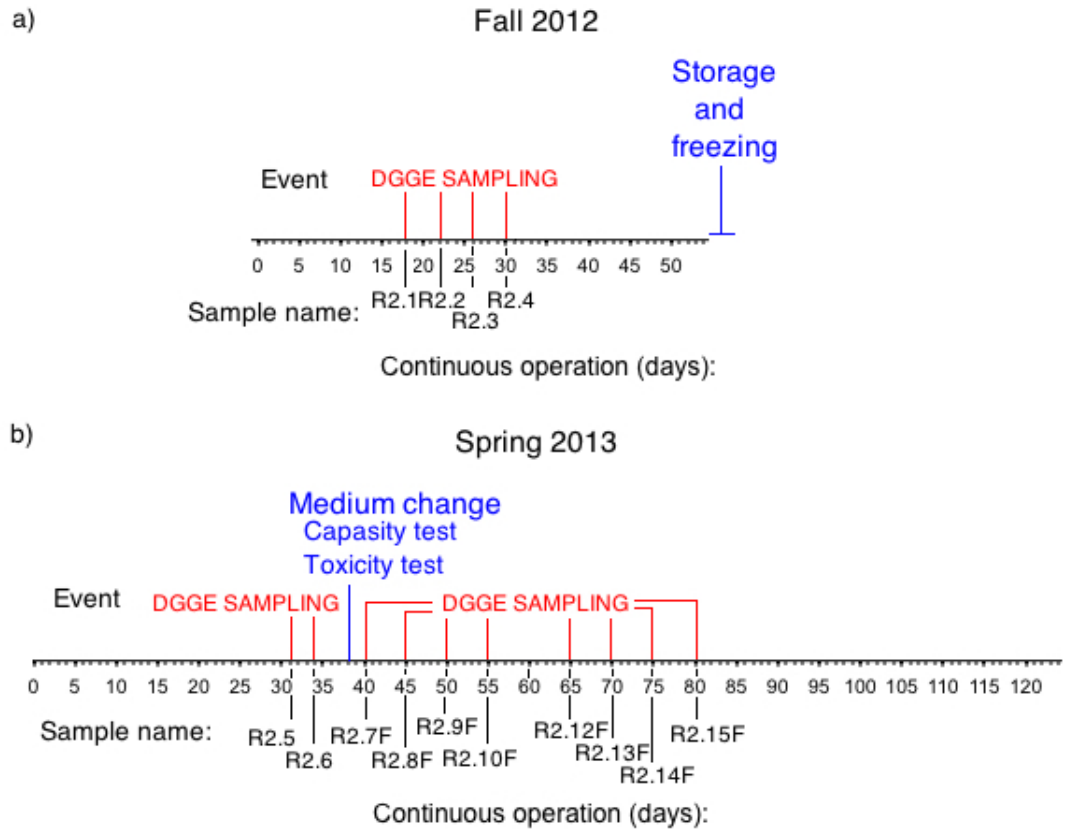

Figure 2.4: Time-lines showing days of continuous operation of Reactor R2. **a)** DNA sampling days after initiation of continuous operation of Reactor R2 with biomass adapted to 33 ppt salinity during the experiment of Jonassen (2012). DNA samples were taken at four day intervals on day 18, 22, 26 and 30 of continuous operation were available for use in the present experiment. **b)** Two DNA samples were taken at three day intervals at day 31 and 34 before the batch capacity- and saline toxicity tests performed at day 37/38. The tests were followed by a change in cultivation medium on day 38: from a 33 ppt salinity based cultivation medium to a 0 ppt salinity based culture medium. During continuous operation DNA were sampled every fifth day from day 40 and until day 80, with a gap at day 60.

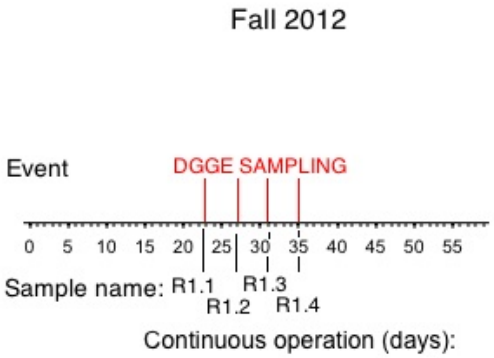

Figure 2.5: Time-line showing days of continuous operation of Reactor R1 with biomass originating from an aerated brackish lagoon at the Mongstad Oil Refinery during the experiment of Jonassen (2012). The reactor was operated with a 22 ppt salinity cultivation medium. DNA were sampled at four day intervals on day 23, 27, 31 and 35 of continuous operation and were used in this experiment.

2.4.2 DNA extraction

DNA extraction from the sampled carriers were performed using the *DNeasy*® Blood and Tissue DNA extraction kit. The extraction comprises of two phases; lysis of the bacterial cells, and elution of the DNA. The protocol used was a modified version of the *DNeasy*® Blood and Tissue handbook protocol for gram-negative bacteria, and is described below.

Each carrier was cut into small fragments with a sterile scalpel and added to 1.5 mL Eppendorf tubes. 180 μL of enzymatic lysis buffer containing 20 mg/mL lysozyme was added to each sample. The samples were then incubated for one hour at 37 °C. 40 μL proteinase K and 180 μL ATL buffer was added and each sample was vortexed and incubated at 55°C for two hours. After the incubation 200 μL AL buffer was added and each sample was incubated at 70 °C for ten minutes followed by addition of 300 μL 96% ethanol. The Eppendorf tubes were vortexed and the liquid was transferred to a DNeasy mini spin columns which were placed in a 2 mL tube and sentrifuged at 8000 rpm for one minute. The filtrate was discharged and 500 μL AW 1 buffer was added. The samples was centrifuged at 8000 rpm, and once again the filtrate was discharged. 500 μL of AW 2 buffer was added and each sample was centrifuged at 15000 rpm for three minutes and the filtrate was discharged. The DNA was eluted in two subsequent steps by adding 50 μL of DNA free water directly on the membrane in the DNeasy column and centrifuging each sample for one minute at 8000 rpm. This gave a total of 100 μL extract.

A *NanoDrop*® ND-1000 spectrophotometer was used to quantify the concentration and purity of the extracted DNA samples.

2.4.3 Polymerase Chain Reaction

The DNA extracts were subjected to DNA amplification by the use of the Polymerase Chain Reaction (PCR). The PCR apparatus used was a Arktik Thermal Cycler (Thermo Scientific) with lid heating to prevent evaporation. Samples with a DNA concentration higher than 10 $ng/\mu L$ were diluted to approximately 10 $ng/\mu L$ before adding the appropriate volume of DNA template to the PCR reaction mix.

A universal primer pair targeting the variable 3 region of the bacterial 16S rRNA gene, 338f-GC (5‘- CGCCCGCCGCGCGCGGCGGGCGGGGCGGGGGCACGGGGGG actcctacgggaggcagcag -3‘) and a 518r (5‘-attaccgcggctgctgg-3‘), commonly used in characterisation of microbial communities were used (Bakke et al., 2011). With this primer pair a sequence of approximately 240 base pairs should be amplified. The forward primer was added a 40 bp GC-clamp in order to add a GC-clamp to the amplified DNA fragments before the denaturing gradient gel electrophoresis (DGGE) described in Sub-chapter 2.3.4.

Chemicals needed to perform the PCR reaction are given in Table 2.4. For simplicity a master mix was first prepared by multiplying all volumes of the PCR components by the total number of samples. From this mix a total 24 μL were added to each of the PCR tubes. Then 1 μL of extracted DNA was added to each PCR tube and all the samples were placed in the PCR thermal cycler.

Table 2.4: PCR reagents including amount used and final concentration for $25\mu L$ reactions.

Component	Amount	Final concentration
10X reaction buffer	2.5 μL	1X
dNTP (10mM)	0.5 μL	200 μM
$MgCl_2$(25 mM)	2 μL	2.0 mM [a]
BSA (10 mg/mL)	0.75 μL	-
Primer 338F-GC (10 μM)	0.75 μL	0.3 μM
Primer 518R (10 μM)	0.75 μL	0.3 μM
Taq DNA polymerase	0.125 μL	-
mqWater	18.125 μL	-
DNA template	1 μL	-

[a] Together with $MgCl_2$ in 10X buffer the final concentration is 2 mM.

Bovine serum albumin (BSA) was supplied from New England Biolabs. $MgCl_2$ and the Taq DNA polymerase was supplied from QIAGEN, and the dNTP and 10X reaction buffer were supplied from VWR.

Table 2.5 shows the cycling conditions used in the PCR reaction. The denaturation, annealing and elongation steps were run for 35 cycles.

Table 2.5: PCR temperature regime.

Step	*Temperature* °C	Time	Cycles
Initial denaturation	95	4 min	1
Denaturation	95	30 sec	
Annealing	53	60 sec	35
Elongation	72	90 sec	
Final elongation	72	30 min	1
Idle	10	infinite	1

To verify the presence of the desired DNA fragments agarose gel electrophoresis was done in an Owl EasyCast Mini Gel System (Thermo Scientific). A 1 % agarose gel was prepared in 1X TAE buffer. The agarose was supplied by $SeaKem^{®}$ LE agarose (Lonza), and the TAE buffer comprised of 5.04 g tris-base, 2 mL 0.5 M EDTA and 1.14 mL of glacial acetic acid per litre. The mixture was heated to reflux and then slowly cooled to 65 °C. 20 μL of $GelRed^{TM}$ Nucleic Acid Gel Stain (QIAGEN) was added to the agarose/TAE-buffer mixture.

5 μL of the PCR product and 1 μL 6X DNA loading dye (Fermentas) was added to each well in the agarose gel. A $GeneRuler^{TM}$ 1 kb Plus DNA ladder (Fermentas) was used to verify the correct sizes of the fragments. The gel was run at 100 V for approximately 75 minutes and transferred to a G:BOX UV visualizer (Syngene). Photos were taken using the associating GeneSnap software.

2.4.4 Denaturing gradient gel electrophoresis

The PCR samples were separated based on the melting characteristics of the DNA through an acrylamide gel in the process of denaturing gradient gel electrophoresis (DGGE). The electrophoresis was conducted with a INGEN PhorU system with self casted 8 % acrylamide gels with different denaturing gradients run at 60 °C. A standard sample, comprising of PCR products from pure cultures of nine different bacterial strains amplified with the 338f-GC and 318r primer, was applied to the gel as a reference. The DGGE gels were stained with SYBR Gold (Life Technologies). During the staining reaction the gel was incubated in darkness for one hour. The gels were then rinsed with mQ-water and transferred to a G:BOX UV visualizer (Syngene). Photos were taken using the associating GeneSnap software. For details see Appendix E.

Two different DGGE runs were performed. In the first run the 12 DNA samples from the three cultures operated by Jonassen (2012) were applied (Figure 2.3.a, 2.4.a and 2.5). The electrophoresis was conducted with a 30 - 50 % denaturing gradient and the gel was run at 100 V in 0.5 X TAE buffer for approximately 18 hours. An overview of the samples analysed on this gel is given in Figure 2.6. The corresponding sampling

times during continuous operation of the three reactors from Jonassen (2012) project work is presented in Chapter 2.4.1.

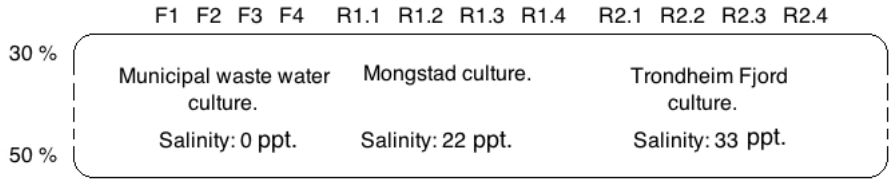

Figure 2.6: Sketch of DGGE gel with DNA samples from Jonassen (2012). Samples marked F.X, R1.X and R2.X corresponds to DNA samples taken from the municipal waste water culture, the Mongstad culture and the Trondheim Fjord culture, respectively.

The second gel was run with a 35 - 50 % denaturing gradient at 100 V in 0.5 X TAE buffer for approximately 20 hours. Only DNA samples from the municipal waste water culture and the Trondheim Fjord culture were applied to the gel. Four DNA samples from the project work of Jonassen (2012) were also applied to this gel. These were: two samples from the continuous operation of Reactor F with a tap water based cultivation medium, and two samples from the continuous operation of Reactor R2 with a sea water based culture medium (Figure 2.3.b and 2.4.b.). An overview of the samples analysed on this gel is given in Figure 2.7. The corresponding sampling times during continuous operation of the three reactors from Jonassen (2012) project work is presented in Chapter 2.4.1.

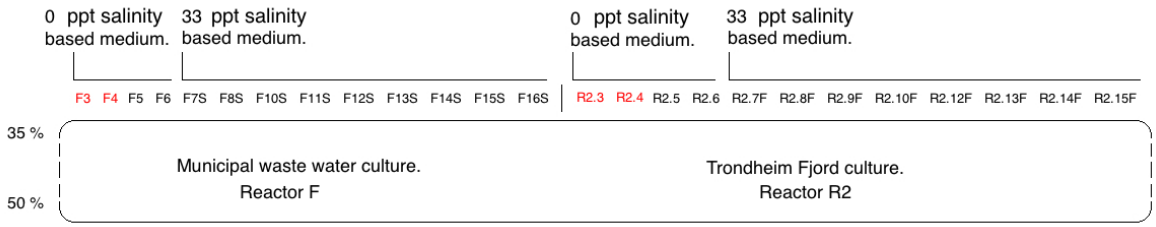

Figure 2.7: Sketch of DGGE gel with DNA samples from the municipal waste water culture and the Trondheim Fjord culture. Samples marked F correspond to samples from the municipal waste water culture, and samples marked R2 correspond to samples from the Trondheim Fjord culture. Red samples are DNA extracts from the project work of Jonassen (2012).

2.5 DGGE analysis and statistics

2.5.1 DGGE anlysis

Pictures of the DGGE gels were analyzed with the use of the computer software tool Gel2k developed by Norland (2004), University of Bergen. Gel2k reads the band profiles and converts these to histograms where the peaks corresponds to bands in the DGGE gel and the area under each peak corresponds to the intensity of the bands. From the histogram a peak area matrix was generated thus generating a numerical fingerprint of the communities. The peak area matrix were normalized by dividing each peak area with the total peak area of each lane, giving a fractional peak area matrix. From the fractional peak area matrix band richness (k) and Shannon diversity index (H') were calculated.

The band richness is simply the number of bands in each lane in the DGGE gel. It was assumed that one band corresponds to a single species and the total number of bands thus reflects the richness of the bacterial community. According to Tuomisto (2010) species richness is related to species diversity, but they are not the same thing. Species richness does not take the abundances into account and is therefore the actual, opposed to the effective, number of species. The Shannon diversity index, which account for both abundance and number of species (Hill et al. (2003), Tuomisto (2010)), were calculated (Equation 2.8).

$$H' = -\sum_{i=1}^{S} p_i ln(p_i) \tag{2.8}$$

p_i is the relative abundance of species i and S is the number of species.

In analysing the DGGE gel the the band richness (k) corresponds to the number of species (S) present in a sample and the peak area corresponds to the relative abundance (p_i). Defined by Equation 2.8 a H' value of zero means that the sample contains one species. Further, H' will reach maximum if the species are distributed evenly throughout the DGGE gel. If one or more species dominates, the resulting Shannon diversity index will be lower. Similar peak area values generated from the band analysis in Gel2k would indicate an even distribution of species present in the sample, whereas dissimilar values would indicate the opposite.

Evenness is a measure range from 0 to 1. The evenness value is maximized when the individuals are equally partitioned among the represented species. Buzas and Gibson evenness measure shown in Equation 2.9 was calculated (Buzas and Gibson, 1969).

$$Evenness = \frac{e^{H'}}{S} \tag{2.9}$$

were H' is the Shannon diversity index and S is the number of species.

An evenness value of 1 means the individuals are uniformly spread across the species present in the sample. A low evenness means that some of the species are over-represented.

2.5.2 Statistical analyses

To visualize the dynamics of the different nitrifying microbial communities non metric multidimensional scaling plots (NMMDS) were generated with the PAST software package (Hammer et al., 2001). The plots were based on Bray-Curtis distance matrices generated from square root transformed fractional peak areas generated from the DGGE analysis (See section 2.5.1). The Bray-Curtis values span from 0 to 1, were 1 corresponds to equal samples. A square root transformation was used in order to down weight particular strong bands in the peak area matrix.

NMMDS is an ordination method based on distances for exploring similarities and/or dissimilarities between objects in a dataset. Similar objects are grouped together and the distance between the objects is related to the similarity between them. In other words, the distance between two points in the plot increases as a function of inequality between the community in the two samples.

Together with the NMMDS plot a stress value (goodness of fit) was assigned. An accurate ordination will give a stress value of zero. An ordination with a stress value below 0.2 is regarded to be sufficient for an accurate ordination.

To test the significant differences between points and groups in the NMMDS plot a non parametric one-way analysis of similarity (one-way ANOSIM) based on Bray-Curtis similarity measures was performed. The p-values were generated based on sequential Bonferoni significance to counteract the problem of multiple comparisons. The one-way ANOSIM test checks whether there are significant differences between groups or points. The H_0 hypothesis states that there is no difference between the groups. While the H_1 hypothesis states that there is a significant difference between the groups or points. If p < 0.05 the H_0 hypothesis was rejected.

In order to assess which bands from the DGGE gel that contributed the most to the observed differences a similarity percentage (SIMPER) was calculated. SIMPER is a simple method for assessing which taxa are primarily responsible for an observed difference between groups of samples under the assumption of independent samples (Clarke, 1993).

Chapter 3

Results

The results are divided into three main chapters. In section 3.1 the operation of the nitrifying reactors is presented. This section also includes a brief summary of the results from previous operation of the reactors (Jonassen, 2012). The results from the capacity- and saline toxic response tests are presented in Chapter 3.2 followed by the results from the DGGE- and statistical analysis related to microbial community dynamics in Section 3.3.

3.1 Operation of the nitrifying reactors

The two reactors with biomass adapted to 0 ppt and 33 ppt salinity water were named F and R2, respectively. All relevant raw-data concerning measured values (inlet/outlet concentrations of ammonium, nitrite, nitrate, pH, dissolved oxygen and temperature) and calculated values (nitrifying activity, HRT, and VNLR) for reactor F and R2 are documented in Appendices A, B and C, respectively.

3.1.1 Operation of adapted and non-adapted cultures in previous experiments

In the previous experiment performed by Jonassen (2012) three nitrifying cultures adapted to different salinities (Chapter 2.2.3) were continuously operated at those salinities in moving bed bio film reactors. When sampled for DGGE (Figure 2.3 - 2.5), the reactors F, R1 and R2 were operated with a hydraulic retention time (HRT) of 24, 13.6 and 12.1 h, respectively. The non-adapted culture (F) showed complete nitrification in the period of sampling, and also throughout the operational period. For the adapted cultures (R1 and R2) the nitrification performance was not stable: the nitrite concentration on the days of sampling were 17.0, 21.1, 16.1 and 4.00 $mg - N/L$ for the 22 ppt adapted culture, and 5.00, 2.00, 1.37 and 0.75 $mg - N/L$ for the 33 ppt adapted culture. Two weeks after the last sampling day of the 22 ppt salinity adapted culture the reactor was performing consistently, and showed complete oxidation of ammonium to nitrate. The culture showed good performance for the rest of the operational period. The 33

ppt reactor was operating consistently from approximately the last day of sampling and throughout the experimental period (Operational data regarding reactor performance, concentration and activity measurements are shown in previous work (Jonassen, 2012)).

3.1.2 The municipal waste water culture

The nitrifying culture adapted to 0 ppt salinity in reactor F was monitored for a total of 122 days. The bio-film carriers of Jonassen (2012) was thawed, and continuous operation at 0 ppt salinity was initiated immediately after. At day 37/38 a capacity and a saline toxicity test were performed. (Se section 3.2) The batch saline toxic response test were run at sea water salinity, and continuous operation with 33 ppt salinity based medium was initiated after the completion of this test.

The average pH, temperature and dissolved oxygen concentration throughout the operational period was 7.6 $\pm$ 0.2, 24.8 $\pm$ 0.7 $^{\circ}C$ and 7.3 $\pm$ 0.6 mgO_2/L, respectively.

Figure 3.1 shows the total amount of nitrogen ($mg - N/L$) fed to the reactor during the operational period along with the effluent concentrations of ammonium, nitrite and nitrate ($mg - N/L$) and the volumetric flow of cultivation medium in the in-fluent.

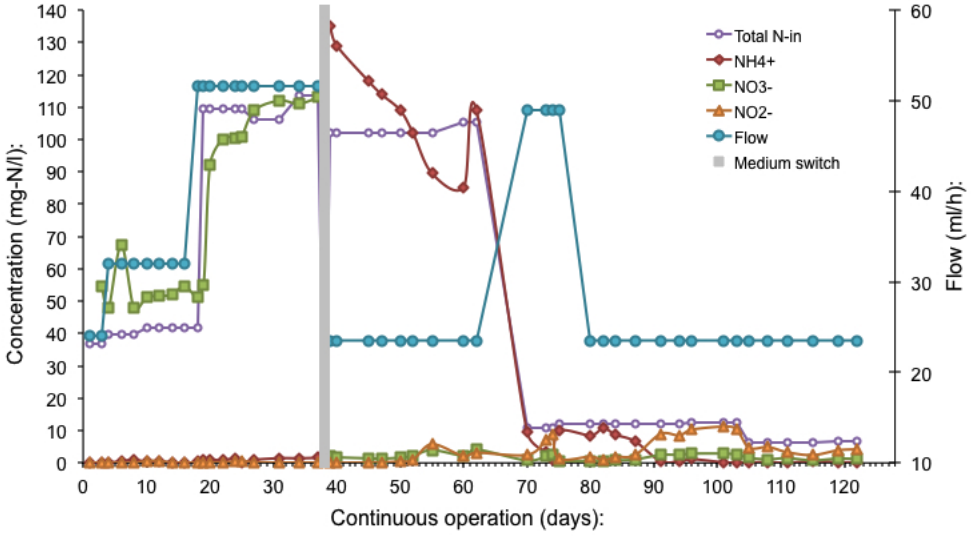

Figure 3.1: Concentration of effluent ammonium, nitrite and nitrate ($mg - N/L$) for Reactor F together with in-fluent volumetric flow (mL/h) and total mass of in-fluent nitrogen ($mg - N/L$) as a function of time. The grey bar corresponds to a change in cultivation medium from a tap-water based medium to a sea water based medium.

Effluent concentration at native salinity

Before the change in cultivation medium salinity the flow was regulated at three occasions. During the three first days of continuous operation the flow was kept low in order

to not wash out bacteria from the reactor. The flow was kept at 24 mL/h, corresponding to a hydraulic retention time (HRT) of 29.2 hours, and the concentration of ammonia in the medium was kept low (36.8 $mg - N/L$). This was done as the thawing of the bio-film carriers could result in pieces of it breaking of and thereby being washed out of the reactor. Moreover, if activity was immediately restored, the ammonium oxidizing bacteria (AOB) would be ammonia limited at an early stage, giving time for the slower growing nitrite oxidizing bacteria (NOB) to get a stronger foothold in the bio-film. There were little or no observed biomass in the settlers, and the concentration of ammonia and nitrite was measured to be 0 and 0.080 $mg - N/L$ on day 3, respectively. This indicated complete conversion of ammonia to nitrate and full nitrification. Between day 4 and 16 the flow was increased to 32 mL/h, giving a HRT of approximately 22 hours. The concentrations indicated full nitrification during that time period. The flow was adjusted to 51.6 mL/h on day 16, giving a HRT of 13.6 h, and the amount of ammonium in the cultivation medium was increased to an average of $109.0 \pm 2.5 mg - N/L$ from day 17 and until day 37. The community seemed to respond well to this increase, showing complete conversion of ammonia to nitrate in that time period.

The average ammonium effluent concentration during continuous operation with the tap-water based cultivation medium was 0.7 ± 0.6 $mg - N/L$, indicating that the 0 ppt salinity adapted culture were ammonium limited in this time period.

Effluent concentration after switch to sea water salinity

After the batch capacity and saline toxic response tests were performed the in-fluent flow was regulated to 24 mL/h, giving a HRT of 29.2 hours. This was done as the 0 ppt adapted municipal waste water culture did not show any signs of nitrifying activity during the batch salinity toxic response test (results presented in Chapter 3.2), and as nitrifying bacteria are slow growers (Henze et al. (1987), Sedlak (1991) and Jimenez et al. (2011)) a high retention time would limit the amount of bacteria being washed out of the reactor.

The concentration of ammonia inside the reactor was 135 $mg - N/L$ when continuous operation was initiated after the batch salinity toxicity test (Chapter 3.2). Figure 3.1 shows a gradual decrease in the concentration of ammonium in the effluent towards the in-fluent concentration from day 39 to day 54, indicating steady state at this point. The next sampling point at day 55 showed a 12 % reduction of the effluent ammonia concentration compared with the in-fluent. The concentration of nitrite and nitrate were 5.8 and 4.0 $mg - N/L$, thus indicating both AOB and NOB activity.

At day 60 a problem with the pH regulation system occurred. The sodium hydroxide container was empty, and the pH in the reactor was 8.60 when the error was discovered. Concentration measurements performed the same day still showed nitrifying activity, but the total nitrogen balance did not add up with a deviation of 15.8 $mg - N/L$ (See N-balance documented in Appendix A). No conversion of ammonia was observed after the concentration measurements performed on day 62 of continuous operation. Due to a period of high pH and a high concentration of ammonia inside the reactor it is possible that the concentration of free ammonia inhibited the nitrifyers. Free ammonia ranged

from 3.3 ± 1.2 mg-N/L from day 40 - 62 according to Equation 1.4 (Chapter 1.2). The flow of cultivation medium was regulated up to 49 mL/h, giving an HRT of 14.1 hours, and the concentration of ammonia in the cultivation medium was changed down to 10.7 $mg - N/L$, thus reducing the loading rate of ammonia with approximately 80 %.

The concentration of ammonium in the effluent decreased from 9.8 to 1.1 $mg - N/L$ between day 70 and 74. Another pH incident occurred between day 74 and 75 - where the pH electrode responded dramatically to minor additions of acid or base. The pH electrode was replaced after this incident. Concentration measurements performed on day 75 did not show any signs of nitrifying activity, so the flow was again reduced to 24 mL/h, (giving a HRT of 29.2 hours) to utterly reduce the loading rate in order for the community to recover. This flow rate was kept throughout the rest of the experiment.

Figure 3.2 shows the concentration development during continuous operation of Reactor F with a sea water based cultivation medium. The time line shown starts from day 75 of continuous operation to better visualize the development.

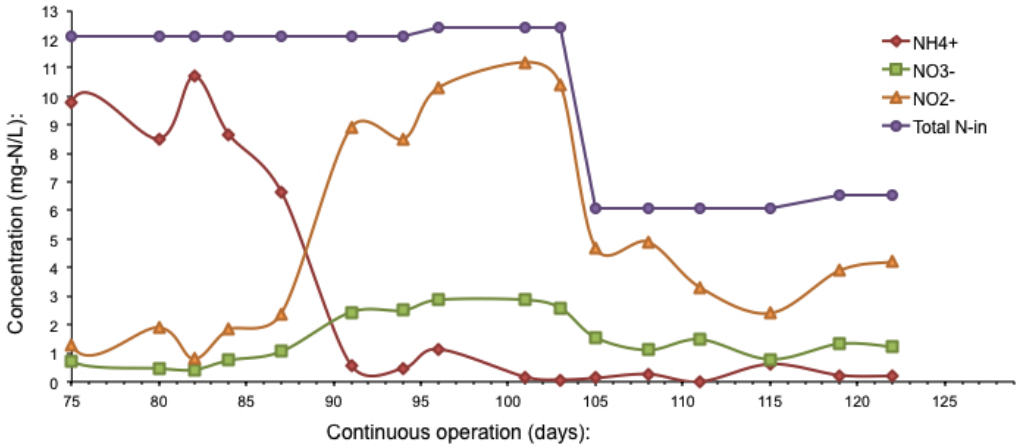

Figure 3.2: Concentration measurements of effluent ammonium, nitrite and nitrate ($mg - N/L$) for Reactor F zoomed in from day 75 of continuous operation. The in-fluent volumetric flow (mL/h) and total in-fluent nitrogen ($mg - N/L$) is also shown. The values are plotted against time of continuous operation.

The ammonium concentration slowly decreased down to 0.58 $mg - N/L$ from day 75 towards day 91 of continuous operation, indicating AOB activity. Between day 91 and 103 the average ammonium effluent concentration was measured to be 0.6 ± 0.4 $mg - N/L$. The average nitrite and nitrate concentrations were 9.7 ± 1.3 $mg - N/L$ and 2.7 ± 0.2 $mg - N/L$. A high nitrite concentration can potentially inhibit the AOBs (Anthonisen et al., 1976), so the in-fluent concentration of ammonium was decreased, in order to minimize this effect, to 5.6 $mg - N/L$ on day 104. From day 105 and toward the end of the experiment the ammonium concentration in the reactor was low and the AOBs was thought to be ammonium limited from day 91 and onwards. The NOB did

not seem to recover from the salinity change and the two pH regulation incidents.

Figure 3.3 shows the ammonium consumption and nitrate formation rates ($mg-N/L\cdot h$) during continuous operation of Reactor F. The volumetric nitrogen loading rate (VNLR) given as $mg-N/L\cdot h$ is also shown.

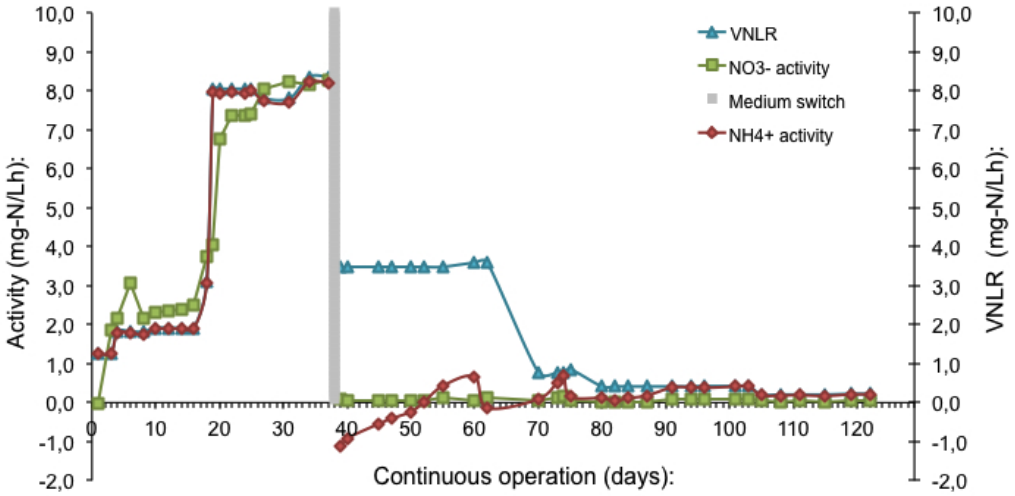

Figure 3.3: Ammonium consumption- and nitrate formation rates ($mg-N/L\cdot h$) during continuous operation of reactor F, and the volumetric nitrogen loading rate (VNLR) ($mg-N/L\cdot h$). The grey bar corresponds to a change in cultivation medium from a tap-water based medium to a sea water based medium. The values are plotted against time of continuous operation.

Nitrification rates at native salinity

The volumetric nitrogen loading rate were gradually increased by increasing the concentration of ammonium and up-regulating flow up to the point of the batch- capacity and saline toxic response test. Calculations showed an ammonium removal rate of 8.21 $mg-N/L\cdot h$ and a nitrate production rate of 8.29 $mg-N/L\cdot h$ at day 37. The VNLR was at this time 8.31 $mg-N/L\cdot h$, indicating complete nitrification. Similar nitrifying activity rates were calculated the last two weeks before the switch in salinity. This indicated a stable and consistent performance in the time before the batch tests and the medium change.

Nitrification rates after switch to sea water salinity

The calculated ammonium consumption rate was negative from day 39 until day 50 of continuous operation with a sea water based medium. A transient due to a change in VNLR and possible cell lysis (see Chapter 3.2) are possible explanations for the negative activity calculations. In the same time period the nitrate production rates was close to

zero. During the proceeding days modest ammonium consumption rates were observed, calculated to be 0.67 $mg - N/L \cdot h$ 27 days after the switch (day 60). The first pH shock on day 60 led to a loss of nitrifying activity, and the loading rate was reduced to give the community time to recover. The ammonium consumption activity slowly rose until the second pH shock, on day 74/75 of continuous operation, which led to a second reset of the ammonium consumption rate. Figure 3.4 shows a close up of the ammonium consumption- and nitrate forming activity rates.

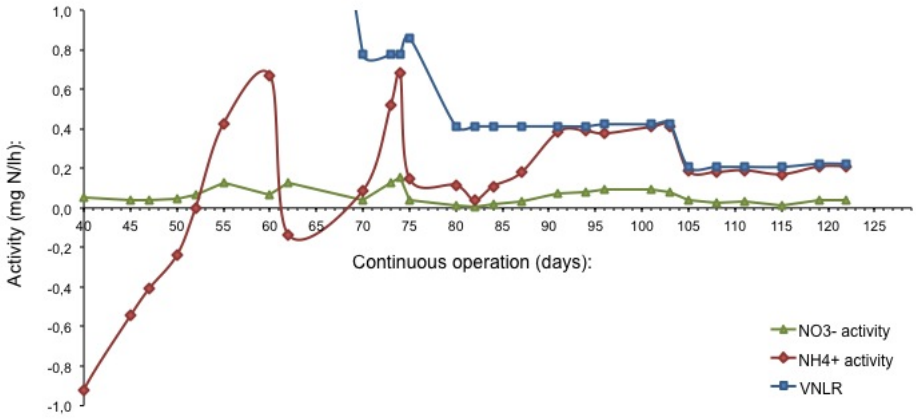

Figure 3.4: Ammonium consuption- and nitrate formation rates, and volumetric nitrogen loading rate ($mg - N/L \cdot h$) against time of continuous operation of reactor F.

The VNLR was reduced to 0.4 $mg - N/L \cdot h$ on day 75 to allow the community to recover from the second pH shock. The ammonium consumption rate slowly increased, and from day 54 to day 64 after the salinity switch (day 91 to 103 of continuous operation) 96 $\pm$ 3 % of the ammonia in the in-fluent was converted. The nitrate formation rates were low in the same period. This led to accumulation of nitrite, and the VNLR was utterly decreased to avoid nitrite inhibition. Towards the end of continuous operation the community showed full consumption of ammonia with consumption rates averaging of 0.20 $\pm$ 0.01 $mg - N/L \cdot h$ from day 66 to 86 after the switch (day 105 to day 123 of continuous operation). The nitrate forming rates were calculated to be 0.05 $\pm$ 0.05 $mg - N/L \cdot h$ in the same time period.

3.1.3 The Trondheim Fjord culture

The culture adapted to 33 ppt salinity was monitored in reactor R2 for a total of 127 days. The bio film carriers of Jonassen (2012) was thawed, and continuous operation at 33 ppt salinity was initiated. The capacity- and saline toxicity test (Chapter 3.2) were followed by a switch in medium, to 0 ppt salinity, on day 38 of continuous operation. The average pH, temperature and dissolved oxygen concentration throughout the experiment was 7.6 ± 0.2, 24.9 ± 0.6°C and 7.5 ± 0.6 $mg - O_2/L$, respectively.

Effluent concentrations at native salinity

Figure 3.5 shows the concentration of effluent ammonium, nitrate and nitrite ($mg - N/L$) in the experimental period. The total concentration of in-fluent nitrogen in the cultivation medium ($Total - N_{in}$) is showed ($mg - N/L$). The grey bar corresponds to the change in cultivation medium salinity.

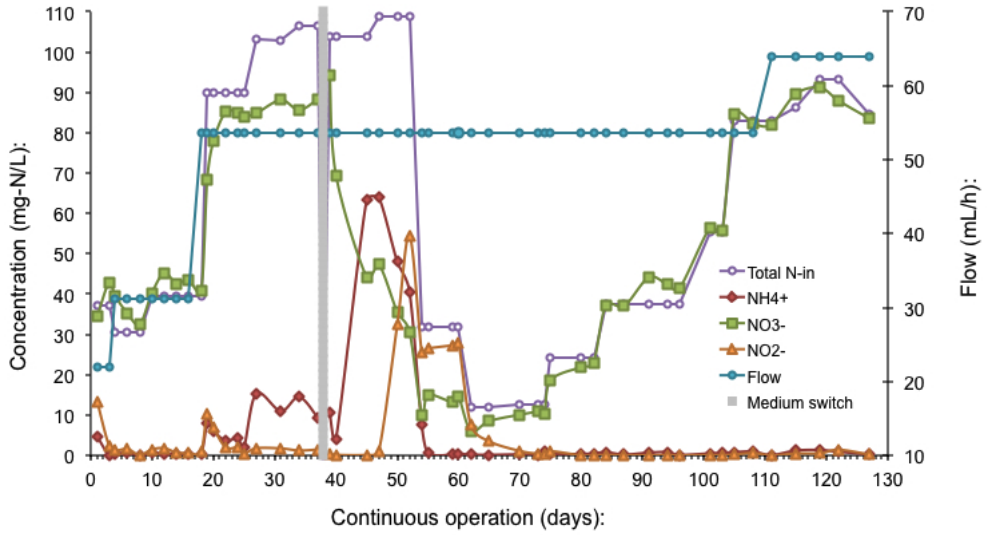

Figure 3.5: Concentration of effluent ammonium, nitrite and nitrate ($mg - N/L$) for Reactor R2 together with in-fluent volumetric flow (mL/h) and total mass of in-fluent nitrogen ($mg - N/L$) as a function of time. The grey bar marks the change in salinity from 33 ppt to 0 ppt salinity.

During continuous operation of Reactor R2 with native saline conditions operational settings such as the volumetric in-fluent flow of medium, and the in-fluent concentration of ammonium was kept almost the same as in Reactor F (Chapter 3.1.2). This was done as the 33 ppt salinity adapted culture showed close to full conversion of ammonia to nitrate during the first 18 days of continuous operation. Some accumulation of nitrite was observed on day 19, when a nitrite concentration of 10.2 $mg - N/L$ was observed. This was probably a transient effect due to the increase in flow and the amount of

ammonium in the in-fluent. The effluent concentration of nitrite was gradually reduced down to 0.43 $mg - N/L$ at day 25, and averaged at 1.33 $\pm$ 0.55 $mg - N/L$ the last 12 days before the medium change.

At day 19 ammonium effluent levels rose from 0.48 to 7.8 $mg - N/L$ as a response to the elevated flow. At day 25 the concentration was measured to be 2.1 $mg - N/L$. A further increase in in-fluent ammonium concentration on day 25 resulted in a further increase, and the ammonium levels averaged 12.6 $\pm$ 1.8$mg - N/L$ towards the point of the change in medium salinity. Complete conversion of ammonium was therefore not achieved before the change in medium salinity.

Effluent concentration after switch to tap-water salinity

Following the batch capacity and saline toxicity test (Chapter 3.2) the sea water based medium was replaced with a tap-water based, low salinity, medium. The effluent concentration of ammonium was at this point (day 39) 10.7 $mg - N/L$. The effluent concentration of ammonium was measured to be 63.3 $mg - N/L$ 8 days after the switch (day 45), before it levelled out and quickly dropped down to 0.65 $mg - N/L$ 18 days after the switch (day 55). The concentration of ammonia was low during the rest of the experiment and averaged 0.55 $\pm$ 0.36 $mg - N/L$ from day 18 to 90 after the switch in salinity (day 55 and onwards). This indicated ammonium limitation throughout this time period.

A period of nitrate accumulation was observed between day 13 and onwards to day 25 after the salinity switch (day 50 to 62 of continuous operation), which peaked at 54.5 $mg - N/L$ on day 15 (day 52) of continuous operation after the medium switch. It seemed like the AOBs adapted more quickly to the change in salinity, and, as the NOBs had a somewhat longer lag time, this resulted in this dramatic increase in effluent nitrate. As a counter measure the amount of ammonia in the in-fluent was reduced with 71 %, from 108 to 31.6 $mg - N/L$, in order to avoid nitrite inhibition. When nitrite levels were sufficiently low an incremental increase in in-fluent ammonium concentration was initiated. This was done to give the NOBs time to gradually adjust to the increased substrate loading. Accumulation of nitrite was not observed onwards of day 33 after the salinity change (day 70).

Flow was adjusted to 64 mL/h (HRT of 11 h.) on day 111 and the concentration of in-fluent ammonium was increased to 92.9 on day 119. Almost complete conversion of ammonium to nitrate was observed after the flow adjustment and increase in ammonium loading.

Figure 3.6 shows the ammonium consumption and nitrate formation activity rates ($mg - N/L \cdot h$) during continuous operation of Reactor R2 together with the volumetric nitrogen loading rate (VNLR) ($mg - N/L \cdot h$).

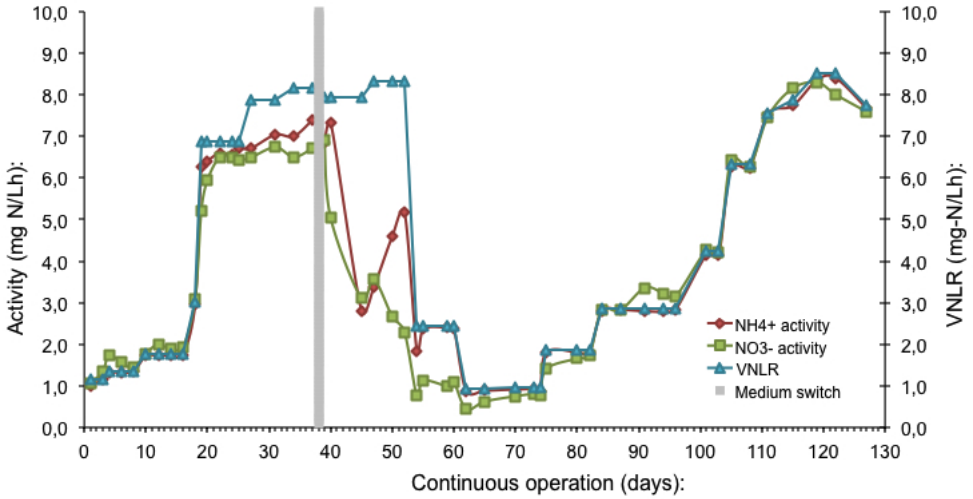

Figure 3.6: Nitrification activity ($mg - N/L \cdot h$ ammonium consumed and nitrate produced) and volumetric nitrogen loading rate ($mg - N/L \cdot h$) plotted against time of continuous operation of reactor R2.

Nitrification rates at native salinity

Operating the 33 ppt salinity adapted culture at native salinity the observations from day zero and until day 25 showed that the ammonium consumption- and nitrate forming rates almost coincided with the volumetric nitrogen loading rate (VNLR) - indicating ammonium limitation and full nitrification. The increase in VNLR up to 7.9 $mg - N/L \cdot h$ from day 27 and until the change in medium salinity did not result in instantly coinciding activity rates, but the ammonium removal- and nitrate formation rates seemed to increase as a response to the raised VNLR towards the change in salinity. Before the change in salinity an ammonium removal rate of 7.4 $mg - N/L \cdot h$ was achieved and the nitrate formation rate was 6.7 $mg - N/L \cdot h$.

Nitrification rates after switch to tap water salinity

The VNLR was kept at approximately the same levels as before the salinity change for the the first 13 days with tap-water saline conditions. A dramatic decrease in the nitrate forming rate, and consequently a big increase in the concentration of nitrite, led to a two step reduction in VNLR. When the nitrate forming rate was close to the ammonium consumption rate and the VNLR, the VNLR was increased in incremental steps from 1.0 $mg - N/L \cdot h$ on day 74 to 8.5 $mg - N/L \cdot h$ on day 122. The nitrification activities and the VNLR almost coincided during this entire period. After the change in salinity an

ammonium removal rate of 8.4 $mg-N/L\cdot h$ and a nitrate formation of 8.0 $mg-N/L\cdot h$ was achieved.

3.1.4 Data quality

Figure 3.7 shows the mass balance for nitrogen, $N_{tot,in} - N_{tot,out}$ for Reactor F (a) and Reactor R2 (b), plotted against time of continuous operation. The gray bars correspond to a change in cultivation medium.

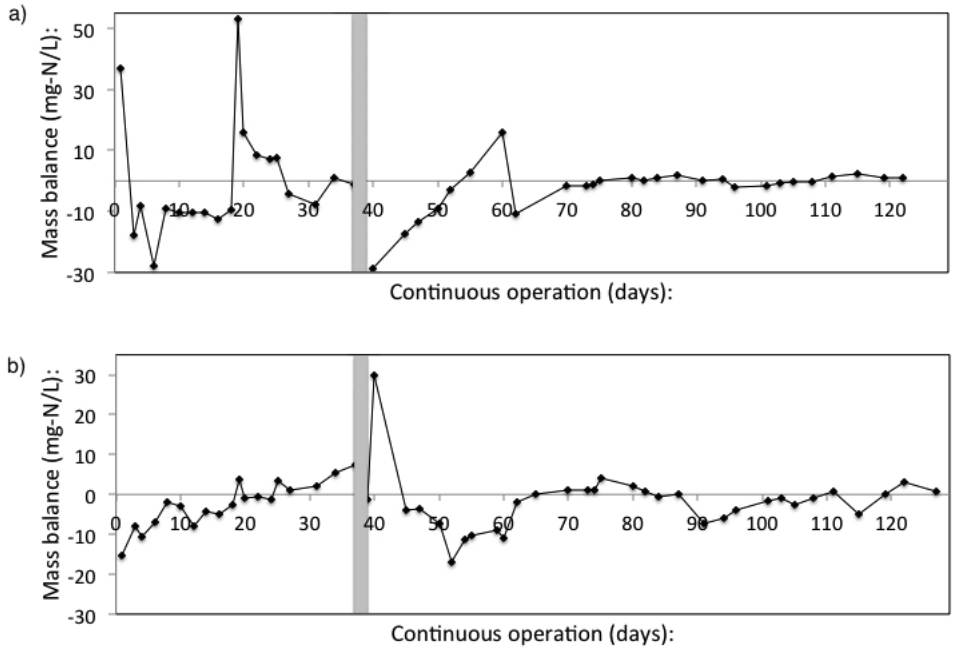

Figure 3.7: Mass balance of total mass nitrogen in the in-fluent subtracted with the mass of nitrogen in the effluent plotted against days of continuous operation. **a)** N-mass balance for reactor F. **b)** N-mass balance for reactor F2.

During continuous operation the mass balance showed an average deviation of -2 ± 14 and -2 ± 7 $mg-N/L$ for Reactor F and R2. Some differences in the mass balance of nitrogen is expected due to loss of nitrogen to gaseous stripping of ammonia and denitrification in anaerobe micro zones. Transients were generally associated with major changes in nitrogen loading rates and would temporarily invalidate the assumption of steady state.

3.2 Nitrification capacity and salinity toxicity tests

During the capacity test the reactors were run in batch with a 0 ppt salinity based cultivation medium for the non-adapted culture, and with a sea water based medium

for the 33 ppt salinity adapted culture. In the batch saline toxicity test the cultivation medium was swapped; operating Reactor F with a sea water based cultivation medium (33 ppt salinity), and Reactor R2 with a tap-water based cultivation medium (0 ppt salinity). The measured concentrations of ammonium, nitrate and nitrite from both tests is documented in Appendix D. Regression analysis gave the nitrification rates.

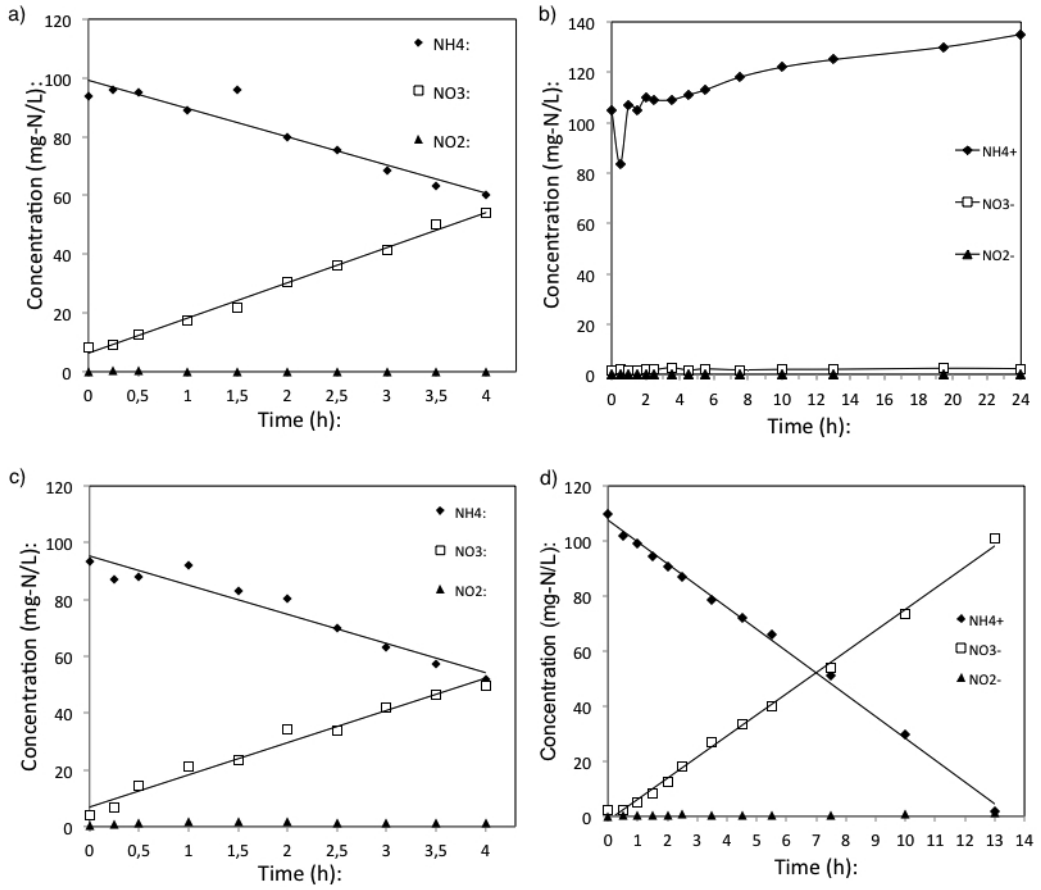

Figure 3.8: a) Batch capacity test with the 0 ppt salinity adapted culture in reactor F. Concentration of ammonium, nitrite and nitrate plotted against time. **b)** Batch salinity toxicity test with the 0 ppt salinity adapted culture in reactor F. Concentration of ammonium, nitrite and nitrate plotted against time. **c)** Batch capacity test with the 33 ppt salinity adapted culture in Reactor R2. Concentration of ammonium, nitrite and nitrate plotted against time. **d)** Batch salinity toxicity test the 33 ppt salinity adapted culture in reactor R2. Concentration of ammonium, nitrite and nitrate plotted against time.

Figure 3.8.a shows the time development of the concentration of ammonium, nitrite and nitrate for the municipal waste water culture (0 ppt salinity adapted) during the batch capacity test. Linear regression analysis showed an ammonium consumption rate

of $9.6 \pm 1.1\ mg-N/L \cdot h$ and a nitrate forming rate of $12.0 \pm 0.3\ mgN/L \cdot h$. Figure 3.8.b shows the concentration measurements of ammonium, nitrite and nitrate over a 24 hour period during the batch saline toxicity test. Observations showed no signs of nitrifying activity. The concentration of ammonium increased with 29 % from 105 mg-$N_{NH_4^+}/L$ at time zero, to 135 mg-$N_{NH_4^+}/L$ at $t = 24h$. This increase could be due to cell lysis when introducing the cells to an abrupt change in osmolarity (Li and Bo Yang, 2011).

In Figure 3.8.c and d the results from the batch- capacity and saline toxicity experiments performed with the 33 ppt salinity adapted culture is presented. In the capacity test activity rates of $10.3 \pm 1.0\ mgN/L \cdot h$ and $11.4 \pm 0.7\ mgN/L \cdot h$ were calculated for ammonium consumption and nitrate formation. Whereas in the saline toxicity test the ammonium consumption rate was $7.95 \pm 0.15\ mgN/L \cdot h$, which corresponds to a 29 % reduction, and the nitrate formation rate dropped approximately 32 % down to $9.6 \pm 1.1\ mgN/L \cdot h$ compared with the capacity test.

The results show that an abrupt change in salinity seemed to affect the nitrification performance in a negative manner. The 0 ppt salinity adapted culture did not show any sign of activity when changing the surrounding environment from a tap water based cultivation medium to a sea water based cultivation medium. On the other hand, the 33 ppt salinity adapted culture responded instantly with no certain observable lag-phase.

The linear correlation was of significance in the regressions done in Figure 3.8a, c and d, with a probability of no correlation below 0.05 for all six regressions.

3.3 Bacterial community structure

In the following sections the results regarding the analysis of the DGGE gels, and computational and statistical analyses of the gels are presented. Chapter 3.3.1 covers the DGGE gel analysis regarding community structure and dynamics of the samples sampled by Jonassen (2012) during continuous operation of the 0, 22 and 33 ppt salinity adapted cultures at native salinities. In Chapter 3.3.2 the results from the DGGE gel analysis for the samples sampled from the 0 and 33 ppt salinity adapted cultures before and after the change in salinity with regards to community structure and dynamics is presented.

3.3.1 Community dynamics at continuous operation at native salinities

Twelve DNA samples from the work of Jonassen (2012) were analysed with DGGE (Figure 3.9) to characterise and compare the nitrifying communities operated at different salinities. The sampling was done at continuous operation with salinities corresponding to community origin. (Se Chapter 2.4.1 for sampling days).

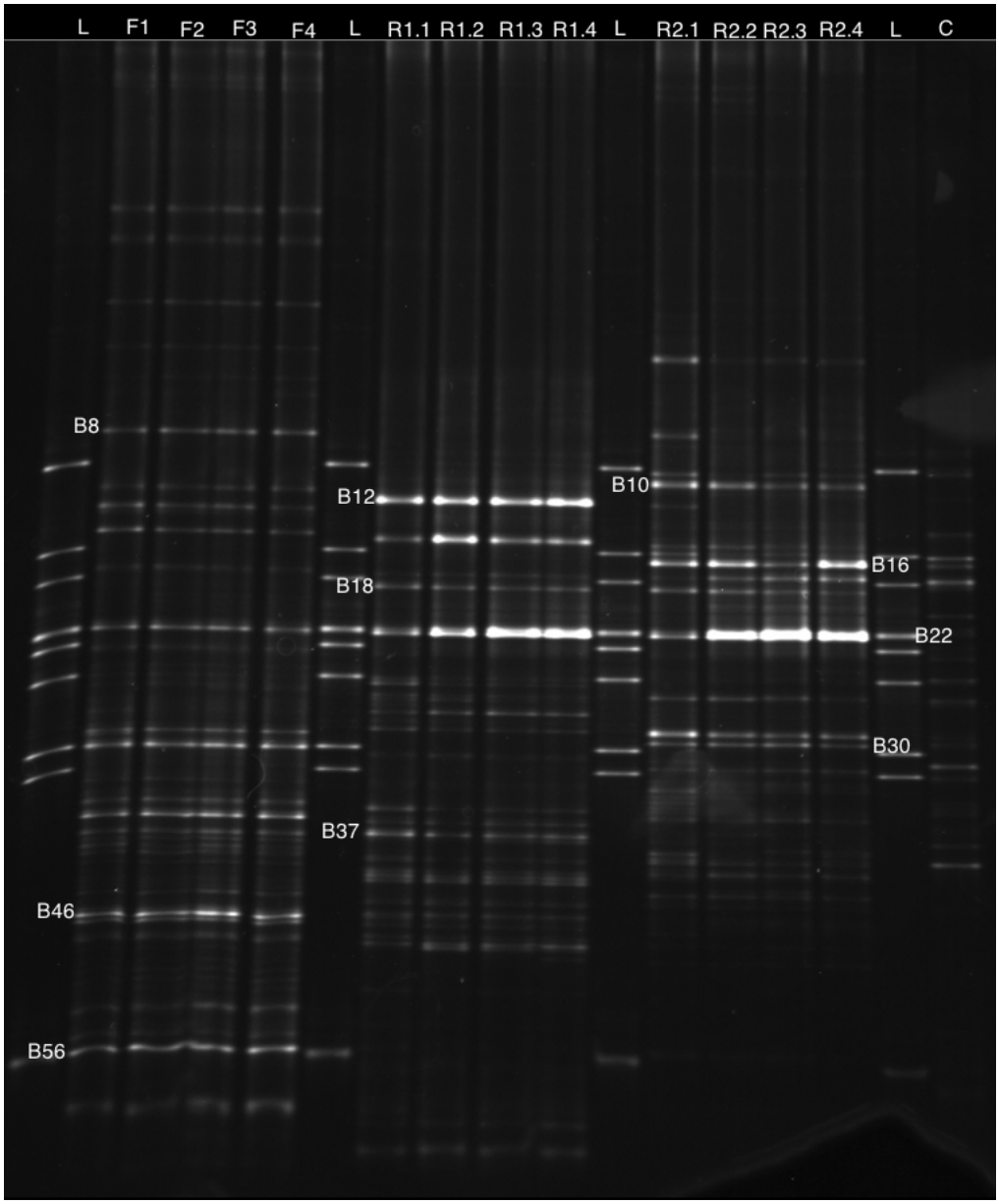

Figure 3.9: 30 to 50 % denaturing DGGE gel with 16S rDNA PCR products from the DNA sampled at continuous operation of reactor F, R1 and R2 during the project work of Jonassen (2012). The samples marked; FX, corresponds to samples from the municipal waste water culture operated with a tap water based cultivation medium (0 ppt salinity) in Reactor F, R1.X, corresponds to samples taken from the Mongstad culture operated with a 22 ppt salinity based medium from Reactor R1, and R2.X, corresponds to samples from the Trondheim Fjord culture operated at sea water salinity (33 ppt) from Reactor R2. Lanes marked with L contains marker DNA. The lane marked C contains DNA from the PCR reaction control.

The samples originated from continuous operation of the 0 ppt salinity adapted municipal waste water culture (F1 - F4) and the 33 ppt salinity adapted Trondheim Fjord culture (R2.1 - R2.4). In addition, DNA from a 22 ppt salinity adapted culture originating from a brackish aerated lagoon at the Mongstad Oil Refinery was used (R1.1 - R1.4).

Table 3.1: Band richness(k), Shannon (H') and Evenness diversity indices for reactor F, R1 and R2.

Reactor	Band richness (k)	Shannon(H')	Evenness ($e^{H'}/S$)
R2	23.3 ± 1.3	2.30 ± 0.30	0.50 ± 0.20
R1	23.0 ± 1.0	2.20 ± 0.20	0.40 ± 0.10
F	36.0 ± 2.0	3.15 ± 0.05	0.64 ± 0.02

The DGGE gel analysis showed a total of 59 unique bands. The municipal waste water culture (Reactor F) showed the highest band richness (k) and the highest Shannon and Evenness diversity indices. The salinity adapted cultures (Reactors R1 and R2) had similar richness and diversity.

Bray-Curtis distance matrices were generated from the square root transformed fractional peak areas generated from the DGGE analysis. Average Bray-Curtis similarities were calculated (Figure 3.10) within groups based on community origin, and between the groups. The average Bray-Curtis similarities seemed to decrease with increasing salinity, with the tap water operated municipal waste water culture (Reactor F) showing the highest similarity (0.81 ± 0.03). For the salinity adapted cultures the similarity within were 0.78 ± 0.08 and 0.65 ± 0.12 for R1 and R2, respectively. Comparing samples from different reactors (cultures) with each other showed that the two cultures originating and operated at saline conditions (R1 vs R2) showed a higher similarity with each other compared to the municipal waste water culture (R1 vs F and R2 vs F). Still, the difference in salinity between the reactors did not seem to influence the similarities between the cultures (Figure 3.11). When comparing the average Bray-Curtis similarity between the reactors and plotting them as a function of $\Delta salinity$, Figure 3.11, there was not observed a consistent trend regarding the differences in salinity. The highest similarity was between Reactor R1 and R2, with 0.35 ± 0.08. Average Bray-Curtis similarities were 0.16 ± 0.04 and 0.22 ± 0.04 for R1 vs F and R2 vs F, respectively.

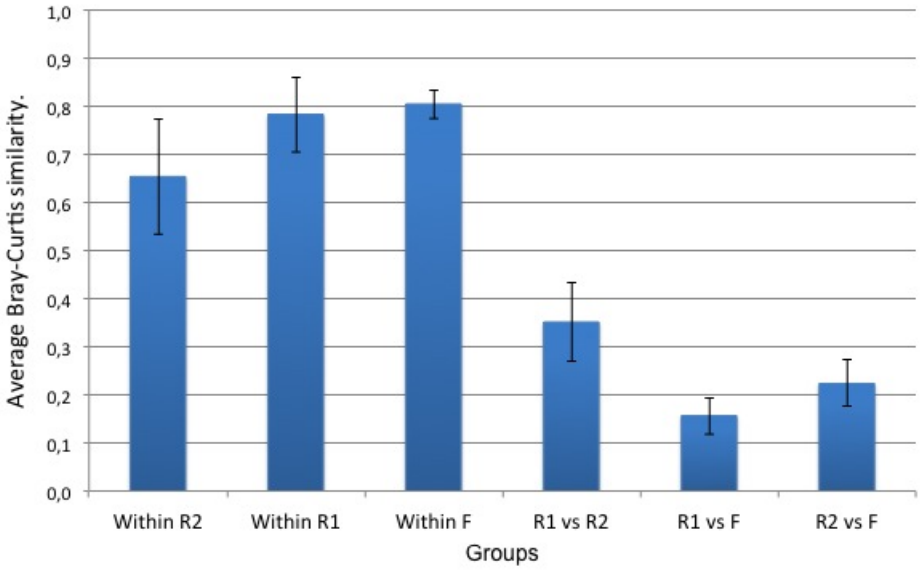

Figure 3.10: Average Bray-Curtis similarities within the communities in Reactor F, R1 and R2 and the average Bray-Curtis similarities between the reactors. The error bars correspond to one standard deviation.

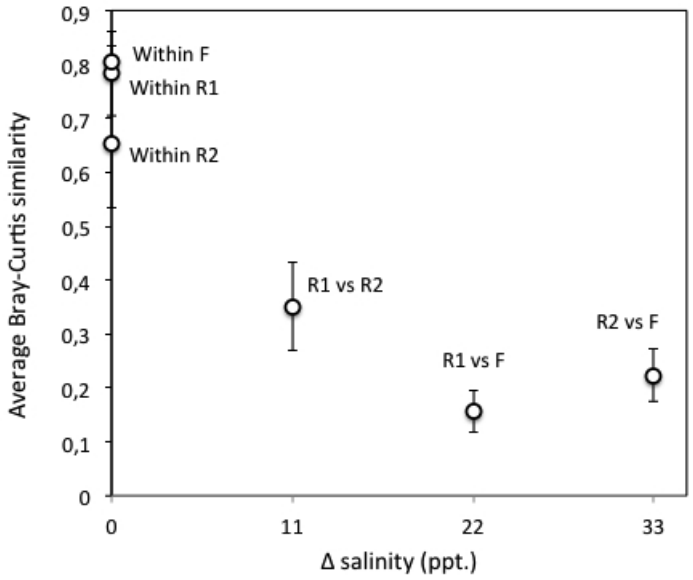

Figure 3.11: Average Bray-Curtis similarities within the communities in Reactor F, R1 and R2 and average Bray-Curtis similarities between the reactors plotted versus $\Delta salinity$. The error bars correspond to one standard deviation.

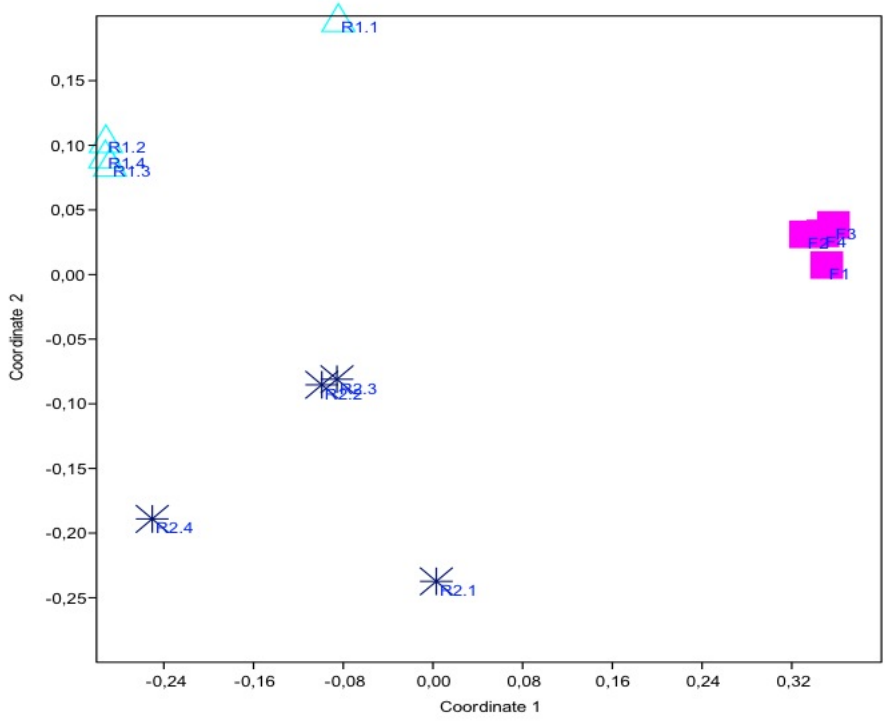

Figure 3.12: NMMDS plot based on Bray-Curtis similarity measure of DGGE gel analysis results. The samples are marked FX, R1.X and R2.X for the municipal waste water-, the Mongstad-, and Trondheim Fjord culture, adapted to 0-, 22-, and 33 ppt salinity, respectively. Stress value: 0.032

An ordination of the different community samples in a non-metric multidimensional scaling plot (NMMDS) based on Bray-Curtis similarity measure of DGGE gel analysis results is shown in Figure 3.12. The NMMDS plot reveals a clear separation between the three communities. The different samples clustered in specific areas in the plot according to community origin. The four samples from the municipal waste water culture clustered most closely together in the upper right side of the plot. The last three samples (R1.2 - R1.4) from 22 ppt salinity adapted Mongstad culture (Reactor R1) clustered closely together, and it appeared that the sample R1.1 was less similar compared with the others. For the Trondheim Fjord culture (from Reactor R2) the samples were distributed more widely, with only two points clustering close together, suggesting a higher variability in community composition between samples. A stress value of 0.032 was generated from the plot, providing evidence of a correct ordination.

A one-way ANOSIM test was conducted in order to determine if there were significant differences between the microbial communities inhabiting the-bio films in the three reactors, Table 3.2. The results indicate significant differences between all communities ($p < 0.05$).

Table 3.2: One-way ANOSIM test for significant differences between the nitrifying cultures adapted to different salinities. (P-values: Bon-Ferroni sequential.)

	R2	R1	F
R2			
R1	0.0287		
F	0.0301	0.0290	

A similarity percentage calculation (SIMPER) showed which bands in the DGGE gel that were responsible for the observed difference between the groups of samples (Table 3.3). The ten most influential bands were included, and are also shown in Figure 3.9.

Table 3.3: Similarity percentage - Showing the ten most influential bands contributing to the total difference between the groups in Figure 3.9.

Band number:	Contrib. %
B22	13.4
B12	11.5
B18	6.66
B16	6.18
B56	4.57
B30	3.95
B46	3.41
B37	3.24
B8	2.62
B10	2.36
Sum:	57.9

As shown in Table 3.3 the ten bands (17 % of the total band number of 59) contributed to 57.9 % of the difference between the three groups in the DGGE gel (Figure 3.9). The 49 other bands contributed to the remaining 42.1 %

3.3.2 Microbial community composition in reactors before and after change in salinity

13 and 12 DNA samples from Reactor F and R2, respectively, were analysed with DGGE (Figure 3.13). The sampling was done at continuous operation at native salinities and after the medium switch (Se Chapter 2.4.1 for sampling days).

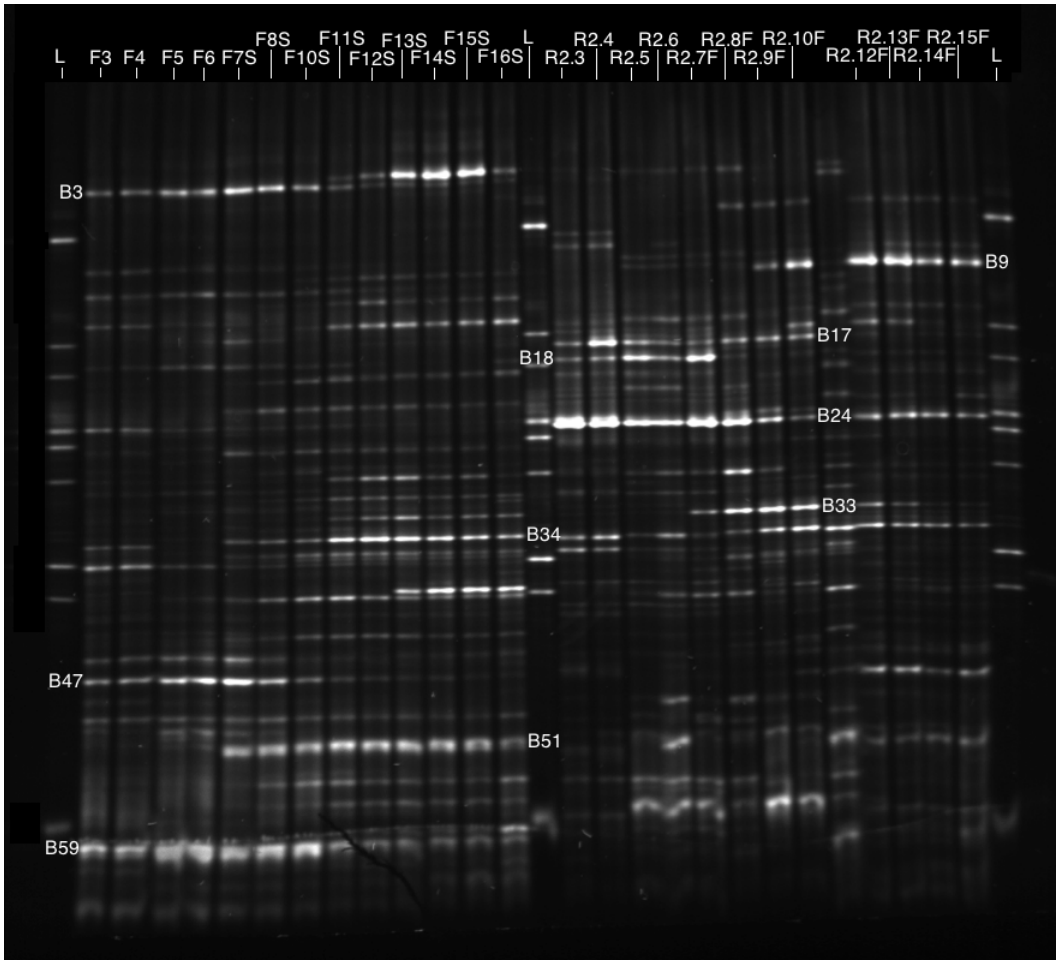

Figure 3.13: Picture of 30 to 50 % denaturing DGGE gel with DNA samples from continuous operation of Reactor F and R2. The samples marked; FX, corresponds to samples from the municipal waste water culture operated with a tap water based cultivation medium in Reactor F (0 ppt salinity). Samples marked FX.S refers to samples from Reactor F taken after the medium switch (33 ppt salinity). R2.X, corresponds to samples from the Trondheim Fjord culture operated with a sea water based medium (33 ppt salinity), whereas the samples marked R2.X.F refers to samples from Reactor R2 taken after the change in salinity (0 ppt salinity). Lanes marked with L contains marker DNA. The samples F3, F4, R2.3 and R2.4 originates from Jonassen (2012).

The DGGE gel analysis of Figure 3.13 showed a total of 59 unique bands, but due to bad separation in the lower most parts of the gel this number could have been higher. Band richness (k), Shannon diversity index (H') and the Evenness index ($e^{H'}/S$) for Reactor F and R2 are shown in Table 3.4.

Table 3.4: Diversity between Reactor F and R2.

Reactor	Band richness (k):	Shannon (H'):	Evenness ($e^{H'}/S$):
F	27.0 ± 5.7	2.79 ± 0.24	0.62 ± 0.06
$R2$	25.6 ± 3.1	2.60 ± 0.12	0.53 ± 0.06

A non-metric multidimensional scaling plot was generated from the Bray-Curtis similarity measures of the DGGE analysis results (Figure 3.14) illustrated that the samples from before the change in salinity grouped together.

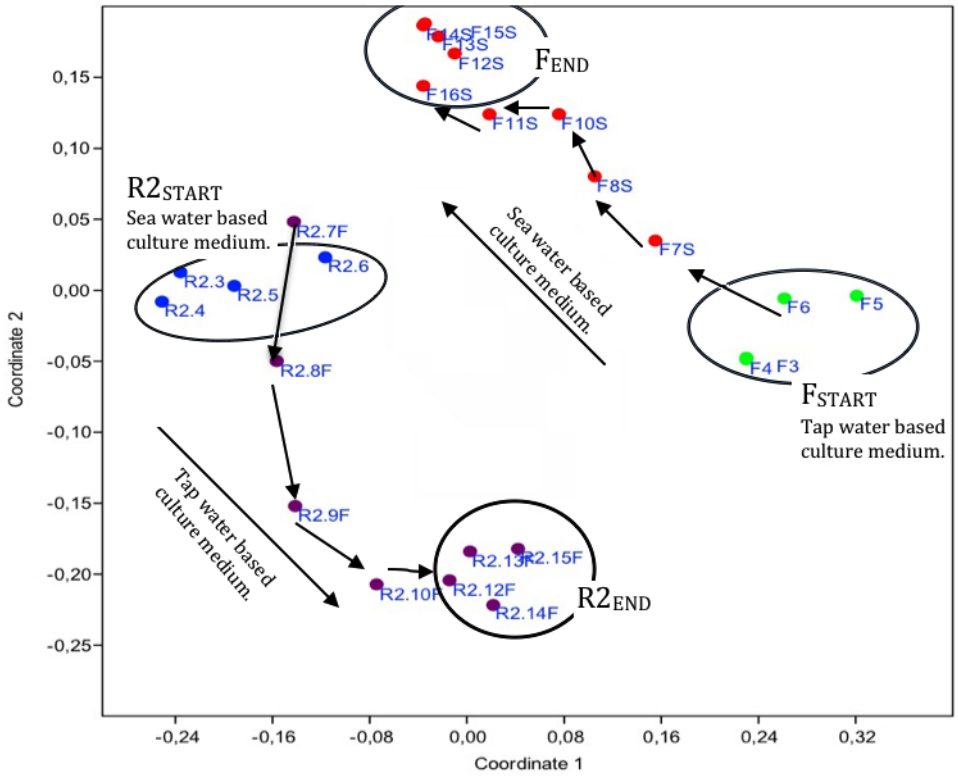

Figure 3.14: NMMDS plot based on Bray-Curtis similarity measure of DGGE gel analysis results. The samples are marked FX, and R2.X for the municipal waste water- and Trondheim Fjord culture. Four distinct groups: F_{start}, F_{end}, $R2_{start}$ and $R2_{end}$, are marked with circles. The arrows between them illustrates the path of movement in order of similarity as the communities changed due to a change in cultivation medium salinity. Stress value: 0.127

When the salinity of the cultivation mediums were swapped, a gradual change as a function of time was observed. In Reactor F the movement was toward the mid-upper part of the plot, while in Reactor R2 the movement was in the opposite direction towards the mid-bottom part. The last four samples from both reactors seemed to cluster into groups. A stress value of 0.127 indicated a reliable ordination.

The four clusters were named F_{start}, F_{end}, $R2_{start}$ and $R2_{end}$, and form the basis for the subsequent calculations. The average Bray-Curtis similarities were calculated within and between the four groups F_{start}, F_{end}, $R2_{start}$ and $R2_{end}$. The average Bray-Curtis similarity calculated within groups was high and ranged between 0.68 and 0.84 (Figure 3.15). The between group similarity was typically only $^1/_3$ of initial groups similarity (ranging from 0.26 to 0.36).

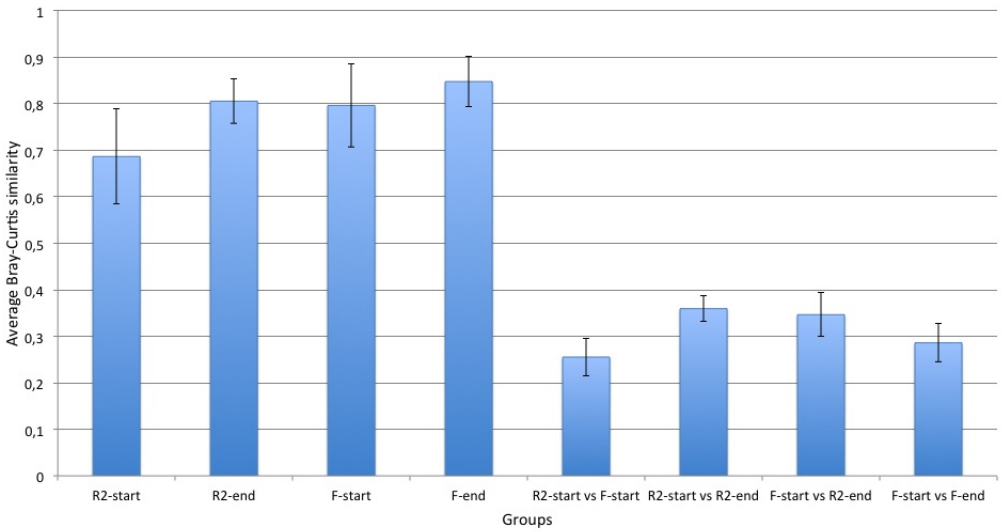

Figure 3.15: Average Bray-Curtis similarities within the four groups F_{start}, F_{end}, $R2_{start}$ and $R2_{end}$. The average Bray-Curtis similarities between the groups is also shown. The error bars corresponds to one standard deviation.

Band richness (k), Shannon diversity index (H') and the evenness index ($e^{H'}/S$ of the four groups F_{start}, F_{end}, $R2_{start}$ and $R2_{end}$ are shown in Table 3.5.

Table 3.5: Diversity between the groups F_{start}, F_{end}, $R2_{start}$ and $R2_{end}$.

Group	Band richness (k):	Shannon (H'):	Evenness ($e^{H'}/S$):
F_{start}	20 ± 2	2.50 ± 0.10	0.63 ± 0.08
F_{end}	30 ± 2	2.95 ± 0.01	0.63 ± 0.05
$R2_{start}$	28 ± 2	2.70 ± 0.10	0.52 ± 0.05
$R2_{end}$	24 ± 3	2.50 ± 0.10	0.50 ± 0.10

When comparing the groups F_{start} and F_{end} the band richness increased as a response to a change in cultivation medium from a tap water to a sea water based medium (Table 3.5). The Shannon diversity index also increased, indicating a more equal distribution of species after the change in salinity. There were no real differences between the evenness values. The calculated band richness, Shannon diversity- and Evenness indices were similar when comparing the groups $R2_{start}$ and $R2_{end}$.

Figure 3.16 shows a comparison of F_{start} with F_{end}, and the intermediate transient samples in between the two groups. The similarities were calculated comparing average Bray-Curtis similarities for F_{start} with the average Bray-Curtis similarities for the transient samples towards F_{end}. Figure 3.17 shows the equivalent development during the transient period for Reactor R2.

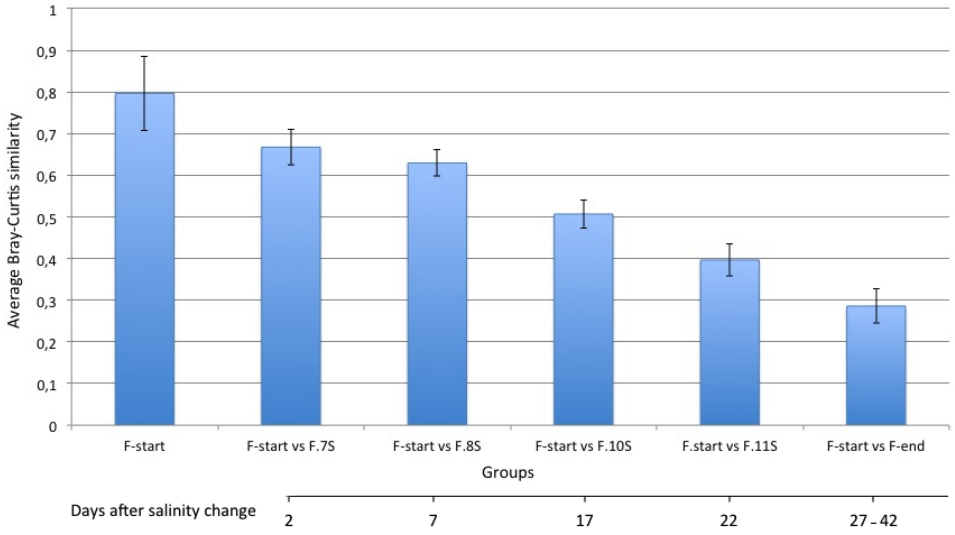

Figure 3.16: Comparison of the average Bray-Curtis values for F_{start} with the time series towards F_{end}. The error bars correspond to one standard deviation.

The community change after the salinity switch from a 0 ppt to a 33 ppt salinity based medium seemed to occur gradually over time. The difference between the comparisons of F_{start} vs F7S, and F_{start} vs F8S showed little difference in the Bray-Curtis similarities. The similarity compared to F_{start} seemed to decrease at a constant rate in the transient period and towards F_{end}. The average Bray-Curtis similarity between F_{start} and F_{end} was 0.29 ± 0.04, and the similarity within the group F_{start} was 0.78 ± 0.09.

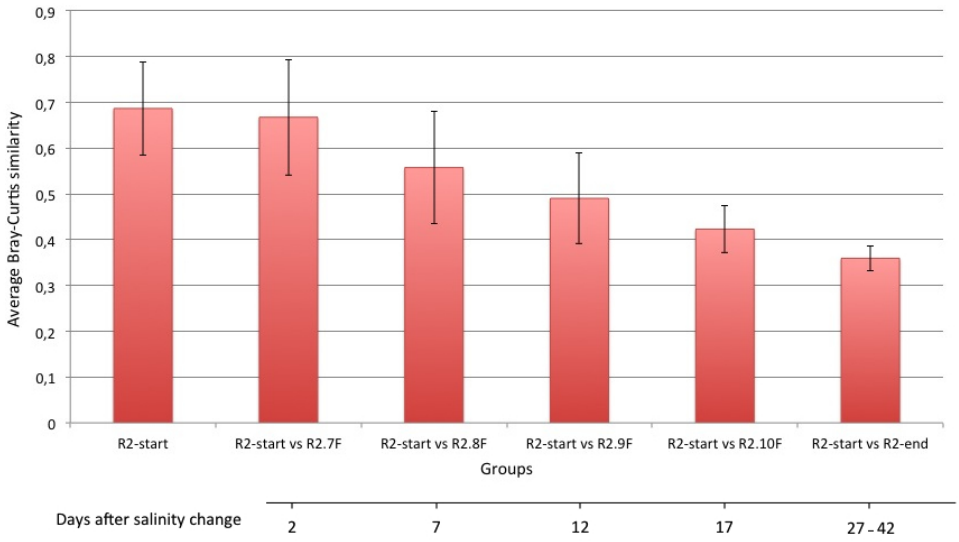

Figure 3.17: Comparison of the average Bray-Curtis values for $R2_{start}$ with the time series towards $R2_{end}$. The error bars corresponds to one standard deviation.

The community change after the salinity switch from a 33 ppt to a 0 ppt salinity based medium seemed to occur gradually as a function time, with a small lag period observed when comparing of $R2_{start}$ and $R2_{start}$ vs R2.7F, which showed a minor difference in the Bray-Curtis similarity. The similarities of the transient samples compared to $R2_{start}$ seemed to decrease at an almost constant rate in the transient period and towards $R2_{end}$. The average Bray-Curtis similarity between $R2_{start}$ and $R2_{end}$ was 0.36 ± 0.03, and the similarity within the group $R2_{start}$ was 0.69 ± 0.10.

A one-way ANOSIM test was conducted in order to calculate if there were significant differences between the microbial communities in the four groups (Table 3.6). There were significant differences between all four groups with p values below 0.03.

Table 3.6: One-way ANOSIM bonferroni seq. F_{start}, F_{end}, $R2_{start}$ and $R2_{end}$.

	$R2_{end}$	$R2_{start}$	F_{end}	F_{start}
R2end				
R2start	0.029			
Fend	0.008	0.009		
Fstart	0.030	0.027	0.008	

A similarity percentage calculation (SIMPER) showed which bands in the DGGE gel that were responsible for the observed difference between the groups of samples (Table 3.7). The ten most influential bands were included, and are also shown in Figure 3.13.

Table 3.7: Similarity percentage - Showing the ten most influential bands contributing to the total difference between the groups in Figure 3.13

Taxon	Contrib. %
B24	9.47
B47	6.86
B9	6.47
B3	4.80
B51	4.73
B59	4.43
B33	3.44
B17	3.35
B34	3.29
B18	3.27
Sum:	50.14

The SIMPER analysis showed that the ten bands (17% of the total band number of 59) explained more than half of the variation between the four groups (F_{start}, F_{end}, $R2_{start}$ and $R2_{end}$) in the DGGE gel (Figure 3.13). The 49 other bands contributed to the remaining variation.

Chapter 4

Discussion and conclusions

4.1 Evaluation of molecular methods

During continuous operation of the reactors it is likely that the nitrifying bio-films retained dead non active biomass. High proportions of dead biomass has been reported by live/dead staining on matured and non-matured bio-films in waste water treatment (Miura et al., 2007b). The turnover rate of biomass withheld in the bio-film depends on several factors with shear forces in the bulk liquid, protozoan grazing, the geometry of the carriers and microbial growth- and death rates being of most importance (Ostgaard, 2005). The live/death ratio was not determined in this study nor was the bio-film turnover rate or the presence of grazers. This led to the possibility that old community members could have vastly influenced the microbial fingerprints (Figure 3.9 and 3.13) when applying DNA based techniques. Further, the use of general bacterial primers when coupling nitrification performance with community changes resulted in displaying the community as a whole, including both the autotrophic nitrifying bacteria and other heterotrophs, on the DGGE community fingerprints. FISH analyses of nitrifying populations within the total bacterial community in sequencing batch reactors with similar operational settings as used in this study (25°C, pH ranging from 7 to 8, DO levels of above $2mg - O_2/L$) was reported by Guo et al. (2013) to constitute of 11.6 - 16% of the total biomass. Xia et al. (2008) showed that the total AOB and NOB population relative to the total population varied between 5.8 - 11% as a response to different C/N ratios in a compact suspended carrier bio-film reactor. Fluorescent *in situ* hybridization (FISH) analyses by Bassin et al. (2011) reported that the AOB and NOB population only constituted 1 - 2 % of the total microbial community in aerobic granular sludge reactors. The proportion of nitrifying bacteria relative to the total community was not determined in this study, still it is likely that most of the biomass retained in the bio-film in this study were heterotrophs and not nitrifying bacteria. DNA based PCR-DGGE fingerprinting can give a somewhat conservative succession regarding community changes, as the turnover of DNA might be slow due to retention of non active biomass in the bio-films.

The DGGE analysis regarding community structure and community dynamics as a

response to a change in salinity (Figure 3.13) did not result in complete separation of the bands in the lower most part of the gel. This probably led to an under estimation of the total number of bands in the gel, and consequently affected the diversity calculations (Table 3.4 and 3.5). In the DGGE gel with samples from Jonassen (2012) project (Figure 3.9) the lane with the control sample from the PCR reaction showed some bands. These bands probably originates from bacterial DNA present in the DNA polymerase used in the PCR reaction. This PCR bias would affect all samples equally, and would therefore not affect the similarity calculations between or within groups. It could have led to a wrong estimation of band richness and diversity indices. Further, due to poor DGGE resolution the presence of minor populations within the community might not have been revealed on the 16S rDNA level. Changes in these minor populations might have had an important effect on the functional stability.

Previous studies of nitrifying communities were DGGE has been the main PCR-based fingerprinting method have resulted in poor gels when applying general bacterial primers targeting the 16S rRNA gene. In general the reported gels show few bands and the separation of the bands is only adequate in most cases (Wu et al. 2008, Bassin et al. 2012). The experimental settings and primers used in this study generated DGGE fingerprints with somewhat better quality and with high band numbers indicating good separation compared to other studies. This gives the results more credibility and the statistical foundation more robustness.

4.2 Nitrification performance before and after the salinity change

Before the change in salinity both reactors showed high nitrification rates at native salinities. Comparing the nitrification rates at those salinities the 0 ppt salinity adapted culture showed 11 % higher ammonium consumption rate, and a 24 % higher nitrate formation rate compared with the 33 ppt adapted culture. The 0 ppt culture showed full nitrification before the change in salinity and the 33 ppt salinity adapted culture oxidised 89 % of the ammonium to nitrate. The salinity increase caused serious inhibition of the performance of the 0 ppt salinity adapted culture. Stable ammonium oxidation rates were not obtained before 54 days after the change in salinity (day 91 of continuous operation). Signs of NOB activity were low, or not present at all, throughout the experiment. It is hard to conclude whether there was some NOB activity, although measurements showed a minor increase in nitrate concentration at this time (54 days after change and towards the end). High concentrations of nitrite is known to influence the Dr. Lange nitrate tests as showed by Rønning (pers. com.). Determining the effects of nitrite concentrations on the Dr. Lange nitrate readings were not performed. A similar experiment by Bassin et al. (2011), where microbial activity was linked to microbial community structure in an aerobic granular sludge process, reported that NOB were severely affected by salt concentrations of 33 g/L. This was likely due to the NOB being more susceptible to osmotic stress than the AOB. Li and Bo Yang (2011) reported a high degree of cell lysis induced by elevated salinity. This could explain why the NOB

did not recover after the increase in salinity in Reactor F, and was probably also the cause of the observed increase in ammonium observed in the salinity toxicity test.

The 33 ppt salinity adapted culture prove to be robust regarding changes in salinity, indicating the presence of halotolerant, and not halophilic, nitrifyers in the bacterial community. Results obtained from the batch salinity toxicity test (Figure 3.8) showed that when subjecting the 33 ppt salinity adapted culture to a 0 ppt salinity cultivation medium the activity rates dropped, 29 % and 32 % for the ammonium oxidation and nitrate formation rates, compared to the activity rates obtained in the nitrifying capacity test. This indicated inhibition due to the change in salinity. No nitrite accumulation was observed, suggesting that the AOB were more severely inhibited by the change. This was in accordance with previous salinity toxicity tests (Jonassen, 2012) performed on the same culture.

On occasions observations showed higher nitrate forming rates than ammonium removal rates. This was probably due to transients which invalidated the assumption of steady state.

4.3 Community structure and dynamics before the change in salinity

Salinity seemed to be a crucial factor for community structure. As shown in Table 3.1 the 0 ppt salinity adapted culture showed 55.5 % higher band richness compared to the two salinity adapted cultures. The Shannon and evenness indices were also higher for the 0 ppt salinity adapted culture compared with the salinity adapted cultures, indicating a more even and uniformly distribution of species within the bacterial community during the time of sampling. Both salinity adapted cultures showed similar band richness and similarity indices, which suggests that the two communities constituted of more dominating populations. The results were expected as previous studies have reported that high salinity systems often show a lower microbial diversity (Moussa et al. 2006, Wu et al. 2008, Bassin et al. 2012). But it contradicts the results of Lefebvre et al. (2004) who found that the microbial structure in salt-adapted system was similar to that of a non-adapted one.

During continuous operation of the three reactors, the ammonium loading rate were similar during the sampling period (VNLR of approximately $2.4 \pm 0.3\ mg - N/l \cdot h$) and the 0 ppt salinity adapted culture was the only one that showed complete nitrification during the this period (Chapter 3.1.1, Jonassen (2012)). The 33 ppt salinity adapted reactor showed full nitrification the preceding few days after the last sampling, and the 22 ppt salinity adapted culture did not show full nitrification performance before two weeks after the last sampling day. Still, the ammonium conversion rates did almost coincide with the VNLR, so the cultures were all ammonium limited during the time of sampling. Nitrite accumulation was observed in both salinity based reactors. Because of the changes in the nitrification rates in the preceding days after sampling, it was likely that the communities in the two salinity based reactors were changing as an adaptive response to the nitrogen loading rates and towards a state were the communities were

able to convert all the in-fluent ammonia to nitrate. This seemed likely as the average Bray-Curtis similarities (Figure 3.10) showed that the similarity within the samples from each community were lower (and had higher standard errors) for the salt adapted cultures, with the 33 ppt showing the lowest similarity within the community. The average Bray-Curtis similarity between the reactors were reduced with a factor of at least two when comparing the communities with each other. Interestingly, the similarity between the two salinity adapted cultures showed higher similarities with each other than when compared to the 0 ppt salinity adapted culture. This indicating that the salinity adapted cultures shared some dominating species. The similarity percentage showed that the ten top contributing bands could explain 57.9 % of the observed difference between the three communities. This indicated that only a minor numbers of species contributed to most of the observed difference between the cultures, and minor changes within these bands could contribute vastly to the total difference.

The high salinity conditions favours the growth of halophilic and halotolerant bacteria as indicated by the nitrification salinity toxicity test (Figure 1.3) of Jonassen (2012). In that experiment it was showed that the salinity adapted cultures still performed good with high nitrification rates even at a lowered salinity. The 22 ppt salinity adapted culture also showed good nitrification performance at elevated salinity levels of 33 ppt. It is possible that a higher degree of community dynamics and flexibility is required in more extreme environments. This raised flexibility/dynamics could be a competitive advantage towards variations in salinity.

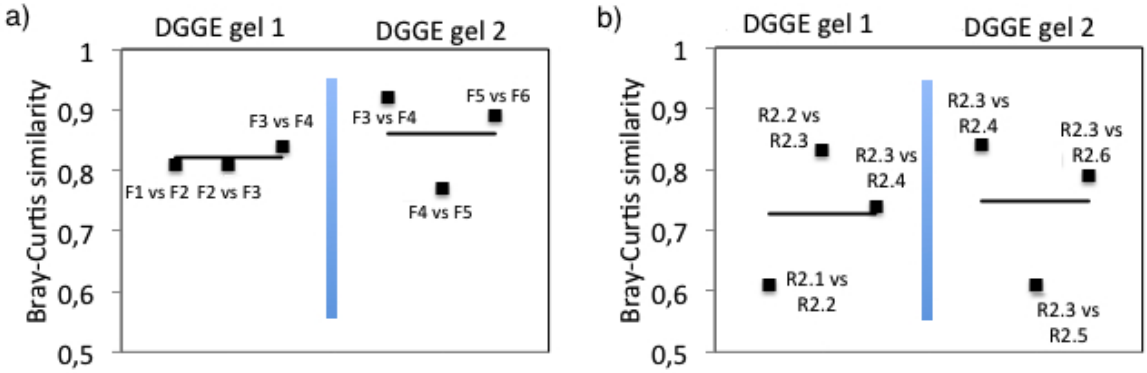

Figure 4.1: Comparison of Bray-Curtis similarities between samples at continuous operation at native salinities. The blue bar corresponds to storage and freezing of the carriers, and divides the experiment of Jonassen (2012) with this study. Black vertical lines is the average Bray-Curtis similarity of the pair wise comparisons. **a)** Bray-Curtis similarities between samples in Reactor F. **b)** Bray-Curtis similarities between samples in Reactor R2.

The similarity between the samples from Reactor F (Figure 4.1.a) fluctuated around a mean before the bio-films were frozen and stored. After thawing and operation at 0 ppt salinity in this study, the fluctuation seemed to increase. This is probably due to the

community response to adapt to the variations in the VNLR in the period of sampling (Sample F5 and F6). It is possible that the samples could have been more similar if the operational conditions were more constant in the sampling period. In Figure 4.1.b, which shows the similarity between the samples from Reactor R2 at native salinity, the fluctuations were more evident. In the experiment of Jonassen (2012) there was some minor accumulation of nitrite at the points of sampling. But the concentration decreased towards the last sampling point. This reduction in nitrite concentration indicates that the NOB were gradually becoming more dominating in the bio-film during this period and the difference in Bray-Curtis similarities between the samples could be explained due to this. In the present study the nitrification performance was good during continuous operation of Reactor R2 at 33 ppt salinity, showing no accumulation of nitrite and converting about 88 % of the in-fluent ammonium. The VNLR was increased in the period of sampling, and the increased loading can explain variations in the Bray-Curtis similarities. Comparing the different samples from Reactor R1 gave Bray-Curtis similarities of 0.71, 0.82 and 0.90. The amount of nitrite accumulation was high in Reactor R1 during the sampling period, and the community did not show good performance until two weeks after the last sample. The community was probably not fluctuating around a possible climax state, but rather moving towards this condition.

The results indicate that stable communities (climax communities) were not achieved when operating the reactors at native salinities, and was in accordance with the experimental results of Moussa et al. (2006). This could be due to variations of different parameters such as in-fluent concentration of ammonium, the volumetric nitrogen load rate, temperature variations, and pH differences. A longer operational period and constant environmental factors could have resulted in a more similar community over time. The results suggest that stable performance is not always coupled to a stable community structure, and consequently that a static nitrifying community is not essential for complete nitrification.

4.4 Community structure and dynamics after the change in salinity

The two cultures showed similar band richness (k) and Shannon diversity (Table 3.4) when comparing the community development throughout the operational period (before and after the change in salinity). There were some differences in the Evenness index where Reactor F showed the highest Evenness, indicating that the species were more uniformly distributed in this community. As the calculated Evenness was an average diversity measure before an after the change in salinity one can expect them to be somewhat similar as the main difference, besides community origin, was the environmental salinity. As discussed in Chapter 4.3 high salinity conditions seemed to reduce the species richness, and similar diversity was therefore expected when performing a comparison that included before and after the change in salinity for both reactors.

According to Kartal et al. (2006) and Dapena-Mora et al. (2010) there are two possible outcomes of the adaptation of a bacterial community to a change in salinity: the

acclimation of the existing population (by physiological or evolutionary adaptation), or a population shift (microbes low in initial number gradually dominates the community due to a competitive advantage towards variations in salinity). The results from the nitrification salinity toxicity test (Chapter 3.2) showed that the community in Reactor R2 quickly acclimatized to the change in salinity. The non-metric multidimensional scaling plot (Figure 3.14) based on Bray-Curtis similarity measures also showed that the community changed as a response to the change in salinity. This indicated that both outcomes of adaptation seemed to occur for the 33 ppt salinity adapted culture. On the contrary, the 0 ppt salinity adapted culture did not show any signs of activity in the salinity toxic response test. But the NMMDS plot (Figure 3.14) showed that the community change was just as eminent as in the 33 ppt salinity adapted culture and, with the modest nitrification rates observed towards the end of the experiment, this suggest population shift as a response to the change in environmental salinity. The ordination in Figure 3.14 showed four distinct clusters, with a successive community change between them. Comparison of the average Bray-Curtis similarity within the samples before the change in salinity with the individual samples in the transient period showed an almost linear decrease in similarity. Indicating a constant development towards a possible final state (Figure 3.16 and 3.17).

The diversity measures (Table 3.5) for the clusters F_{start} and F_{end} showed that the band richness increased with 50% after the change in salinity. This was not expected and contradicts studies reporting that an increase in salinity cause a reduction in community richness (Moussa et al. 2006, Wu et al. 2008, Bassin et al. 2012). The Shannon diversity index was also higher indicating less dominating species after the change. This was also unexpected as an increase in salinity would probably select a narrower group of bacteria able to function at high salinity. It is likely that this could be due to poor band separation in the lower most parts of the DGGE gel (Figure 3.13) which led to an underestimation of the bands present (Chapter 4.5). The diversity indices of $R2_{start}$ and $R2_{end}$ were more similar with small changes in band richness, Shannon diversity and Evenness. This was considered plausible and in accordance with the results from the batch salinity toxicity test, and the community origin, suggesting a more robust community with respect to changes in the salinity. The similarity percentage between the four groups showed that the ten most contributing bands could explain approximately 50 % of the total variance between the groups. This was in accordance with the results obtained before the change in salinity (Chapter 4.3) and indicated that variations in a few key players in the community, would influence the similarity between the groups substantially. These key players may further possess important roles regarding functional stability within the communities.

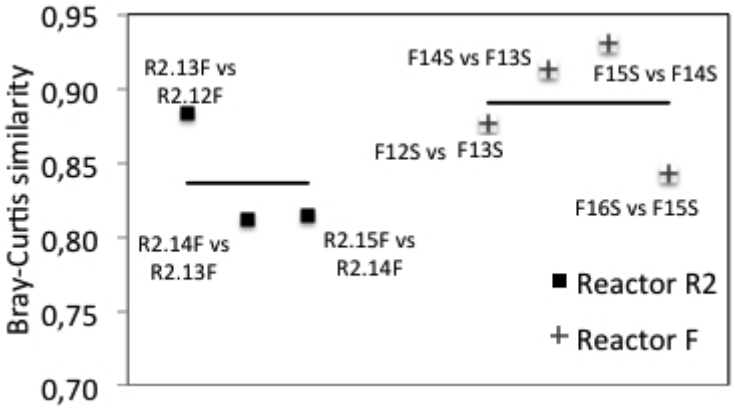

Figure 4.2: Comparison of Bray-Curtis similarities between the samples in the groups F_{end} and $R2_{end}$ during continuous operation after the salinity switch. Black vertical lines is the average Bray-Curtis similarity of the pair wise comparisons.

The similarity between the samples constituting the groups F_{end} and $R2_{end}$ from Reactor F and R2, respectively, seemed to fluctuate around a mean which indicate that stable communities were not obtained (Figure 4.2). This was probably due to the communities response to adapt to the variations in the VNLR in the period of sampling, and it is possible that the observed difference between the samples could have been more similar if the operational conditions were more constant in the sampling period. In Reactor R2, the fluctuations seemed more evident, and the Bray-Curtis similarities were less similar compared to the F_{end} group of Reactor F. In the sampling period the community showed full nitrification, but changes in the VNLR may have caused a change in the community. In reactor F it was observed stable ammonium oxidizing activity towards the end of operation at 33 ppt salinity (Sample F16S). This suggested that the AOB were gradually becoming more dominating in the bio-film during this period and the decrease in Bray-Curtis similarities between the samples could be explained due to this. The VNLR were decreased in the period of sampling, and the difference in nitrogen loading rates could further explain the variations in the Bray-Curtis similarities.

It was hard to determine whether the nitrogen loading rates or hydraulic retention time did result in changes in the microbial population in Reactor F and R2. When coupling nitrification performance with community changes it should be stated that the recorded community changes displays the community as a whole, thus including both the autotrophic nitrifying bacteria and other heterotrophs present in the bio film. This makes it hard to conclude if changes in activity are associated with big differences in community structure. Environmental factors such as pH, temperature and dissolved oxygen concentration remained fairly constant during the operational period, and it is not likely that these factors contributed in a decisive manner towards the community change after the salinity change. The pH incidents in Reactor F may have directed the community towards the final state, as reported by Princic et al. (1998).

The results indicate that the microbial adaptation strategy was not determined by

either acclimation or by population shift, but rather a combination of the two determined by the communities inherent prerequisites. These results may contradict the results of Bassin et al. (2011) who concluded that the AOB population did not change but adapted to changing salinities in their experiment. Bassin et al. (2011) based this on sequencing of bands from DGGE runs with general bacterial primers and primers targeting the *amoA* gene and concluded based on the presence or absence of AOB. As this present study examined the community changes in the community as a whole, it is hard to say if the nitrifying population varied in the transient period and towards the more stable end state. But it seems highly unlikely that the nitrifying population was stagnant in the same period.

During adaptation to a change in salinity a stable nitrification performance was not necessarily coupled to a stable community structure. Towards the end of the experiment Reactor R2 showed full nitrification, but minor fluctuations in the community was still observed. This indicates, in accordance with the results from continuous operation at the cultures native salinity (33 ppt), that a static nitrifying community is not essential for complete nitrification.

4.5 Conclusions

- The microbial community adapted to 33 ppt was halotolerant and showed robustness to changes in the salinity.
- A static nitrifying community is not essential for complete nitrification, but rather an advantageous community trait regarding robustness to perturbations in environmental factors such as pH, temperature and nitrogen loading.
- The microbial adaptation strategy was not determined by either acclimation or by population shift for the 33 ppt salinity adapted halotolerant culture. But rather a combination of the two, determined by the community's inherent prerequisites.
- Population shift was probably the main adaptation strategy for the 0 ppt adapted culture when adapting to 33 ppt salinity.
- During adaptation to a change in salinity a stable nitrification performance was not necessarily coupled to a stable community structure.
- Only a few species contributed to the majority of variance between the different communities. The degree of abundance of these key players may have important roles regarding functional stability at different salinities.

4.6 Future perspectives

DNA based PCR-DGGE prove to be a sufficient way to describe the community dynamics and structure as a response to environmental changes, and this study has resulted in new knowledge and insight regarding functional performance, community dynamics and adaptation strategies as a response to a low salinity adaptation of high salinity adapted cultures (as most studies have their focus on the opposite scenario). But as DNA based fingerprinting is afflicted with the presence of non active biomass due to retention in the bio-film, and a long DNA turnover rate, it is suggested that more work should be directed towards a RNA (cDNA) based DGGE gel analysis. This would probably result in a more accurate description of the successive community changes that occurred as a response to the change in salinity in the communities as the turnover rate of RNA is substantially lower than DNA in most cases. In particular when considering short term operation of bio-film based reactor systems with few days between sampling. More work should further be directed towards identification of the species inhabiting the bio-film, in particular the bands corresponding to species thought to be key players in the communities. Sequencing DNA from the DGGE gels has resulted in deficient results in previous experiments at the department (Hjort, 2010), so other sequencing options should also be applied (*e.g.* 454 pyrosequencing). Supplementing the DGGE analysis with fluorescent *in situ* hybridisation (FISH) analyses could also give more information regarding the relative abundance of NOB and AOB as a function of time during the adaptation and give more knowledge regarding the physical distribution of nitrifying bacteria within the bio-films. Alternatively, the use of specific AOB and NOB primers for the PCR-DGGE could give further insight in community dynamics and structure only accounting for the nitrifying bacteria.

The cultures, DNA extracts and biomass samples from this study are available for further investigation.

Bibliography

AnalystSoft (2012). Statplus.

Anthonisen, A., Loehr, R., Prakasam, T., and Srinath, E. (1976). Inhibition of nitrification by ammonia and nitrous acid. *Journal of the water pollution federation*, 48(5):835–852.

Bakke, I., Schryver, P. D., Boon, N., and Vadstein, O. (2011). Pcr-based community structure studies of bacteria associated with eukaryotic organisms: A simple pcr strategy to avoid co-amplification of eukaryotic dna. *Journal of Microbiological Methods*, 84:349 – 351.

Bassin, J., Pronk, M., Muyzer, G., Kleerebezem, R., Dezotti, M., and Van Loosdrecht, M. (2011). Effect of elevated salt concentrations on the aerobic granular sludge process: Linking microbial activity with microbial community structure. *Applied and Environmental Microbiology*, 77(22):7942–7953.

Bassin, J. P., Kleerebezem, R., Muyzer, G., Rosado, A. S., van Loosdrecht, M. C. M., and Dezotti, M. (2012). Effect of different salt adaptation stratergies on the microbial diversity, activity and settling of nitrifying sludge in sequencing batch reactors. *Appl Microbiol Biotechnol*, (93):1281–1294.

Bernhard, A., Landry, Z., Blevins, A., De La Torre, J., Giblin, A., and Stahl, D. (2010). Abundance of ammonia-oxidizing archaea and bacteria along an estuarine salinity gradient in relation to potential nitrification rates. *Applied and Environmental Microbiology*, 76(4):1285–1289.

Bibiloni, R. c., Simon, M., Albright, C., Sartor, B., and Tannock, G. (2005). Analysis of the large bowel microbiota of colitic mice using pcr/dgge. *Letters in Applied Microbiology*, 41(1):45–51.

Boon, N., De Windt, W., Verstraete, W., and Top, E. (2002). Evaluation of nested pcr-dgge (denaturing gradient gel electrophoresis) with group-specific 16s rrna primers for the analysis of bacterial communities from different wastewater treatment plants. *FEMS Microbiology Ecology*, 39(2):101–112.

Brunvold, L., Sandaa, R.-A. b., Mikkelsen, H., Welde, E., Bleie, H., and Bergh, Ø. b. (2007). Characterisation of bacterial communities associated with early stages of

intensively reared cod (gadus morhua) using denaturing gradient gel electrophoresis (dgge). *Aquaculture*, 272(1-4):319–327.

Buzas, M. and Gibson, T. (1969). Species diversity: Benthonic foraminifera in western north atlantic. *Science*, 163(3862):72–75.

Catalan-Sakairi, M. A. B., Wang, P. C., and Matsumura, M. (1997). Nitrification performance of marine nitrifiers immobilized in polyester- and macro-porous cellulose carriers. *Journal of Fermentation and Bioengineering*, 84(6):563 – 571.

Clarke, K. (1993). Non-parametric multivariate analysis of change in community structure. *Australian Journal of Ecology*, (18):117–143.

Dapena-Mora, A., Vázquez-Padín, J., Campos, J., Mosquera-Corral, A., Jetten, M., and Méndez, R. (2010). Monitoring the stability of an anammox reactor under high salinity conditions. *Biochemical Engineering Journal*, 51(3):167–171.

Francis, C., Beman, J., and Kuypers, M. (2007). New processes and players in the nitrogen cycle: The microbial ecology of anaerobic and archaeal ammonia oxidation. *ISME Journal*, 1(1):19–27.

Gafan, G. P. and Spratt, D. A. (2005). Dentaturing gradient gel electrophoresis gel expansion (dggege) - an attempt to resolve the limitations of co-migration in the dgge of complex polymicrobial communities. *FEMS Microbiology Letters*, (253):303–307.

Graham, D., Knapp, C., Van Vleck, E., Bloor, K., Lane, T., and Graham, C. (2007). Experimental demonstration of chaotic instability in biological nitrification. *ISME Journal*, 1(5):385–393.

Guo, C.-Z., Fu, W., Chen, X.-M., Peng, D.-C., and Jin, P.-K. (2013). Nitrogen-removal performance and community structure of nitrifying bacteria under different aeration modes in an oxidation ditch. *Water Research*.

Gutierrez-Wing, M. T. and Malone, R. F. (2005). Biological filters in aquaculture: Trends and research directions for freshwater and marine applications. *Aquacultural Engineering*, (34):163–171.

Hammer, Ø., Harper, D., and Ryan, P. (2001). Past: Paleontological statistics software for education and data analysis. *Palaeontologia Electronica*, 4(1).

Hellinga, C., Schellen, A., Mulder, J., Van Loosdrecht, M., and Heijnen, J. (1998). The sharon process: An innovative method for nitrogen removal from ammonium-rich waste water. *Water Science and Technology*, 37(9):135–142.

Henze, M., Grady C.P.L., J., Gujer, W., Marais, G., and Matsuo, T. (1987). Activated sludge model no. 1. *Activated Sludge Model No. 1*.

Hill, T., Walsh, K., Harris, J., and Moffett, B. (2003). Using ecological diversity measures with bacterial communities. *FEMS Microbiology Ecology*, 43(1):1–11. cited By (since 1996)204.

Hjort, I. (2010). Molecular genetic analysis of the microbial community structure in nitrifying biofilms adapted to different salinities. Master's thesis, Norwegian University of Science and Technology.

Hunik, J., Meijer, H., and Tramper, J. (1992). Kinetics of nitrosomonas europaea at extreme substrate, product and salt concentrations. *Applied Microbiology and Biotechnology*, 37(6):802–807.

Jimenez, J., Melcer, H., Parker, D., and Bratby, J. (2011). The effect of degree of recycle on the nitrifier growth rate. *Water Environment Research*, 83(1):26–35.

Jonassen, K. R. (2012). Microbial communities in nitrifying biofilm at different salinities. Project work.

Kartal, B., Koleva, M., Arsov, R., van der Star, W., Jetten, M., and Strous, M. (2006). Adaptation of a freshwater anammox population to high salinity wastewater. *Journal of Biotechnology*, 126(4):546–553.

Konneke, M., Bernhard, A., De La Torre, J., Walker, J., Waterbury, J., and Stahl, D. (2005). Isolation of an autotrphic ammonia oxidizing archaeon. *Nature*, (437):453–546.

Kristoffersen, M. (2004). Nitrifikasjon for resirkulerte oppdrettsanlegg; salinitetsadaptering. Project work.

Kusar, D. and Avgustin, G. (2012). Optimization of the dgge band identification method. *Folia Microbiology*, (57):301–306.

Lefebvre, O., Habouzit, F., Bru, V., Delegenes, J., Godon, J., and Moletta, R. (2004). Treatment of hypersaline industrial wastewater by a microbial consortium in a sequencing batch reactor. *Environmental Technology*, 25(5):543–553.

Li, L. and Bo Yang, P. Z. (2011). Effect of acclimation stratergy on the biological nitrification in the saline wastewater. *Advanced Materials Research*, 183-185:522–526.

Madigan, Martinko, Dunlap, and Clark (2009). *Brock Biology of microorganisms*. Pearson Education Inc, 12 edition.

Miura, Y., Hiraiwa, M. N., Ito, T., Itonaga, T., Watanabe, Y., and Okabe, S. (2007a). Bacterial community structures in mbrs treating municipal waste water: Relationship between community stability and reactor performance. *Water Research*, (41):627–637.

Miura, Y., Watanabe, Y., and Okabe, S. (2007b). Membrane biofouling in pilot-scale membrane bioreactors (mbrs) treating municipal wastewater: Impact of biofilm formation. *Environmental Science and Technology*, 41(2):632–638.

Moussa, M., Sumanasekera, D., Ibrahim, S., Lubberding, H., Hooijmans, C., Gijzen, H., and Van Loosdrecht, M. (2006). Long term effects of salt on activity, population structure and floc characteristics in enriched bacterial cultures of nitrifiers. *Water Research*, 40(7):1377–1388.

Mumy, K. L. and Findlay, R. H. (2004). Convenient determination of dna extraction efficiency using an external dna recovery standard and quantitative-competitive pcr. *Journal of Microbiological Methods*, 57(2):259–268.

Muyzer, G., De Waal, E., and Uitterlinden, A. (1993). Profiling of complex microbial populations by denaturing gradient gel electrophoresis analysis of polymerase chain reaction-amplified genes coding for 16s rrna. *Applied and Environmental Microbiology*, 59(3):695–700.

Myers, R., Fischer, S., Lerman, L., and Maniatis, T. (1985). Nearly all single base substitutions in dna fragments joined to a gc-clamp can be detected by dentaturing gradient gel electrophoresis. *Nucleic Acids Res.*, 13(9):3131–3145.

Norevik, E. (2004). Removal of ammonium from "produced water" from offshore operations. Master's thesis, Norwegian University of Science and Technology.

Norland, S. (2004). Gel2k. *Dept. of Biology University of Bergen.*

Ostgaard, K. (2005). *Miljøbioteknologi Del II - Biologisk vannrensing.* Institutt for bioteknologi NTNU.

Ostgaard, K., Lee, N., and Welander, T. (1994). Nitrification at low temperatures. In *Institution of Chemical Engineers Symposium Series*, pages 134–137.

Princic, A., Mahne, I., Megusar, F., Paul, E. A., and Tiedje, J. M. (1998). Effects of ph and oxygen and ammonium concentrations on the community structure of nitrifying bacteria from wastewater. *Applied and Environmental Microbiology*, 64(10):3584–3590.

Regjeringen.no (2012). Fiskeri og kystdepartementet: Sjømatrådet presenterer solide eksporttall for 2011. *http://www.regjeringen.no/nb/dep/fkd/aktuelt/nyheter/2012/sjomatradet-presenterer-solide-eksportta.html?id=668071.*

Sedlak, R. (1991). *Phosphorus and Nitrogen Removal from Municipal Wastewater.*

Selvik J., Tjomsland T., E. H. (2007). Teoretiske tilførseslberegninger av nitrogen og forsfor til norske kystområder. *Technical report, Norsk institutt for vannforskning for statens forurensingstilsyn.*

Shimano, S., Sambe, M., and Kasahara, Y. (2012). Application of nested pcr-dgge (denaturing gradient gel electrophoresis) for the analysis of ciliate communities in soils. *Microbes and Environments*, 27(2):136–141.

Staley, J. and Konopka, A. (1985). Measurement of in situ activities of nonphotosynthetic microorganisms in aquatic and terrestrial habitats. *Annual Review of Microbiology*, 39:321–346.

Sudarno, U., Bathe, S., Winter, J., and Gallert, C. (2010). Nitrification in fixed-bed reactors treating saline wastewater. *Applied Microbiology and Biotechnology*, 85(6):2017–2030.

Taylor, J. R. (1997). *An introduction to error analysis, the study of uncertainties in physical measurements*, volume 2. University Science Books.

Treusch, A., Leininger, S., Kietzin, A., Schuster, S., Klenk, H.-P., and Schleper, C. (2005). Novel genes for nitrite reductase and amo-related proteins indicate a role of uncultivated mesophilic crenarchaeota in nitrogen cycling. *Environmental Microbiology*, 7(12):1985–1995.

Tuomisto, H. (2010). A consistent terminology for quantifying species diversity? yes, it does exist. *Oecologia*, 164(4):853–860.

Ward, B. B., Arp, D. J., and Klotz, M. G. (2011). *Nitrification*. ASM Press, Washington.

Wittebolle, L., Vervaeren, H., Verstraete, W., and Boon, N. (2008). Quantifying community dynamics of nitrifiers in functionally stable reactors. *Applied and Environmental Microbiology*, pages 286–289.

Wright, P. and Wood, C. (2012). Seven things fish know about ammonia and we don't. *Respiratory Physiology and Neurobiology*, 184(3):231–240.

Xia, S., Li, J., and Wang, R. (2008). Nitrogen removal performance and microbial community structure dynamics response to carbon nitrogen ratio in a compact suspended carrier biofilm reactor. *Ecological Engineering*, 32(3):256–262.

Appendices

Appendix A

Operation of the nitrifying reactor F, with biomass originating from low salinity municipal waste water

Table A.1 shows operating conditions for the reactor during the test period. This include parameters such as concentrations of ammonia, nitrite and nitrate in the effluent and concentration of ammonia, nitrite and nitrate in the cultivation media. Calculated nitrification activities, hydraulic retention time and volumetric nitrogen load rate are also presented. The N-balance refers to the mass of nitrogen in the effluent, subtracted the total mass of nitrogen sent into the reactor.

On day 37/38 the batch capasity- and toxic salinity tests were conducted.

Table A.1: Operation of the nitrification reactor with biomass originating from low salinity municipal waste water. Shown are the inlet concentrations of ammonia, nitrite and nitrate, the outlet concentration of ammonia, nitrifying activities, hydraulic retention time and volumetric nitrogen load rate.

Time	$C_{influent}(mg-N/L)$			$C_{effluent}(mg-N/L)$				HRT	VNLR	Activity (mg-N/lh)		
(day)	NH_4^+	NO_2^-	NO_3^-	NH_4^+	NO_2^-	NO_3^-	N-balance	(h)	$(mg-N/lh)$	NH_4^+	NO_2^-	NO_3^-
1	36.8	0	0.219	0.089	0.07		36.9	29.2	1.27	1.26	0.00	-0.01
3	36.8	0	0.219	0	0.080	54.6	-17.7	29.2	1.27	1.26	0.00	1.86
4	39.4	0.006	0.491	0.123	0.019	47.8	-8.05	21.9	1.82	1.80	0.00	2.16
6	39.4	0.006	0.491	0.463	0.110	67.3	-28.0	21.9	1.82	1.78	0.00	3.05
8	39.4	0.006	0.491	1.03	0.004	48.0	-9.14	21.9	1.82	1.75	0.00	2.17
10	41.8	0.007	0.148	0.327	0.600	51.2	-10.2	21.9	1.92	1.90	0.03	2.33
12	41.8	0.007	0.148	0.403	0.600	51.5	-10.5	21.9	1.92	1.89	0.03	2.35
14	41.8	0.007	0.148	0.148	0.06	52.1	-10.4	21.9	1.92	1.90	0.00	2.37
16	41.8	0.007	0.148	0	0.071	54.6	-12.7	21.9	1.92	1.91	0.00	2.49
18	41.8	0.007	0.148	0.354	0.062	51.2	-9.66	13.6	3.09	3.05	0.00	3.76
19	109	0.002	0.311	0.873	0.07	55.1	53.3	13.6	8.06	7.97	0.01	4.04
20	109	0.002	0.311	1.08	0.17	92.1	16.0	13.6	8.06	7.95	0.01	6.76
22	109	0.002	0.311	0.776	0.18	100	8.26	13.6	8.06	7.98	0.01	7.35
24	109	0.002	0.311	1.38	0.435	101	7.00	13.6	8.06	7.93	0.03	7.38
25	109	0.002	0.311	0.042	0.636	101	7.64	13.6	8.06	8.03	0.05	7.42
27	106	0.007	0	0.937	0.209	109	-4.14	13.6	7.81	7.74	0.01	8.03
31	106	0.007	0	1.45	0.098	112	-7.54	13.6	7.81	7.70	0.01	8.25
34	113	0	0.463	1.43	0.123	111	0.910	13.6	8.36	8.22	0.01	8.15
37	113	0	0.463	1.57	0.117	113	-1.22	13.6	8.36	8.21	0.01	8.29
38	Batch											
39	102	0	0.186	135	0.014	2.35	-35.2	29.3	3.48	-1.12	0.00	0.07
40	102	0	0.186	129	0.015	1.76	-28.6	29.3	3.48	-0.92	0.00	0.05
45	102	0	0.186	118	0.15	1.41	-17.4	29.3	3.48	-0.55	0.01	0.04
47	102	0	0.186	114	0.159	1.31	-13.3	29.3	3.48	-0.41	0.01	0.04
50	102	0	0.186	109	0.452	1.64	-8.91	29.3	3.48	-0.24	0.02	0.05
52	102	0	0.186	102	0.905	2.18	-2.90	29.3	3.48	0.00	0.03	0.07
55	102	0	0.186	89.5	5.79	3.97	2.93	29.3	3.48	0.43	0.20	0.13

Continued on next page

Table A.1 – *Continued from previous page*

Time	$C_{influent}(mg-N/L)$			$C_{effluent}(mg-N/L)$				HRT	VNLR	Activity (mg-N/lh)		
(day)	NH_4^+	NO_2^-	NO_3^-	NH_4^+	NO_2^-	NO_3^-	N-balance	(h)	$(mg-N/lh)$	NH_4^+	NO_2^-	NO_3^-
60	105	0.011	0.349	85.3	2.02	2.26	15.8	29.3	3.59	0.67	0.07	0.07
62	105	0.011	0.349	109	3.16	4.15	-11.0	29.3	3.59	-0.14	0.11	0.13
70	10.7	0.061	0.181	9.46	2.48	0.726	-1.72	14.1	0.78	0.09	0.17	0.04
73	10.7	0.061	0.181	3.36	7.01	2.02	-1.45	14.1	0.78	0.52	0.49	0.13
74	10.7	0.061	0.181	1.10	8.80	2.40	-1.36	14.1	0.78	0.68	0.62	0.16
75	11.90	0.027	0.188	9.81	1.30	0.712	0.293	14.1	0.86	0.15	0.09	0.04
80	11.9	0.027	0.188	8.52	1.90	0.463	1.23	29.3	0.41	0.12	0.06	0.01
82	11.9	0.027	0.188	10.7	0.800	0.416	0.199	29.3	0.41	0.04	0.03	0.01
84	11.9	0.027	0.188	8.67	1.83	0.750	0.865	29.3	0.41	0.11	0.06	0.02
87	11.9	0.027	0.188	6.66	2.39	1.06	2.01	29.3	0.41	0.18	0.08	0.03
91	11.9	0.027	0.188	0.584	8.90	2.44	0.191	29.3	0.41	0.39	0.30	0.08
94	11.9	0.027	0.188	0.474	8.50	2.50	0.641	29.3	0.41	0.39	0.29	0.08
96	12.2	0.014	0.198	1.14	10.3	2.87	-1.90	29.3	0.42	0.38	0.35	0.09
101	12.2	0.014	0.198	0.166	11.2	2.87	-1.82	29.3	0.42	0.41	0.38	0.09
103	12.2	0.014	0.198	0.071	10.4	2.58	-0.639	29.3	0.42	0.41	0.35	0.08
105	5.62	0.045	0.425	0.128	4.70	1.55	-0.288	29.3	0.21	0.19	0.16	0.04
108	5.62	0.045	0.425	0.268	4.90	1.11	-0.188	29.3	0.21	0.18	0.17	0.02
111	5.62	0.045	0.425	0.004	3.30	1.48	1.31	29.3	0.21	0.19	0.11	0.04
115	5.62	0.045	0.425	0.620	2.40	0.783	2.29	29.3	0.21	0.17	0.08	0.01
119	6.39	0.044	0.124	0.228	3.90	1.33	1.10	29.3	0.22	0.21	0.13	0.04
122	6.39	0.044	0.124	0.197	4.20	1.22	0.941	29.3	0.22	0.21	0.14	0.04
127	6.39	0.044	0.124	0.133	1.10	5.30	0.025	29.3	0.22	0.21	0.04	0.18

Appendix B

Operation of the nitrifying reactor R2, with biomass originating from the Trondheim Fjord

Table B.1 shows operating conditions for the reactor during the test period. This include parameters such as concentrations of ammonia, nitrite and nitrate in the effluent and concentration of ammonia, nitrite and nitrate in the cultivation media. Calculated nitrification activities, hydraulic retention time and volumetric nitrogen load rate are also presented. The N-balance refers to the mass of nitrogen in the effluent, subtracted the total mass of nitrogen sent into the reactor.

On day 37/38 the batch capasity- and toxic salinity tests were conducted.

Table B.1: Operation of the nitrification reactor with biomass originating from high salinity sea water from the Trondheims Fjord. Shown are the inlet concentrations of ammonia, nitrite and nitrate, the outlet concentration of ammonia, nitrifying activities, hydraulic retention time and volumetric nitrogen load rate.

Time	$C_{influent}(mg-N/L)$			$C_{effluent}(mg-N/L)$				HRT	VNLR	Activity (mg-N/lh)		
(day)	NH_4^+	NO_2^-	NO_3^-	NH_4^+	NO_2^-	NO_3^-	N-balance	(h)	$(mg-N/lh)$	NH_4^+	NO_2^-	NO_3^-
1	37.0	0.012	0.138	4.79	13.3	34.4	-15.3	31.94	1.16	1.01	0.42	1.07
3	37.0	0.012	0.138	0	2.40	42.8	-8.05	31.94	1.16	1.16	0.07	1.34
4	30.4	0.029	0.131	0.41	1.20	39.5	-10.6	22.5	1.36	1.33	0.05	1.75
6	30.4	0.029	0.131	0.623	1.60	35.2	-6.86	22.5	1.36	1.32	0.07	1.56
8	30.4	0.029	0.131	0	0.09	32.5	-2.03	22.5	1.36	1.35	0.00	1.44
10	39.3	0.018	0.272	0.604	1.50	40.3	-2.81	22.5	1.76	1.72	0.07	1.78
12	39.3	0.018	0.272	0.465	1.80	45.2	-7.88	22.5	1.76	1.73	0.08	2.00
14	39.3	0.018	0.272	0.441	0.71	42.6	-4.16	22.5	1.76	1.73	0.03	1.88
16	39.3	0.018	0.272	0.418	0.58	43.6	-5.01	22.5	1.76	1.73	0.02	1.93
18	39.3	0.018	0.272	0.475	0.91	40.7	-2.50	13.07	3.03	2.97	0.07	3.09
19	89.9	0.006	0.063	7.83	10.2	68.3	3.64	13.07	6.88	6.28	0.78	5.22
20	89.9	0.006	0.063	6.13	6.90	77.8	-0.86	13.07	6.88	6.41	0.53	5.95
22	89.9	0.006	0.063	3.62	2.01	85.1	-0.76	13.07	6.88	6.60	0.15	6.51
24	89.9	0.006	0.063	4.31	1.96	84.9	-1.20	13.07	6.88	6.55	0.15	6.49
25	89.9	0.006	0.063	2.06	0.43	84.1	3.38	13.07	6.88	6.72	0.03	6.43
27	103	0.021	0	15.3	1.78	84.8	1.14	13.07	7.88	6.71	0.13	6.49
31	103	0.021	0	11.0	1.74	88.1	2.16	13.07	7.88	7.04	0.13	6.74
34	106	0.008	0.619	14.5	1.22	85.6	5.31	13.07	8.16	7.00	0.09	6.50
37	106	0.008	0.619	9.42	1.46	88.3	7.45	13.07	8.16	7.39	0.11	6.71
38	Batch											
39	100	0.110	3.64	10.7	0.32	94.1	-1.37	13.07	7.94	6.83	0.02	6.92
40	100	0.110	3.64	4.14	0.13	69.5	30.0	13.07	7.94	7.33	0.00	5.04
45	100	0.110	3.64	63.3	0.15	44.2	-3.90	13.07	7.94	2.81	0.00	3.10
47	108	0.013	0.728	63.9	1.16	47.3	-3.62	13.07	8.32	3.37	0.09	3.56
50	108	0.013	0.728	48.0	32.4	35.6	-7.26	13.07	8.32	4.59	2.48	2.67
52	108	0.013	0.728	40.5	54.5	30.6	-16.86	13.07	8.32	5.16	4.17	2.29
54	31.6	0	0.216	7.49	25.6	10.1	-11.37	13.07	2.43	1.84	1.96	0.76

Continued on next page

Table B.1 – *Continued from previous page*

Time	$C_{influent}(mg-N/L)$			$C_{effluent}(mg-N/L)$				HRT	VNLR	Activity (mg-N/lh)		
(day)	NH_4^+	NO_2^-	NO_3^-	NH_4^+	NO_2^-	NO_3^-	N-balance	(h)	$(mg-N/lh)$	NH_4^+	NO_2^-	NO_3^-
55	31.6	0	0.216	0.653	26.5	15.0	-10.34	13.07	2.43	2.37	2.03	1.13
59	31.6	0	0.216	0.200	27.3	13.2	-8.88	13.07	2.43	2.40	2.09	0.99
60	31.6	0	0.216	0.408	27.8	14.5	-10.89	13.07	2.43	2.39	2.13	1.09
62	11.7	0.012	0.385	0.203	7.60	6.14	-1.85	13.07	0.93	0.88	0.58	0.44
65	11.7	0.012	0.385	0.145	3.50	8.51	-0.06	13.07	0.93	0.88	0.27	0.62
70	12.2	0.013	0.286	0.265	1.10	10.1	1.03	13.07	0.96	0.91	0.08	0.75
73	12.2	0.013	0.286	0.177	0.38	10.8	1.14	13.07	0.96	0.92	0.03	0.80
74	12.2	0.013	0.286	1.04	0.22	10.3	0.94	13.07	0.96	0.85	0.02	0.77
75	24.0	0	0.238	0.393	1.06	18.6	4.19	13.07	1.85	1.81	0.08	1.40
80	24.0	0	0.238	0.364	0.010	21.9	1.96	13.07	1.85	1.81	0.00	1.66
82	24.0	0	0.238	0.496	0.010	23.0	0.73	13.07	1.85	1.80	0.00	1.74
84	37.2	0.016	0.228	0.800	0.121	37.0	-0.48	13.07	2.86	2.79	0.01	2.81
87	37.2	0.016	0.228	0.235	0.060	37.0	0.15	13.07	2.86	2.83	0.00	2.81
91	37.2	0.016	0.228	0.672	0.020	44.1	-7.35	13.07	2.86	2.79	0.00	3.36
94	37.2	0.016	0.228	0.832	0.110	42.4	-5.90	13.07	2.86	2.78	0.01	3.23
96	37.2	0.016	0.228	0.138	0.000	41.4	-4.09	13.07	2.86	2.84	0.00	3.15
101	54.8	0.035	0.764	0.501	0.090	56.5	-1.54	13.07	4.25	4.15	0.00	4.26
103	54.8	0.035	0.764	0.617	0.100	55.8	-0.97	13.07	4.25	4.14	0.00	4.21
105	82.6	0.005	0.26	0.798	0.220	84.5	-2.65	13.07	6.34	6.26	0.02	6.45
108	82.6	0.005	0.26	0.976	0.620	82.3	-1.03	13.07	6.34	6.25	0.05	6.28
111	82.6	0.005	0.26	0.087	0.000	82.1	0.68	10.95	7.57	7.54	0.00	7.47
115	85.9	0.013	0.321	1.21	0.480	89.6	-5.06	10.95	7.88	7.73	0.04	8.15
119	92.9	0.062	0.259	1.34	0.540	91.1	0.24	10.95	8.51	8.36	0.04	8.30
122	92.9	0.062	0.259	0.912	1.42	87.9	2.99	10.95	8.51	8.40	0.12	8.00
127	84.3	0.035	0.352	0.234	0.190	83.5	0.76	10.95	7.73	7.68	0.01	7.59

Appendix C

pH, temperature and dissolved oxygen measurements

Tables C1 and C2 shows the measured pH, temperature and dissolved oxygen (DO) concentration for the nitrifying reactor with biomass originating from high salinity sea water and municipal waste water respectively. Measurements are shown as days after initiation of continuous operation.

Table C.1: pH, dissolved oxygen (DO) and temperature measurements from the nitrifying reactor with biomass originating from the Trondheim Fjord.

Day:	pH:	DO (mg/L):	T (°C):
1	7.80	6.96	25.0
3	7.70	7.36	21.8
4	7.37	6.93	25.0
6	7.71	6.94	25.0
8	7.71	6.89	25.0
10	7.76	7.10	24.3
12	7.73	6.91	25.0
14	7.79	6.88	25.0
16	7.74	6.72	25.0
18	7.29	6.73	24.9
19	7.76	6.53	25.0
20	7.58	6.69	24.5
22	7.38	6.73	24.8
24	7.39	6.61	24.7
25	7.66		
27	7.25	6.82	24.8
31	7.21	6.87	24.8
34	7.21	6.87	24.8
37	7.28	6.78	24.8
38			

Continued on next page

Table C.1 – *Continued from previous page*

Day:	pH:	DO (mg/L):	T (°C):
39			
40	7.68	7.92	25.2
45	7.78	8.01	25.1
47	7.72	7.81	25.5
50	7.74	7.54	25.3
52	7.71	7.67	25.4
54	7.70	7.45	25.3
55	7.29	8.20	25.0
59	7.36	8.12	25.2
60	7.65	8.09	24.6
62	7.80	8.15	24.9
65	7.82	8.13	25.2
70	7.74	8.36	25.6
73	7.79	8.27	24.8
74	7.72	8.05	25.7
75	7.76	8.05	25.2
80	6.77	8.16	25.0
82	7.63	7.94	25.5
84	7.79	7.82	25.0
87	7.40	7.86	24.5
91	7.76	7.59	24.7
94	7.80	7.54	25.2
96	7.52	7.97	24.8
101	7.72	7.47	24.5
103	7.77	7.53	24.5
105	7.39	7.62	24.4
108	7.27	7.87	24.5
111	7.69	7.97	26.4
115	7.23	7.71	24.3
119	7.22	7.59	23.4
122	7.29	7.23	25.5
127	7.27	7.01	26.5

Table C.2: pH, dissolved oxygen (DO) and temperature measurments from the nitrifying reactor with biomass originating from municipal waste water.

Day:	pH:	DO (mg/L):	T (°C):
1	7.54	7.54	25.1
3	7.8	8.82	21.3
4	7.62	8.27	24.8
6	7.53	8.09	25.1
8	7.73	8.24	24.9
10	7.76	8.22	24.9
12	7.76	8.08	24.9
14	7.33	8.13	24.9
16	7.44	7.92	24.9

Continued on next page

Table C.2 – *Continued from previous page*

Day:	pH:	DO (mg/L):	T (°C):
18	7.76	8.04	24.8
19	7.76	7.86	25.0
20	7.23	7.86	24.1
22	7.24	7.87	24.4
24	7.22	7.22	24.3
25	7.34		
27	7.68	7.75	24.6
31	7.24	7.90	24.6
34	7.74	7.73	24.6
37	7.24	7.73	24.6
38			
39			
40	7.77	7.05	24.9
45	7.76	7.07	24.9
47	7.72	6.94	25.3
50	7.45	6.73	25.1
52	7.66	6.85	25.2
55	7.68	6.96	25.0
60	7.70	6.88	24.7
62	7.30	6.92	24.8
70	7.68	7.06	25.2
73	6.96	7.10	24.6
74	7.33	6.90	25.7
75	7.72	6.94	25.1
80	7.56	6.41	25.0
82	7.74	6.90	25.5
84	7.78	6.98	25.0
87	7.77	7.00	24.4
91	7.68	6.91	24.6
94	7.73	6.84	25.0
96	7.52	6.90	24.5
101	7.67	6.90	24.6
103	7.77	6.87	24.5
105	7.63	6.93	24.4
108	7.75	6.76	24.8
111	7.35	6.81	26.2
115	7.44	7.01	24.3
119	7.79	7.01	23.5
122	7.73	6.74	25.5
127	7.75	6.76	26.5

Appendix D

Capasity and toxicity tests

Tables D1 and D2 shows the measured concentrations of ammonia, nitrite and nitrate for Reactor F and Reactor R2 during the batch capacity test.
Tables D3 and D4 shows the measured concentrations of ammonia, nitrite and nitrate for Reactor F and Reactor R2 during the salinity toxic response test.

Table D.1: Concentration measurements of ammonium, nitrite and nitrate ($mg-N/L$) for the municipal waste water culture in Reactor F during the batch capacity test.

Time (h):	$C^+_{NH_4}$:	$C^-_{NO_2}$:	$C^-_{NO_3}$:
0	93.8	0.107	8.26
0.25	96	0.18	9.07
0.5	94.9	0.192	12.5
1.0	88.9	0.090	17.6
1.5	96	0.073	21.6
2.0	79.9	0.076	30.4
2.5	75.3	0.173	36.3
3.0	68.3	0.113	41.5
3.5	63.3	0.080	50.0
4.0	60.1	0	54.1

Table D.2: Concentration measurements of ammonium, nitrite and nitrate ($mg-N/L$) for the Trondheims Fjord culture in Reactor R2 during the batch capacity test.

Time (h):	$C^+_{NH_4}$:	$C^-_{NO_2}$:	$C^-_{NO_3}$:
0	93.2	0.400	3.89
0.25	87.0	0.765	6.88
0.5	87.9	1.24	14.2
1.0	92.2	1.82	21
1.5	83.0	1.92	23.6
2.0	80.4	1.52	34.4
2.5	69.8	1.41	34
3.0	63.0	1.14	41.7
3.5	57.4	1.17	46.6
4.0	51.7	1.17	49.4

Table D.3: Concentration measurements of ammonium, nitrite and nitrate ($mg-N/L$) for the municipal waste water culture in Reactor F during the salinity toxic response test.

Time (h):	$C^+_{NH_4}$:	$C^-_{NO_2}$:	$C^-_{NO_3}$:
0	105	0.075	1.78
0.5	83.6	0.007	2.08
1.0	107	0.001	1.75
1.5	105	0.006	1.69
2.0	110	0.008	1.91
2.5	109	0.003	1.88
3.5	109	0.070	2.75
4.5	111	0	1.78
5.5	113	0.006	2.23
7.5	118	0	1.86
10.0	122	0.002	2.04
13.0	125	0	2.09
19.5	130	0.001	2.48
24.0	135	0.014	2.35

Table D.4: Concentration measurements of ammonium, nitrite and nitrate ($mg-N/L$) for the Trondheim Fjord culture in Reactor R2 during the salinity toxic response test.

Time (h):	$C^{+}_{NH_4}$:	$C^{-}_{NO_2}$:	$C^{-}_{NO_3}$:
0 .0	110	0.039	2.10
0.5	102	0.163	2.46
1.0	99.3	0.352	5.07
1.5	94.3	0.390	8.40
2.0	90.8	0.570	12.7
2.5	87.1	0.650	17.9
3.5	78.5	0.470	26.9
4.5	72.0	0.230	33.2
5.5	65.8	0.260	39.8
7.5	51.2	0.420	54.0
10.0	29.6	0.710	73.4
13.0	1.62	1.10	101

Appendix E

DGGE protocol

Mounting of glass plates

1. Wash the two glass plates, the spacer and the comb using Deconex soap and hot tap water. Finally rinse well with water to remove any traces of soap. Polish one side of each glass plate using 96% ethanol and Kimwipe paper.
2. Assemble the glass plates and spacer, and place it all in the gel box. Assure that the spacer is aligned to the lower edge of the glass plates. Tighten the screws.
3. Loosen the two uppermost screws, mount the comb, and then tighten the screws again.

Preparation of DGGE solutions

1. Determine the acrylamide percent and the denature gradient of the gel. (For recipes og solutions, see below.)
2. Make acrylamide solutions with the desired denaturing percentage in two 50 ml tubes. (Total volume in each tube will be 24 mL; see table below for volumes of 0% and 80% denaturing solutions.)
3. The 0% denat. acrylamide solution can be added to the 50 mL tubes without filtration. The 80% denat. acrylamide solution needs to be filtered before upon addition. (In order to remove urea crystals).
4. Prepare a 50 mL tube with 8 mL 0% denat. acrylamide solution. (Stacking gel for the top part of the gel.)
5. When ready to pour the gel, add $16\mu L$ tetramethylethylenediamine (TEMED) to the 24 mL gel solutions, and $10\mu L$ TEMED to the 8 mL stacking solution.
6. Prior to pouring the gel, add $87\mu L$ APS (10% ammonium per-sulphate) in both 24 mL gel solutions. (For the stacking gel, add $40\mu L$ APS, but not until the stacking gel is ready for pouring.)

Casting the gel

1. Rinse the gradient mixer and the tubes by pumping mq-water through the system.
2. Turn off the pump, close the valve between the chambers off the gradient mixer, and put the gradient mixer on stirring.
3. Pour the gel solution with low denat. percentage in the left chamber. Quickly open and close the valve to remove any air bubbles in the channel between the chambers. Use a pipette to remove any small amounts of gel solution in the right chamber.
4. Pour the gel solution with high denat. percentage in the right chamber.
5. Start the pump and wait a few seconds until the solution from the right chamber has migrated 7-8 cm out in the tube. Then open the valve between the chambers. Assure stirring in both chambers.
6. Place the syringe between the glass plates. (Assure no water from the washing step is left in the tube.)
7. When the gel reaches approximately 1 cm below the comb, stop the comb, remove the syringe, and empty any leftovers from the mixing chamber and tubes. Rinse the system with a small amount of mq-water.
8. When the mixing chambers are empty from water, close the valve and stop the pump. Add APS to the stacking gel solution, mix, and pour into the right chamber of the mixer.
9. Start the pump. When the glass plates are completely filled with the stacking gel, turn of the pump, and press the comb down and in to the gel. Tighten the screws.
10. Leave the gel for polymerization for at least two hours.
11. Pump mq-water through the system to avoid gel polymerization in the tubes.

Preparations and addition of samples

1. Make 20 L of 0.5X TAE buffer (200 mL 50X TAE and 20 L of mq-water) and add approximately 17 L to the buffer tank. (The buffer may be used for three runs.) Turn on the instrument to heat the buffer to 60°C.
2. Carefully remove the comb from the gel. Loosen all screws, and carefully press down the spacer. Tighten the screws at the sides of the glass plates. (The screws on the bottom should be loose throughout the electrophoresis.)
3. Place the gel system in the buffer tank. Avoid air bubbles beneath the gel.

4. Attach the electrical wires and recirculation tube and turn on the recirculation. Rinse the wells using a syringe with buffer. Turn the power on (100 V; should result in approximately 27 - 35 mA) and let run while preparing the samples.

5. Add 3 μL loading dye to 5 μL PCR sample. When all samples are ready for loading, turn off the recirculation and push the "low voltage" button. Apply the samples to the wells. Avoid using the 2-3 outermost wells due to "smiling" effects.

Running the gel

1. Turn on the "high voltage" button, set the voltage to 100 V. Run the gel for 5-10 minutes without buffer recirculation.

2. Turn on the recirculation and run gel for 17-18 hours.

Staining and visualization

1. Turn of the instrument; lift the gel system out.

2. Loosen the screws, and lift out the gel. Carefully separate the glass plates.

3. Transfer the gel to a plastic foil sheet and place it in a suitable lidded box.

4. Prepare the staining solution by adding 30 mL mq-water, 3μL SYBR Gold, 600 μL 50X TAE buffer in a 50 mL tube.

5. Distribute the staining solution evenly on the gel. Put the lid on the box, and leave for 1-2 hours.

6. Carefully take out the gel and rinse with mq-water. Carefully let the water run of the gel, use a paper towel at the edges of the gel to remove excess water.

7. Wash the UV plate of the "gel dock" with distilled water and ethanol. Use Kimwipe papers to remove any dust or other particles on the UV plate. Distribute some mq-water on the plate (This allows for easy movement of the gel on the plate).

8. Carefully transfer the gel from the plastic foil to the UV plate (by turning the plastic foil "upside down"). Before removing the foil, position the gel on the plate.

9. Photograph the gel at different exposures, and save the pictures in the original format, and *e.g.* pdf or other formats.

Eluation of bands for sequencing

1. Print out a picture of the gel, and number the bands that are to be sequenced.

2. Add 20 μL sterile mq-water to eppendorf tubes, and number the tubes according to the number of bands.

3. Pull out the UV plate, and pull down the UV screen. Cover the wrists to avoid UV radiation. Use blue 1 mL pipette tips to stick out material from the bands. Take care to avoid touching other bands. Use a pipette to blow out the material in the eppendorf tube with water.

4. Place the tubes in the fridge over night.

5. Use $1\mu L$ of the eluate as template in a $25\mu L$ PCR reaction.

Chemical recipes

For all the solutions mention under, add distilled water to obtain the final volume.

50X TAE buffer

The 50 X TAE buffer is prepared according to Table F.1. Prior of use, autoclave the buffer.

Table E.1: 50 X TAE Buffer (20 L).

Compound	*Amount*
Tris base	242 g
Glacial acetic acid	57.1 mL
0.5 M EDTA (pH 8.0)	100 mL

Deionized formamide

Deionize 200 mL formamide by adding 7.5 g DOWEX RESIN AG 501X8, and stir for one hour at room temperature.

Acrylamid solution (0% denaturing)

8% acrylamide in 0.5 X TAE buffer (per 250 ml):

1. 50 mL of 40% acrylamide solution (BioRadLab Inc)

2. 2.5 mL of 50 X TAE buffer

Store solution at 4°C, protected from light.

Acrylamid solution (80% denaturing)

8% acrylamide, 5.6 M urea, 32% formamide, in 0.5 X TAE buffer (per 250 ml):

1. 50 mL of 40% acrylamide solution (BioRadLab Inc.)

2. 2.5 mL of 50 X TAE buffer

3. 84 g of urea

4. 80 mL of deionized formamide

Store solution at 4°C, protected from light. Must be sterile filtered before pouring the gel.

0% stacking gel

Prepared by taking 8 mL of the 0% acrylamide solution and adding $40\mu L$ 10% APS and $10\mu L$ TEMED.

10% ammonium per-sulphate (APS)

1. Dissolve 10 g of ammonium per-sulphate in 100 mL dH_2O.

2. Sterile filter the solution.

3. Divide solution in $250\mu L$ fractions in eppendorf tubes and store in freezer.

4. Used eppendorf tubes are discharged after use.

Composition of low and high denaturing solutions

Table E.2 shows the composition of low and high denature solutions. 0%- and 80% stock refers to the amount of the 0% and 80% acrylamid solutions needed.

Table E.2: Composition of low and high denature solutions. 0%- and 80% stock refers to the amount of the 0% and 80% acrylamid solutions needed

Denaturing %	0% stock	80% stock	TEMED + 10% APS	Total volume
15	19.5	4.5	16 + 87	24
25	16.5	7.5	17 + 87	24
30	15	9	18 + 87	24
35	13.5	10.5	19 + 87	24
40	12	12	20 + 87	24
45	10.5	13.5	21 + 87	24
50	9	15	22 + 87	24
55	7.5	16.5	23 + 87	24
60	6	18	24 + 87	24
75	1.5	22.5	25 + 87	24